UC Berkeley
UC Berkeley Electronic Theses and Dissertations

Title
Cellular Mechanobiology of Glioblastoma Multiforme

Permalink
https://escholarship.org/uc/item/99n9177g

Author
Ulrich, Theresa Ann

Publication Date
2011

Peer reviewed|Thesis/dissertation

Cellular Mechanobiology of Glioblastoma Multiforme

by

Theresa Ann Ulrich

A dissertation submitted in partial satisfaction of the

requirements of the degree of

Joint Doctor of Philosophy

with University of California, San Francisco

in

Bioengineering

in the

Graduate Division

of the

University of California, Berkeley

Committee in charge:

Professor Sanjay Kumar, Chair

Professor Mohammad Mofrad

Professor Tejal Desai

Professor Andrew Wurmser

Spring 2011

Cellular Mechanobiology of Glioblastoma Multiforme

By Theresa Ann Ulrich

Abstract

Cellular Mechanobiology of Glioblastoma Multiforme

by

Theresa Ann Ulrich

Joint Doctor of Philosophy in Bioengineering
with University of California, San Francisco

University of California, Berkeley

Professor Sanjay Kumar, Chair

The rapid progression of high-grade brain tumors is related to diffuse infiltration of single tumor cells into the surrounding brain parenchyma, a process that involves aberrant interactions between tumor cells and the extracellular matrix (ECM). Tremendous effort has been devoted to elucidating the genetic and biochemical underpinnings of these tumors; however, poor translation of candidate therapies from animal models to human patients has only increased the sense of urgency for the development of new approaches in both the laboratory and the clinic. Indeed, despite decades of extensive clinical and biological research, the life expectancy of patients with grade IV glioblastoma multiforme (GBM) brain tumors is still approximately one year at diagnosis. The work presented in this dissertation has approached this problem from a biophysical perspective, demonstrating that biomechanical cues from the ECM serve as regulators of key GBM tumor cell properties relevant to invasion in both two-dimensional (2D) and three-dimensional (3D) culture models.

We first investigated the role of ECM rigidity in regulating the structure, migration, and proliferation of a panel of glioma cell lines on 2D fibronectin-coated polymeric ECM substrates of defined mechanical rigidity. We found that on highly compliant ECMs, tumor cells appear rounded and fail to productively migrate. As ECM rigidity is increased, tumor cells spread extensively, form prominent stress fibers and mature focal adhesions, and migrate rapidly. Remarkably, cell proliferation is greatly enhanced on rigid versus compliant ECMs. Pharmacological inhibition of nonmuscle myosin II-based contractility blunts this rigidity-sensitivity and rescues motility on highly compliant substrates, providing support for a novel model in which ECM rigidity provides a transformative, microenvironmental cue that acts through actomyosin contractility to regulate the invasive properties of GBM tumor cells.

We next explored glioma mechanosensitivity in 3D by introducing a novel biomaterial platform in which we progressively modulate the biophysical properties of collagen I matrices by adding agarose. We found that agarose increases the bulk elasticity of 3D collagen ECMs over two orders of magnitude by forming a dense meshwork that intercalates between the entangled

collagen fibers. Embedded glioma cells exhibit a pronounced transition from mesenchymal to amoeboid modes of motility, accompanied by severe limitation of cellular invasion from multicellular spheroids as the agarose content of the hydrogels increases from 0-1% w/v. Furthermore, addition of agarose progressively inhibits cell-directed macroscopic gel compaction, concomitant with restriction of cell spreading and reduced cytoskeletal stress fiber and focal adhesion assembly. While time-of-flight secondary ion mass spectrometry and scanning electron microscopy fail to reveal agarose-induced alterations in collagen ligand presentation, the latter modality shows that agarose strongly impairs cell-directed assembly of large collagen bundles. Our results support a model in which agarose structurally couples and reinforces individual collagen fibers, simultaneously introducing steric barriers to cell motility while shifting ECM dissipation of cell-induced stresses from the non-affine deformation of individual collagen fibers to the bulk-affine deformation of a continuum network.

Additionally, we found that agarose-mediated inhibition of cell spreading and cytoarchitecture on 3D collagen-agarose composite hydrogels can be rescued by partial β-agarase digestion of the agarose network or by covalently crosslinking the matrix with glutaraldehyde. Based on these results, we argue that cell spreading and motility on collagen requires local matrix stiffening, which can be achieved via cell-mediated fiber remodeling or by chemically crosslinking the fibers. These findings underscore the critical role of ECM mechanics in regulating glioma tumor cell behaviors in 3D matrices, and bear general implications for micromechanical regulation of cell adhesion and motility in composite fibrillar-nonfibrillar ECMs in vivo and the use of such matrices in tissue engineering and regenerative medicine applications.

This dissertation is dedicated to each and every member of my family.

I may have left our small town in search of bigger and better things, but what I have truly gained on this adventure is an appreciation for the lessons I have learned from you – especially, that a capacity for love, kindness, generosity, honesty, and hard work is ultimately more valuable than anything I could have learned or accomplished in graduate school.

Table of Contents

Acknowledgements

I could never have imagined how fun and rewarding my experience as a Ph.D. student would turn out to be, and I would like to begin my dissertation by sincerely thanking all of the people who have been a part of my life over these last years. Although I will be unable to formally acknowledge the many ways in which you have each touched and enriched my life, I have appreciated every one of you and all of your many kindnesses.

First and foremost, I thank my Ph.D. advisor and mentor, Prof. Sanjay Kumar. Sanjay took me into his fledgling bioengineering laboratory as a young physicist with little to no experience in cell biology, biomaterials, or cancer research, and the fact that I have done well is a testament to his patience and outstanding mentorship abilities. It has been an honor and a privilege to complete my training with an advisor who is not only an extraordinarily gifted scientist, communicator, and teacher, but who also possesses an uncommonly sincere and consistent humility, integrity, balance, and professionalism. From my first day in the lab, Sanjay has always showed a sincere interest and enthusiasm for my ideas and my progress and development as both an academic and a person. His endless supply of optimism, encouragement, and sage advice has lifted me to greater heights than I could have ever imagined. Although one short paragraph could never do justice to the depth and extent to which he has helped me to learn and grow over the last five years, I will say this: Sanjay is one of very few people I truly look up to as a model of the kind of person that I hope to become, and I leave his lab knowing that if I can be half as good a mentor in my career as he has been to me over the last five years, my trainees will be very lucky indeed.

I would also like to acknowledge the outstanding faculty in the Bucknell University Physics Department, who taught me how to think critically and gave me the confidence, skills, and an early push into academia that has continued to propel me forward to this day. Profs. Sally Koutsoliotas, Tom Solomon, and especially my undergraduate research advisor, Krishna Chowdary, played exceptionally important roles in my development as a scientist and an academic, and will always be among my heroes and role models in science and education.

I owe a large debt of gratitude to the federal and California state governments and their taxpayers for funding my education and training as a scientist and engineer. Without the generous support of undergraduate and graduate scholarships, including graduate research fellowships from the National Science Foundation, the Department of Defense, and the UC Berkeley Graduate Division, as well as undergraduate opportunities in the National Science Foundation Research Experience for Undergraduates program and the Bucknell University Presidential Fellowship program, I would never have made it this far.

I have been privileged to have Prof. Elena de Juan Pardo, Prof. Shamik Sen, Dr. Amit Pathak, Prof. Cristina Davis, Prof. Terry Johnson, Dr. Rahul Thakar, and Prof. Wilbur Lam as mentors at various points as I have progressed through graduate school, and I thank them each for their patience, friendship, and good advice. I would also like to sincerely thank Amit Jain, Vaibhavi Umesh, Sophie Wong, and the many other exceptionally bright and talented students I have worked with in the lab and the classroom over the past six years – I am certain that I learned more from them than they learned from me. I thank all of the past and present members of the

Kumar Lab, including Albert Keung, Anuj Patel, Joanna MacKay, Yushan Kim, Dr. Kandice Tanner, Dr. Badri Ananthanarayanan, Dr. Sebastian Rammensee, Dr. Ching-Wei Chang, Dr. Nithya Srinivasan, Meimei Dong, Rosalia de las Rivas Astiz, Alvaro Jorge, Matthew Chown, Dexter D'Sa, Lizhi Cao, Diana Guo, and Charmaine Ramos, who have made the day-to-day working conditions and atmosphere in our lab so enjoyable and memorable. I will miss you all, but I am already so excited to see all of the wonderful directions that your science and your lives will take.

I thank the members of my dissertation committee, Profs. Tejal Desai, Mohammad Mofrad, and Andrew Wurmser, for all of their encouragement and advice, and for taking an active interest in my success. I thank my academic advisor, Prof. Steve Conolly, for our many interesting discussions, for challenging me to "think big" by distilling complex scientific issues to the essential underlying problem or issue, and for always being one of my biggest fans. I thank Prof. Dorian Liepmann for recruiting me to Berkeley in the first place, and for taking such an active interest in my success and happiness as I settled into the bioengineering program, including serving as chair of my qualifying exam committee. I thank Profs. Seung-Wuk Lee and Amy Herr for all of their advice and encouragement, and I thank Prof. Kevin Healy for all of his valuable advice in my first year of graduate school, including suggesting that I consider a research rotation in the Kumar Laboratory. The staff members in the Bioengineering office have been amazingly cheerful and helpful throughout my graduate career, and I extend a special thank you to Rebecca Pauling, Tere Falciglia, Jennifer Davidson Teverbaugh, and Catherine Ocampo Galicia for going above and beyond the call of duty to help me sort out all kinds of arcane questions and bureaucratic issues over the years.

I have been honored to have made many wonderful friends here in Berkeley, all of whom hold a special place in my heart. I trust that you all know how much I have valued your friendship and how much I have treasured our adventures together. Here, I will just extend a special thank you to Janet Casperson for organizing and hosting our Wednesday girls' night over the last several years, which was always a happy and extraordinarily refreshing escape from a long week in lab. I would also like to extend a special thank you to our camping, hiking, and football comrades, including Scott and Jenn Mansell, Paul Koster Van Groos, April and Nick Mostek, and Anh Pham, for many fun and memorable excursions.

I am deeply grateful to my parents, grandparents, and extended family for all of their love, for encouraging my creativity and infusing my childhood with a sense of wonder about the natural world, and for helping me to develop so many of the traits and values that I have needed to succeed throughout my education. I thank my sisters, best friends, and confidantes, Amanda and Laura, for their endless supply of support, encouragement, and understanding, and for always believing in me, even when I did not believe in myself.

Finally and most importantly, I would like to express my gratitude to my husband, Patrick, who continues to amaze and inspire me each and every day. Few people have the privilege to truly spend a lifetime with their best friend and better half, and even fewer find such a joyful and meaningful day-to-day existence. Graduate school has been the grandest of adventures because we did it together.

Chapter 1. Introduction to mechanobiology in health and disease in the central nervous system

1.1 Introduction

Over 2300 years have passed since Aristotle first identified touch as one of the five exteroceptive senses, marking one of the first discussions in the academic literature of mechanosensation, the ability to sense mechanical forces. In the intervening time, we have learned a great deal about how cells convert mechanical sensations into chemical signals, a process known as mechanotransduction. Importantly, we have learned that mechanotransduction serves not only as a sensory mechanism for cells and tissues, but as a regulatory mechanism as well. Numerous studies over the last several decades have revealed the robust sensitivity of mammalian cells to mechanical cues such as shear flow, cyclic strain, and microenvironmental stiffness, demonstrating that the mechanical microenvironment participates centrally in the homeostasis of cells and tissues, and that disruptions of these mechanical cues can contribute to the onset and progression of disease (1, 2). The field of mechanobiology, which examines how cells sense, process, and respond to mechanical stimuli, has emerged at the intersection of the physical and biological sciences to examine the often subtle, yet complex relationship between mechanical force and cell and tissue behavior.

The central nervous system (CNS) has been the focus of extensive tissue biomechanics research for over three decades, spurred in part by widespread public interest in brain and spinal cord trauma in automobile accidents, sports injuries, and other traumatic settings. Yet, despite this history of pioneering work in tissue-level biomechanics, investigation of cellular mechanobiology in the CNS has been comparatively limited. While the earliest work in this field stemmed directly from studies of neuronal trauma and regeneration (e.g. cell-level studies of axonal repair following injury), the last decade has seen rapid acceleration in the pace of research exploring how the properties of the normal (non-traumatized) mechanical microenvironment affect the health and disease of CNS cells and tissues.

This chapter provides an overview of the nascent field of cellular mechanobiology in the CNS, beginning with a description of the structure and mechanical microenvironment within the brain and spinal cord, continuing with an overview of the mechanobiological characteristics of cells in the CNS, and concluding with demonstrated and potential roles for how dynamic interactions between cells and their mechanical microenvironment can contribute to the onset or exacerbation of disease in the nervous system. Section 1.7 focuses on cellular mechanobiology in the setting of glioblastoma multiforme brain tumors, providing specific context for the remaining chapters of this dissertation.

1.2 The mechanical microenvironment of CNS tissues

No other organ system in the body is as carefully protected from external mechanical forces as the CNS by its encasement within the bony skull and vertebral column (and as a consequence, no other organ system is as vulnerable to the buildup of excess pressure during disease or injury, as we will discuss in the last sections of this chapter). The soft tissues inside the CNS are further protected by three membranes known as meninges (the superficial dura mater, central arachnoid mater, and deep pia mater) and by the serum-like cerebrospinal fluid (CSF) that bathes both the brain and spinal cord. A network of cavities deep within the brain, known as ventricles, is lined

by a population of epithelial cells whose main function is to secrete CSF and to aid its circulation throughout the ventricles, the subarachnoid space (located between the arachnoid mater and pia mater) and the central canal of the spinal cord.

The brain parenchyma is organized into distinct anatomical structures (the cerebral hemispheres, diencephalon, brain stem, and cerebellum), which are crisscrossed by blood vessels and defined by a complex and highly organized neuroarchitecture of white matter (composed of neuronal axons) and grey matter (composed of nerve cell bodies). Far less is known about the structure and function of the extracellular matrix (ECM) in CNS tissues than in most other organ systems in the body. A well-defined ECM containing large amounts of collagen, fibronectin, and laminin exists in the basement membrane of the cerebral vasculature and in the meninges surrounding the brain cortex; however, these structures stand in stark contrast to the rest of the brain parenchyma, which consists of a relatively amorphous, anisotropic, and heterogeneous matrix containing mainly hyaluronic acid as well as various other glycosaminoglycans and proteoglycans (3, 4).

The spinal cord is similarly heterogeneous, consisting of longitudinally-oriented white matter tracts surrounding a central, butterfly-shaped region of gray matter. Like the brain, the spinal cord is organized into distinct anatomical structures with specialized functions (e.g., the ascending and descending sensory and motor white matter tracts), and contains an anisotropic ECM that consists mostly of hyaluronic acid (5). The structural inhomogeneities within both the brain and spinal cord lead to extensive heterogeneity in the mechanical and biochemical microenvironment of resident cells, however, cyclic mechanical strain is generated throughout the CNS by pulsatile flow of CSF at a rate of approximately 1 Hz (6-8).

The mechanical stiffness of human tissues varies widely, ranging from very soft brain, fat, and mammary tissues with elastic moduli of less than 1 kPa to calcified bone tissues with elastic moduli near 10,000 kPa (10 MPa). Reported measurements of the mechanical properties of human and animal brain and spinal cord tissues have varied by more than an order of magnitude from several hundred Pa to several kPa, likely due to variations in species, age, sample size and anatomic origin, sample preparation, testing conditions, and time post-mortem (9-13).

The spectrum of available methods and published results for mechanical analysis of CNS tissues has recently been reviewed in considerable detail (14, 15). Here, we will focus our discussion on the two methods that are most commonly used today: rotational rheometry and magnetic resonance elastography (MRE). Rotational rheometry has been employed in materials characterization for decades and generally involves the small-amplitude oscillatory deformation of a sample of known geometry, measurement of the resulting stress within the sample, and calculation of material properties such as the shear modulus and elastic modulus (see (16) for a straightforward and detailed explanation of rheometry theory and methods in the context of biological samples). MRE, on the other hand, is a noninvasive alternative that allows determination of tissue stiffness in living subjects, and therefore has become increasingly popular for measuring the mechanical properties of brain tissue (17-20). This technique involves application of acoustic shear waves to the tissue of interest; a phase-sensitive MR imaging sequence is then used to visualize and quantitatively measure propagating strain waves throughout the tissue, and an algorithm is subsequently used to generate a map of the elastic modulus of the imaged region (21).

A recent report by Vappou and colleagues demonstrated a surprisingly strong agreement between the linear viscoelastic behavior of brain tissues measured by rotational rheometry and MRE (22), which may facilitate longitudinal or comparative studies of brain tissue mechanics in healthy and diseased individuals in the future. However, an important caveat of both rotational rheometry and MRE is that both measurements require a macroscopic sample of tissue that may contain multiple cell types and ECM with microscale heterogeneities, thereby complicating inference of the local mechanical microenvironment of single cells. This limitation was illustrated by a recent atomic force microscopy (AFM) indentation study by Elkin et al., which measured the apparent elastic modulus of the cell-scale microenvironment in anatomical subregions of the rat hippocampus, revealing spatial heterogeneity in local tissue mechanics (11).

The brain is generally considered to be a nonlinear viscoelastic material with mechanical properties that exhibit relatively low but measurable inter-species variability. These mechanical properties appear to be independent of perfusion pressure and cranial confinement as long as strains are modest. Importantly, the mechanics of brain tissue change rapidly and dramatically within hours after death (23), which may account for some of the variability in reported measurements of brain tissue elasticity. Rheological studies of immature and adult porcine and rat brain tissue have revealed that an additional source of variability may be a decrease in the mechanical stiffness of the brain parenchyma with age, an observation that has been attributed in part to the increasing lipid content associated with myelination of rapidly branching axonal and dendritic arbors during development as well as reduction in water content with age (24, 25). Dynamic magnetic resonance imaging (MRI) studies appear to support the idea of age-dependent alterations in the mechanical properties of mature CNS tissues (10). While dynamic phase contrast MRI is not traditionally thought of as a measurement of tissue mechanics, it can be used to measure the coupling of brain, spinal cord, and CSF pulsations to the driving vascular pulsations; because the biomechanical properties of CNS tissues exert strong influence over this coupling, observed differences between adult and elderly individuals provide indirect evidence that human CNS tissue mechanics progressively change with age.

In one of the earliest studies of brain tissue biomechanics, Metz et al. compared the viscoelastic properties of living tissue in anesthetized animals with post-mortem and post-fixation tissue samples; although the authors reported significant increases in the elastic modulus of the fixed tissue, they surprisingly observed very little change in the nonlinearity of the stress-strain relationship (26). Numerous studies have since reported nonlinear stress-strain responses in mammalian brain tissue, similar to the characteristic strain-stiffening observed in collagenous soft tissues (27-32); these nonlinearities feature prominently in models of traumatic injury, but their significance to cellular mechanobiology remains incompletely understood because the range of frequencies at which cells probe their environment is not yet well determined.

1.3   Mechanobiology in CNS development

The mechanical properties of the ECM can direct a wide range of cellular properties, including cell shape and cytoarchitecture (33-35), motility (36, 37), matrix remodeling (38), differentiation (39-42), and the extension of functional cellular projections (43-46). As the human brain

develops, billions of cells are generated in the proliferative tissues lining the lateral ventricles of the brain. These cells migrate throughout the developing CNS, differentiate into neurons or glial cells, and establish a diverse array of organized structures with distinctive shapes and intricate internal architecture (47). Neurogenesis continues, albeit in a much more limited way, into adulthood through the self-renewal and differentiation of adult neural stem cells (aNSCs) found within the hippocampus and subventricular zone (48). The mechanosensitivity of aNSCs was recently explored by Saha and colleagues, who demonstrated that the differentiation and self-renewal of aNSCs can be modulated by controlling the mechanical stiffness of the surrounding microenvironment (42). In particular, culturing aNSCs on the surface of soft polymeric substrates with stiffnesses close to living brain tissue (~100-500 Pa) favored differentiation into neurons, whereas culturing aNSCs on polymeric substrates with identical surface chemistry but much greater mechanical rigidity (~1-10 kPa) favored differentiation into glial cell types. The latter finding raises the intriguing possibility that tissue stiffening may play an instructive role in glial scar formation rather than merely serving as a passive consequence of the process. This mechanosensitivity, coupled with the mechanical heterogeneity present throughout the normal and diseased brain, lends support to the hypothesis that mechanical cues may be dynamically involved in CNS development, in the maintenance of homeostasis, and in the development of disease.

The mechanisms governing morphogenesis (the development of shape, organization and structure) in CNS tissues have long been the subject of vigorous investigation and debate, but one of the most elegant and robust hypotheses that has emerged is the tension-based theory of morphogenesis proposed by David Van Essen in 1997 (47). This theory holds that mechanical tension along axons, neurites and glial cell extensions is sufficient to generate many of the structural features of the mammalian CNS, including the folding patterns of the cortex and the observed compactness of the neural circuitry. This hypothesis is supported by the unique mechanical properties of neurons (described below), which would be expected to facilitate regulation of steady tension in neuronal processes during development through both passive and active mechanisms.

1.4   Mechanobiology of neurons in the CNS

The notion that mechanosensation is a central function of many neurons, such as the somatosensory neurons that transduce tactile and sound cues, was clear long before the recent surge of interest in cellular mechanotransduction mechanisms. It was less obvious whether differentiated neurons in the CNS, which are largely shielded from external mechanical loading by the presence of the cranium and vertebral column, should be expected to retain similar sensitivity to the mechanical properties of their microenvironment. Yet, a growing body of work has indicated that the relationship between mature neurons and microenvironmental mechanics is as dynamic and delicate in the CNS as in tissues which routinely experience mechanical loading. For example, the growth and functionality of neurons appears to be tightly coupled to microenvironmental rigidity. Two recent studies by Janmey and colleagues revealed that substrate rigidity can modulate the outgrowth of cells from explants of spinal cord (45) and cortical brain tissue (49) in a manner that mirrors the stiffness-dependence of aNSC differentiation discussed previously (42). Specifically, explanting CNS tissues onto substrates

that match the approximate stiffness of CNS tissues (several hundred Pa) was found to optimally support both neuronal and glial survival while suppressing overgrowth of the cultures by astrocytes, whereas explanting onto softer substrates selected for neuronal survival and growth and explanting onto stiffer substrates selected for glial survival and proliferation.

The extension and branching of neurites (thin projections from the cell body, including axons and dendrites) in culture can be similarly regulated by the rigidity of the cellular microenvironment (43-46); substrates which are either much softer or much stiffer than the normal brain microenvironment often do not support robust neurite extension in vitro, although the details of this relationship appear to depend upon the cell source and substrate geometry and composition. This correlation may have implications for neuroregeneration and tumorigenesis; for example, it was recently proposed that the softening of reactive astrocytes following mechanical injury may provide a compliant, brain-like mechanical substrate that promotes neurite extension (50). In addition, it was recently shown that the potency with which retinoic acid can induce neurite extension, reduce proliferation and suppress N-Myc expression in human neuroblastoma cells all depend strongly on ECM stiffness (51). Given the substantial mechanical stress exerted by neurites on adhesive substrates (52-54), this phenomenon is likely related to the capacity of the underlying substrate to support generation of contractile forces within elongating projections. Interestingly, neurites have been elicited in vitro by direct application of tensile forces with glass microneedles, where active elongation is observed when tension is maintained above a threshold value, and active retraction is observed when tension is released (53-56). Follow-up studies using magnetic beads to apply external loads to elongating neurites showed that forces on the order of 1.5 nN are required to elicit neurites, and that force-induced neurite initiation and elongation appears to be a highly conserved property that is largely independent of cell age and synaptic phenotype (57, 58).

The initiation, extension, and maintenance of neurites is key to the functional integrity of the CNS, and importantly, these processes are intimately related to the mechanical properties of neurons and their subcellular components. AFM characterization of individual neurons showed that retinal neurons display the rheological characteristics of elastic solids, with cell processes that are often softer than the cell body (59). Individual neurites display simple elastic behavior under transient stretching (neurite length increases in proportion to applied tension) (54) and viscoelastic properties under sustained stretching (60); specifically, the initial tension relaxes passively to a lower level on the timescale of minutes, and when resting tension is released, the neurite shortens slightly prior to active retraction. Interestingly, cytoskeletal elements within the cell are known to behave in similar fashion; actin stress fibers in living cells also retract as viscoelastic cables following incision with a femtosecond laser nanoscissor (61), and curved microtubules have been observed to straighten briefly following nanoscissor incision due to release of elastic energy prior to rapid depolymerization (62). This is also consistent with the viscoelastic behavior that has been measured in a wide variety of cultured non-neuronal cell types by magnetic twisting cytometry (35, 63-65), atomic force microscopy (66-69), micropipette aspiration (70-72), optical trapping (73, 74), cellular de-adhesion measurements (75), and a variety of other methods (76).

Biochemical modifications to cytoskeletal elements may play a key role in neurite mechanics as well; in particular, it has long been known that cytoskeletal dynamics play a central role in

driving the directionality of axonal growth (77-79). More recently, however, contributions of cytoskeletal networks to the shape and mechanics of mature axons have begun to emerge. For example, repulsive forces between phosphate groups on neurofilament sidearm domains contribute to the organization of neurofilament networks within axons (80-82). Indeed, enzymatic dephosphorylation of neurofilaments significantly alters the mechanical properties of both purified neurofilament gels and single neurofilament proteins (83, 84). Conversely, traumatic nerve injury is sometimes accompanied by altered posttranslational modification and organization of neurofilaments and other cytoskeletal proteins (85, 86). Similar mechanisms have been proposed for the organization of microtubule bundles, which are commonly found in both axons and dendrites, by microtubule-associated proteins (87). Modulators of the actin cytoskeleton also play a prominent role in regulating axonal growth and guidance; for example, activation of myosin motors and Rho-family GTPases, (e.g. Rho, Rac, Cdc42) play vital roles in regulating axon growth dynamics, and dysfunctional Rho family GTPase signaling has been tied to a surprisingly wide variety of adult and congenital neurological disorders (88-90). Mechanosensitive ion channels have also been implicated in neurite growth kinetics (91-93) in addition to their well-documented role in fast sensation of stretch and other forces (94-96). For example, inhibition of Ca^{2+} influx through stretch activated ion channels in neurons from explanted *Xenopus laevis* spinal cord tissue was found to dramatically accelerate the rate of neurite extension, implying that calcium influx through mechanosensitive channels can inhibit outgrowth (92).

1.5   Mechanobiology of glial cells in the CNS

Neurons have traditionally commanded the vast majority of attention in neurobiology research due to their propagation of action potentials, electrical impulses which travel along axons to facilitate quick and efficient transmission of signals over distances that can be greater than a meter. Non-neuronal cells within the CNS, known as glia (derived from the Greek word for "glue"), have historically been relegated to the accessory role of "support cells", with known functions ranging from the secretion and cilia-driven circulation of CSF by ependymal cells, to the myelination of axons by oligodendrocytes, to the structural support presumably provided by astrocytes, the most abundant cell type in the CNS. Over the last twenty years, new discoveries have challenged these old stereotypes and have stimulated renewed interest in the biology of glial cells, particularly astrocytes. Far from serving simply as the "glue of the nervous system," astrocytes are now thought to regulate adult neurogenesis (97-99), learning and synaptic plasticity (100-105), and orchestration of the host response to injury in addition to protecting the CNS via maintenance of homeostasis and induction and maintenance of the blood-brain barrier (106).

The first direct viscoelastic characterization of individual glia and neurons, published in 2006, directly challenged the dogma of glia as structural support cells. These atomic force microscopy indentation measurements revealed that glial cells are softer than neurons (and would therefore provide poor structural support) and that elastic forces dominate viscous forces in glial mechanics (therefore making them a poor glue) (59). Yet, in 2008, direct probing of this hypothesis in situ via comparative tensile testing of spinal cord explants with an intact or disrupted glial matrix demonstrated that glia do provide significant mechanical support to spinal

cord tissue under uniaxial tension (107). While this is still an active area of debate, it is possible that the high compliance of individual glial cells allows them to protect neurons by cushioning them during trauma, whereas the architectural arrangement of star-shaped astrocytes into a cellular scaffold that physically couples blood vessels, neurons, and other glia may be critical in providing mechanical support to the tissue, especially given the absence of a robust ECM.

The idea that astrocytes may be ideally situated to sense and resist mechanical disruption in the brain through their unique scaffold architecture is not new; in fact, it has been over two decades since Alen Mathewson and Martin Berry first hypothesized that "architectural disruption" in the brain may be responsible for the phenomenon of astrocyte activation (108). This activation, also referred to as reactive gliosis or astrogliosis, involves both astrocyte hypertrophy (abnormal enlargement of cell size) and hyperplasia (increase in cell number) in response to CNS pathologies ranging from neurodegenerative diseases to direct trauma, and often results in the formation of a glial scar (109). Because astrocytes function as a syncytium of interconnected cells, mechanical deformation in one area of the brain due to primary stress (e.g. the mass effect of a tumor or direct stress due to trauma) or secondary stress (e.g. increasing pressure due to edema, the buildup of fluid following tissue insult) could quickly be biochemically and mechanically communicated to distant astrocytes, allowing rapid induction of reactive gliosis and other host response mechanisms.

Mathewson and Berry's architectural disruption hypothesis has been supported by in vitro observations of strain rate-dependent gliosis in 3-dimensional (3D) cell culture models (110) and also by growing evidence that the mechanosensory machinery of astrocytes is particularly robust. For example, astrocytes directly convert mechanical stimuli into chemical signals using stretch-activated or stretch-inactivated ion channels. Ostrow and colleagues used micropipette indentation to directly demonstrate this phenomenon, showing that deformation of a single astrocyte induces transmembrane flux of Ca^{2+}, which propagates as a transcellular wave through gap junctions to neighboring astrocytes in confluent culture (111). Chemical stimuli such as glutamate can similarly trigger the initiation and propagation of calcium waves in cultured astrocytes (112, 113); these calcium waves are believed to constitute a key signaling mechanism to orchestrate astrocytic functions ranging from guidance of CNS growth cones (114) to alterations in cell structure, gene expression, and proliferation (115, 116). Importantly, mechanical induction of intracellular second-messengers (e.g. inositol triphosphate and release of intracellular calcium) have been observed in cultured astrocytes as well (111).

Mounting evidence suggests that the components of the cellular contractile machinery regulate calcium signaling via gap junctions in addition to traditional mechanotransductive pathways. A relationship between a functional cytoskeleton and active calcium signaling in astrocytes was clearly established in 1998 by Cotrina and colleagues, who demonstrated that neonatal astrocytes are unable to propagate calcium waves until the actin cytoskeleton is fully developed (a process that takes several hours), despite the existence of extensive gap junctional coupling shortly after subculture (117). Furthermore, the radius of propagated calcium waves increases in direct proportion to the percentage of cells exhibiting a well-organized actin cytoskeleton (measured as the fraction of cells with visible actin stress fibers). Importantly, associated pharmacologic inhibition experiments revealed that calcium wave propagation is significantly attenuated by

inhibition of myosin light chain kinase activity or actin polymerization but does not require microtubule organization.

In addition to these specialized mechanotransductive mechanisms, glia also exhibit many of the mechanobiological properties that are typical of cell types outside of the CNS. For example, mechanical stress induces rapid reorganization of both the intermediate filament network and the actin cytoskeleton (118, 119). The unique coupling of cytoskeletal elements across the astrocyte syncytium (e.g. organization of stress fibers into parallel bundles spanning multiple cells), however, suggests that transmission of mechanical signals in the brain may act across an unexpectedly long range (120). This is potentially important as a mechanism for the dynamic production and regulation of coordinated responses to CNS injury and disease, as we will explore next.

1.6   CNS mechanobiology in injury and disease

Many CNS diseases are intimately associated with structural changes that would be expected to alter the mechanical properties of the ECM and resident cells. For example, Alzheimer's disease involves the gradual buildup of amyloid plaques and neurofibrillary tangles in the brain (121), a process which may affect both macroscopic and microenvironmental mechanics. Enhanced cell proliferation, de novo secretion of ECM proteins, and increased interstitial pressure within tumors increase the mechanical rigidity of tumor tissues relative to normal brain, as visualized by MRI and ultrasound elastography imaging of CNS malignancies (17, 122-125). It has even been hypothesized that some diseases may actually be *caused* by changes in the brain's mechanical properties; for example, it is thought that loss of tissue tensile strength following infarction can lead to physical obstruction of CSF flow, resulting in normal pressure hydrocephalus (126, 127).

On the cellular level, the innate physiological response to CNS trauma or disease is related to mechanobiological phenomena in a number of interesting ways. For example, one of the hallmarks of astrocyte activation is increased expression of cytoskeletal intermediate filaments, including glial fibrillary associated protein (GFAP), vimentin, and nestin, in addition to upregulation of focal adhesion proteins such as vinculin, talin, and paxillin, and the actin crosslinking protein alpha-actinin, implying that activated astrocytes should express a highly contractile phenotype (118, 119, 128). The increase in tissue volume accompanying astrocyte hypertrophy and hyperplasia increases the stress on surrounding cells, as does secretion of additional ECM proteins such as collagen IV and laminin (129), which subsequently form a scar of collagenous basement membrane that is thought to be one of the major impediments to axonal regeneration (130). This local increase in stress can produce positive feedback to initiate further pathological changes, including enhanced expression of endothelin, a potent vasoconstrictor and astrocytic mitogen that is also associated with astrocyte activation in response to a variety of pathologies (116).

There are few other organ systems in which changes in local stress or tissue volume have the same implications as in the brain, where the maximum tissue volume is resolutely fixed by the encasing skull and local mechanical disturbances can be rapidly transmitted over long distances by the unique architecture of the astrocyte syncytium. As a result, secondary increases in mass

or pressure that accompany many CNS diseases and injuries (e.g. from edema or the mass effects of tumor growth) can often contribute more to morbidity and mortality than the primary insult. The distinction between primary and secondary mechanical effects is especially significant in the case of traumatic brain injury, where direct trauma often imparts large, transient forces to CNS soft tissues, resulting in a complex cascade of secondary mechanical and biochemical responses. Investigations of tissue and cell-scale responses to traumatic CNS injury have broadly sought to understand not only how the transient forces present during the injury are directly transmitted to cells and tissues, but also what acute and long-term host response mechanisms are subsequently activated, and how these mechanisms can be exploited to enhance repair and the return of function (131).

Having reviewed general concepts in CNS mechanobiology, we now turn to a specific CNS pathology for which we and others have recently begun to elucidate the role of mechanobiology: the growth and invasion of the brain tumor glioblastoma multiforme (GBM).

1.7 Mechanobiology of Glioblastoma Multiforme

Primary brain tumors are abnormal masses of tissue that originate in the brain; they can be malignant (cancerous) or benign (non-cancerous, i.e. not recurrent or progressive). Tumors arising from glia or their progenitors are called gliomas and are clinically divided into four grades according to the level of malignancy at diagnosis (132). Grade IV gliomas, also known as glioblastoma multiforme (GBM), represent the most common, aggressive, and neurologically destructive primary brain tumors. As the name would imply, GBM tumors are grossly heterogeneous (both inter- and intratumorally and at all levels, from tissue to cell to molecular and genetic), which may help explain why they are remarkably refractory to therapy. It has been over 80 years since the *Journal of the American Medical Association* (JAMA) published neurosurgeon Walter Dandy's report of what is perhaps the most radical GBM therapy to date: surgical hemispherectomy – literally, removal of an entire hemisphere of brain cortex (133). Yet, Dandy concluded that even this radical procedure is ineffective at preventing rapid recurrence of the tumor, and sadly, an editorial published in JAMA almost 80 years later still cites a brain tumor diagnosis as one of the most feared by patients, physicians, and oncologists alike (134). This fearsome reputation is well-deserved: despite extensive clinical and biological research efforts over the past several decades, there are still few proven risk factors for the development of GBM and little hope for long-term survival (134, 135). Even with the best available surgical care, chemotherapy, and radiation therapy, the average life expectancy at diagnosis is 12-15 months (136).

Clearly, the factors driving GBM progression are tightly woven into a complex network that has not yet been adequately dissected from either a basic science or therapeutic perspective. Tremendous effort has been devoted to elucidating the genetic and biochemical underpinnings of GBM over the last several decades; however, poor translation of candidate therapies from animal models to human patients has only increased the sense of urgency for the development of new approaches in both the laboratory and the clinic. Using words that could as easily have been written by Walter Dandy in 1928, the aforementioned 2005 JAMA editorial ended with a warning: "Advancements for patients with malignant glioma have been negligible, and there is a

real risk of going nowhere by simply continuing to travel the same path." (134) Indeed, the survival time for GBM has increased only incrementally over the past 25 years, with the most substantial recent advance (due to the alkylating agent temozolomide) improving survival by only an additional few months.

One novel path that is addressed in this dissertation is investigation of GBM tumor cell mechanobiology. It has been known for decades that glioma cells retain many of the mechanosensory abilities of their nonmalignant counterparts, including stretch-activated ion channels and the ability to communicate transcellularly via gap junction-mediated calcium signaling (137-140). Increased expression of connexins, the molecular building blocks of gap junctions, is correlated with enhanced calcium signaling between glioma cells and host astrocytes in rat xenograft models, and results in glioma cell invasion through a greater volume of brain parenchyma (141). This implies that functional integration into the astrocytic syncytium, which itself is ideally posed to sense and transmit mechanical and biochemical signals over long distances in the brain, may constitute a significant support system for invasive GBM cells as they migrate away from the tumor mass into the surrounding tissue.

The remarkable capacity of single GBM tumor cells to diffusely infiltrate the surrounding brain parenchyma prior to diagnosis and following treatment is often cited as one of the key factors driving the uncommon aggressiveness of GBM. This infiltration ultimately renders surgical debulking and tumor bed irradiation ineffective, as was powerfully demonstrated by the failure of even Walter Dandy's hemispherectomies to prevent tumor recurrence. A central therapeutic goal in GBM has therefore been to develop new strategies to limit tumor cell invasion, thereby rendering the tumor more susceptible to anatomically-directed therapies. While it is clear that biochemical signaling from the ECM is an important regulator of GBM tumor cell invasion, the biophysical components of this crosstalk have received comparatively little attention to date.

Hints that glioma invasion may be partly regulated by cell and tissue biomechanics have been inconspicuously scattered throughout the academic literature for over half a century. For example, neuropathologist Hans Scherer published extensive observations in 1940 describing the organization of invasive glioma cells into distinctive and predictable patterns that radiate away from the main tumor mass into the surrounding brain parenchyma (142). Importantly, he noted that invasive cells spread preferentially along the surface of anatomical structures in the brain, including the basement membrane of blood vessels, white matter tracts, and the pia mater. These infiltrative patterns are now commonly known as the "secondary structures of Scherer", and their association with biomechanically distinct components of the brain architecture may be especially informative from a mechanobiological perspective.

Importantly, there is evidence that the mechanobiological machinery of glioma cells differs from that of their nonmalignant counterparts, a crucial prerequisite for the development of mechanobiologically-inspired therapeutics. For example, glioma cells exhibit reduced expression of cadherins (calcium-dependent transmembrane glycoproteins that facilitate cell-cell adhesion), enhanced expression of matrix metalloproteinases, increased expression of focal adhesion proteins such as focal adhesion kinase (FAK), and altered expression of integrins compared to normal astrocytes (4, 143-147). These differences are potentially significant from the standpoints of both basic pathophysiology and therapeutics. For example, integrin-mediated

11

adhesion of tumor cells to ECM proteins has been associated with greater resistance to ionizing radiation and chemotherapies, a phenomenon known as cell adhesion-mediated radioresistance/drug resistance (CAM-RR/CAM-DR) (148).   Recent studies have linked $\beta1$ integrin signaling in particular with inhibition of drug-induced apoptosis (149) and promotion of radioresistance (150). Enhanced expression of integrins $\alpha2$, $\alpha3$, $\alpha5$, and $\beta1$ in drug-resistant glioma cells has been correlated with enhanced adhesivity to ECM proteins such as fibronectin and collagen as well (151); these proteins are more commonly found in tumor tissue and basement membrane than normal brain parenchyma, suggesting that CAM-DR may also promote tumor progression and invasiveness. Surprisingly, a recent study showed that pharmacologic inhibition of fibronectin assembly in the ECM can enhance sensitivity of GBM cells to nitrosourea chemotherapy in vitro and in vivo (152); however, the dynamics of this relationship and the mechanisms driving ECM-derived chemosensitivity are not yet understood. Nevertheless, promising new chemotherapeutics are already beginning to target components of the contractility and adhesion machinery, including the potent integrin antagonists Cilengitide and SJ749 (153, 154), radioiodinated antibodies directed against tumor-secreted ECM proteins (155, 156), drugs that inhibit Rho GTPase-based signaling (157), and small-molecule inhibitors of FAK and other focal adhesion proteins (158).

Contractility-mediating pathways are also intimately related to cell migration and invasion, which depend on actomyosin-generated contractile forces and involve a variety of dynamic and spatially-regulated changes to both the cytoskeleton and the adhesion complexes that mediate interactions with the surrounding ECM. In an important study that has general implications for cell migration through 3D ECMs, Rosenfeld and colleagues recently demonstrated that NMMII is needed to deform the nucleus of glioma cells to enable amoeboid motion through ECM pores, and invading tumor cells in vivo significantly upregulate NMMII expression relative to endogenous brain cells (159). Other recent work has shown that pharmacologic inhibition of myosin light chain kinase results in dramatic inhibition of glioma cell motility (160) and that ROCK-dependent mechanisms are important in GBM cell migration and therapeutic sensitivity (161-168). Rho/ROCK signaling is thought to be especially important in regulating cell survival and tumorigenesis as well; for example, the ROCK inhibitor Y-27632 and transfection with dominant negative RhoA and ROCK were each found to induce apoptosis *in vitro* and resulted in significantly smaller tumor mass following tumor inoculation *in vivo* (169).

In summary, while GBM tumor cells have been extensively studied from both genetic and biochemical perspectives over the course of many decades, advances in the laboratory have not translated into needed benefits in life expectancy in the clinic, leaving physicians and patients in desperate need of new perspectives and new approaches. As described above, a growing body of literature has begun to consider the role of matrix biology and cellular contractility in glioma cell pathophysiology, providing tantalizing hints that a mechanobiological approach may be able to provide a valuable new set of perspectives and therapeutic handles to address this problem.

1.8   Open questions and scope of thesis

The last several decades have seen an emerging appreciation for the complex and unexpected ways in which mechanobiology can regulate the CNS in health and disease. This introductory

chapter has reviewed this growing field, starting with the structure and mechanical microenvironment of the brain and spinal cord, continuing with the mechanobiological characteristics of cells in the CNS, and concluding with the importance of mechanobiology to the progression of specific CNS disease states including glioblastoma multiforme brain tumors. Despite remarkable progress, many key challenges remain. In particular, it will be critical to determine how mechanobiological signaling in the CNS fits into the context of traditionally-understood genetic and biochemical control of neurobiology; cells in vivo are simultaneously subjected to space- and time-dependent mechanical and soluble/matrix-bound biochemical signals, and their response to this constellation of inputs undoubtedly depends on cell-intrinsic factors (e.g., regulation of gene expression) that may dramatically change from one cell to another in the same microenvironment. Understanding which signals dominate cell behavior in specific physiological settings will be key to dissecting the relative contributions of these cues to normal function and pathophysiology in the CNS. Related to this, it will be essential to extend the many elegant tools that have been developed for studying the mechanics and mechanobiology of single cells in culture to living tissues and organisms. As discussed earlier, noninvasive imaging methodologies that derive contrast from variations in tissue mechanics, such as ultrasound and magnetic resonance elastography, hold great promise along these lines. One would also expect that increased use of mechanosensitive optical probes and fluorescently-labeled mechanosensory proteins in animal models may also enable in vivo visualization of CNS mechanotransduction. We anticipate that careful attention to these and other challenges will bring us closer to a day when both the CNS mechanical microenvironment and cellular mechanotransductory signaling systems can be exploited to regenerate nerve tissue, attack complex neuropathologies, and combat invasive brain tumors.

The emerging field of glioma mechanobiology has specifically begun to infuse an appreciation for mechanics into our overall understanding of GBM pathophysiology over the last several years. The goal of the work presented in the following chapters of this dissertation has been the application, adaptation, and development of technologies in bioengineering and biomaterials to establish and then further our understanding of glioma cell mechanobiology. In Chapter 2, we use a previously established polyacrylamide gel culture system to demonstrate that clinically-relevant glioma cell behaviors, including motility and proliferation, can be directly regulated by microenvironmental stiffness in 2-dimensional (2D) culture. Importantly, we show that these responses can be directly modulated with pharmacologic inhibitors of actomyosin contractility. In Chapters 3 and 4, we develop, characterize, and utilize a composite collagen-agarose biomaterial system to study GBM mechanobiology in 3-dimensional (3D) culture, revealing intriguing differences between the mechanoresponsive behaviors of glioma cells in 2D and 3D culture that derive from equally intriguing and instructive disparities between local (cell-scale) and bulk mechanics in 3D fibrillar culture systems. Finally, Chapter 5 concludes this dissertation with a summary of the results and significance of the work presented in the preceding chapters, plus a brief summary of several ongoing projects that have directly grown out of the studies in Chapters 2-4. Collectively, these promising and surprising early results suggest that further exploration of the mechanobiological aspects of GBM tumor cells may constitute a new and valuable path toward the identification of novel therapeutic targets, and that these paradigms and approaches might be productively extended to other pathologies.

Chapter 2. The mechanical rigidity of the extracellular matrix regulates the structure, motility, and proliferation of glioma cells in 2-dimensional culture

2.1   Abstract

Glioblastoma multiforme (GBM) is a high-grade malignant astrocytoma of the central nervous system associated with a mean survival time of approximately one year, even with aggressive surgical care, chemotherapy, and radiotherapy. This rapid progression is due in part to the diffuse infiltration of single tumor cells into the normal brain parenchyma, which is thought to involve aberrant interactions between tumor cells and the extracellular matrix (ECM).   Here we test the hypothesis that mechanical cues from the ECM contribute to key tumor cell properties relevant to invasion. We cultured a series of glioma cell lines (U-373 MG, U-87 MG, U-251 MG, SNB19, C6) on fibronectin-coated polymeric ECM substrates of defined mechanical rigidity and investigated the role of ECM rigidity in regulating tumor cell structure, adhesion, migration, and proliferation.   On highly rigid ECMs, tumor cells spread extensively, form prominent actomyosin stress fibers and mature focal adhesions, and migrate rapidly. As ECM rigidity is lowered to values comparable to normal brain tissue, tumor cells appear rounded and fail to productively migrate. Remarkably, cell proliferation is also strongly regulated by ECM rigidity, with cells dividing much more rapidly on rigid ECMs than on compliant ECMs.   Direct or indirect pharmacological inhibition of nonmuscle myosin II-based contractility significantly blunts this rigidity-sensitivity and rescues cell motility on highly compliant substrates. Collectively, our results provide support for a novel model in which ECM rigidity provides a transformative, microenvironmental cue that acts through actomyosin contractility to regulate the invasive properties of GBM tumor cells.

2.2   Introduction

Glioblastoma multiforme (GBM) is a high-grade malignant astrocytoma of the central nervous system associated with a median survival time of 15 months, even with aggressive surgical care, chemotherapy, and radiotherapy (136).   This uncommon aggressiveness is derived in part from the marked capacity of single tumor cells to diffusely infiltrate the surrounding brain parenchyma prior to diagnosis, making complete debulking of the tumor virtually impossible.   A central therapeutic goal in GBM has been to develop new strategies to limit tumor cell invasion, thereby rendering the tumor addressable by local therapies. This in turn has led to an expansive effort to identify key molecular regulators of GBM tumor cell motility *in vitro* and *in vivo* (159, 162, 167, 170, 171).

Among the key regulators of cell motility are the extracellular matrix (ECM) and the cellular components needed to recognize and process ECM-derived cues, including adhesion proteins and molecular motors. The importance of ECM proteins such as fibronectin, laminin, and collagen in stimulating a migratory phenotype has been demonstrated in a number of *in vitro* studies using both established GBM cell lines and biopsy explants (172). Strong correlations between matrix metalloproteinase (MMP) activation, GBM invasion, and poor prognosis indicate that tumor cells are able to extensively remodel the surrounding matrix during invasion (3). This remodeling is frequently accompanied by *de novo* secretion of ECM proteins such as tenascin-C, which has been associated with angiogenesis and enhanced cell motility (173, 174). Because these behaviors are central to tumor progression, a growing body of work is now beginning to address the functional contributions of key mediators of cell-ECM interactions, including

integrins (153, 175, 176), focal adhesion proteins such as vinculin and focal adhesion kinase (FAK) (158, 177, 178), and molecular motors such as nonmuscle myosin II (NMMII) (159). These studies have begun to elucidate the crucial and complex role that cytoskeletal proteins play in regulating GBM tumor cell migration and invasion. These interactions have taken on new significance in light of the recent Cancer Genome Atlas (TCGA) sequencing effort, which has revealed a preponderance of genomic lesions across GBM tumors in the EGFR/Ras/PI3K pathway (179), which has been previously linked at multiple levels to ECM-based signaling in the context of glioma invasion (180, 181).

However, while it is clear that biochemical signaling from the ECM is an important regulator of GBM tumor cell invasion, the biophysical components of this crosstalk are comparatively poorly understood. Improving this understanding is important given the recent explosion of work demonstrating the powerful influence of biophysical inputs such as the density, rigidity, and geometry of the ECM on cell fate, migration, and pathogenesis, even in the presence of seemingly contradictory biochemical cues (182-184). For example, recent studies have shown that manipulating substrate elasticity or cell geometry in a 2D cell culture system can strongly influence lineage specification of naïve human mesenchymal stem cells (39, 41, 185), the random-walk migration velocity, cell spreading area, and cytoskeletal architecture of smooth muscle cells (37), and the outgrowth of neurons versus glial cells in mixed cortical cultures (49).

A growing body of literature indicates that the biomechanical properties of cells, subcellular structures, and the surrounding ECM directly influence and are influenced by the onset and progression of neoplastic disease (1, 186, 187). For example, a change in substrate elasticity of less than one order of magnitude during 3D *in vitro* culture of mammary epithelial cells is enough to cause otherwise normal cells to begin developing physiological and morphological characteristics of a developing tumor (188). With respect to invasion, ECM rigidity can also powerfully regulate both the motility and speed of human prostate carcinoma cells through 3D ECMs (189) and the density and activity of podosomes, which spatially focus proteolytic secretion. Recent work specifically suggests that podosomes act as dynamic mechanosensors (190) and that the number and activity of tumor cell invadopodia are correlated with ECM stiffness (191). Promising new chemotherapeutics are already beginning to target components of the contractility and adhesion machinery, including the potent integrin antagonist Cilengitide (153) and small-molecule inhibitors of focal adhesion proteins such as FAK (158).

Several lines of evidence indirectly suggest that ECM-derived biomechanical cues may play an important role in GBM specifically. Neurosurgeons anecdotally report that GBM tumor tissue is typically substantially stiffer than the surrounding parenchyma, an observation which is supported by the efficacy of ultrasound elastography for guiding surgical resection (122-125). Moreover, there is tremendous anatomic variation in mechanical stiffness within the adult brain (11), and these conspicuous rigidity differentials may also feature prominently in invasion. For example, the infiltrative path of GBM cells tends to favor interfaces between mechanically distinct anatomical structures in the brain, such as the basement membrane of blood vessels and white matter tracts (146). Although ECM stiffness is known to be a transformative factor in breast tumors, the pathophysiological significance of the mechanical difference between normal and malignant tissue in the brain remains very poorly understood.

Recent work has provided clues that the mechanical properties of the cellular microenvironment may fundamentally alter the migration of human glioblastoma cells *in vitro* as well as *in vivo* (159, 192-194). For example, Thomas and DiMilla reported that the migration rate of human SNB19 glioblastoma cells cultured on elastomeric films change as a function of substrate mechanical properties (controlled by altering the duration of heating and distance from a Bunsen burner) (192), and several 3D studies have shown a strong correlation between matrix density and invasion from tumor spheroids (194, 195). Cell migration and invasion depend on actomyosin-generated contractile forces and involve a variety of dynamic and spatially-regulated changes to both the cytoskeleton and the adhesion complexes that mediate interactions with the surrounding ECM. Many of these motility-mediating interactions are shaped by the mechanics of the extracellular milieu, and the expression levels of several contractility-mediating signaling molecules, including RhoA and RhoB, are known to correlate with tumor malignancy (196). Indeed, Rosenfeld and colleagues recently demonstrated that nonmuscle myosin II (NMMII) is needed to deform the nucleus of glioma cells to enable amoeboid motion through ECM pores, and invading tumor cells *in vivo* significantly upregulate NMMII expression relative to endogenous brain cells (159).

Motivated by the growing evidence that mechanobiological cues are present in human gliomas, by the limited amount of information that exists regarding the role of ECM elasticity in glioma pathogenesis, and by the significant implications that this knowledge could have toward the development of mechanobiologically-inspired therapeutics, we sought to test the hypothesis that micromechanical cues from the ECM could influence fundamental properties of GBM tumor cells relevant to tumor growth and invasion. Our approach is based on fabrication of ECM substrates with independently-defined mechanical and biochemical properties, which enables us to create cellular microenvironments whose rigidities span the range between normal and tumor tissue. Our studies reveal for the first time that ECM elasticity strongly affects GBM cell structure, motility, and proliferation, and that this mechanosensing requires a competent actin cytoskeleton, Rho GTPase, and NMMII.

2.3   Materials and Methods

2.3.1   Synthesis of ECM substrates

We followed a previously-established method for fabricating defined-rigidity polyacrylamide ECM substrates (34, 37), with minor modifications. Solutions of acrylamide and N-N'-methylene-bis-acrylamide (Bio-Rad, Hercules, CA) were combined in various percentages (acrylamide: 3-15%, bis-acrylamide: 0.02-1.2%) with ultra pure water (Gibco BRL, Grand Island, NY), perfused with nitrogen gas for 30 minutes, placed under vacuum for at least an hour, and then transferred to a sterile environment. Free radical initiators ammonium persulfate (10% solution, 1/200 v/v, Bio-Rad) and TEMED (1/2000, Sigma-Aldrich, St. Louis, MO) were added to solution immediately prior to syringe filtering (0.22 μm filter). Droplets of sterile solution were sandwiched between a glutaraldehyde-activated glass coverslip and a hydrophobic glass coverslip (Superhydrophobic Solution, OMS Optochemicals, Pointe Claire, Quebec, Canada). Following polymerization, the substrates were immersed in 50 mM HEPES buffer (Gibco) and the top coverslip was detached with a pair of sterile forceps. All substrates were activated with

the heterobifunctional crosslinker Sulfo-SANPAH (0.5 mg/ml, Pierce Chemical Co., Rockford, IL) in two 8 min. UV exposures, functionalized with 10-16 µg/ml human plasma fibronectin (Millipore Corp., Temecula, CA) in HEPES at 4°C overnight in order to achieve a nominal surface density of 2.6 µg/cm^2, washed with PBS, and soaked in complete culture medium at 37°C and 5% CO_2 for at least 30 minutes prior to cell seeding.

2.3.2 Characterization of mechanical properties

The macroscopic elastic shear modulus of each gel formulation was measured at 37°C using an Anton Paar Physica MCR 301 rheometer with a 25-mm parallel plate geometry. Amplitude sweeps over the range γ=0.1-10% were used to identify the linear regime; frequency sweeps at 5% strain over the range 0.1-10 Hz were then used to extract the storage modulus, loss modulus, and complex modulus of each sample. Three measurements were made on each sample, and at least three independent samples were measured per condition. Elastic moduli of 0.08 kPa, 0.25 kPa, 0.8 kPa, 19 kPa, and 119 kPa were measured for gels containing final acrylamide/bis-acrylamide (A/B) percentages of 3%A/0.05%B, 4%A/0.075%B, 5%A/0.1%B, 8%A/0.6%B, and 15%A/1.2%B, respectively, as described in detail elsewhere[*].

2.3.3. Cell culture

U-373 MG human glioma cells were obtained from the Tissue Culture Facility at the University of California, Berkeley, U-87 MG and U-251 MG human glioma cells were kindly provided by Dr. C. David James (University of California, San Francisco), and human SNB19 and rat C6 glioma cells were kindly provided by Dr. Andrew Wurmser (University of California, Berkeley). U-373 MG and U-87 MG cells were cultured in Dulbecco's Modified Eagle's medium (DMEM, Gibco) supplemented with 10% Calf Serum Advantage (J.R. Scientific, Woodland, CA) and 1% penicillin/streptomycin, MEM nonessential amino acids, and sodium pyruvate (Gibco). SNB19, U-251 MG, and C6 cells were cultured in DMEM supplemented with 10% calf serum and 1% penicillin/streptomycin.

2.3.4 Fluorescence staining of F-actin and vinculin-positive focal adhesions

Cells were washed once with 1x PBS, pH 7.4 (Fisher Scientific, Pittsburgh, PA), prior to fixation with 4% paraformaldehyde (Fisher Scientific) in PBS for 10-12 minutes. A staining buffer of 1% goat serum (Gibco) and 0.05% sodium azide (Sigma-Aldrich) in PBS was used for all subsequent washing steps and dilutions. Cells were permeabilized with 0.1% Triton-X 100 (EMD Biosciences, San Diego, CA) for 10 minutes at room temperature prior to blocking with 5% goat serum in PBS. Cells were subsequently stained for focal adhesions with mouse monoclonal anti-vinculin IgG (Sigma-Aldrich; diluted 1:200) and Alexa Fluor 546-labeled goat anti-mouse IgG (H+L) antibody (Invitrogen, Carlsbad, CA; diluted 1:250).   F-actin was stained with Alexa Fluor 488 phalloidin (Invitrogen; diluted 1:200), and the nucleus was stained with 4′,6-diamino-2-phenylindole (DAPI) (Invitrogen; diluted 1:200).

---

[*] A. J. Keung, E. M. de Juan Pardo, D. V. Schaffer, and S. Kumar (2011). Rho GTPases Mediate the Mechanosensitive Lineage Commitment of Neural Stem Cells (manuscript in preparation).

2.3.5 Microscopy and morphometric analysis

All live-cell and fluorescence imaging was performed using an inverted Nikon TE2000-E2 microscope equipped with a motorized, programmable stage (Prior Scientific, Inc, Rockland, MA), an incubator chamber to maintain constant temperature, humidity, and CO_2 levels (In Vivo Scientific, St. Louis, MO), a digital camera (Photometrics Coolsnap HQ II, Roper Scientific, Tucson, AZ), and SimplePCI software (Hamamatsu Corporation, Sewickley, PA). Measurements of cell spreading area were obtained by quantifying the area of phalloidin-stained cells using Image J software (National Institutes of Health, Bethesda, MD). High-magnification epifluorescence images acquired through polyacrylamide gels in Figs. 2 and 5 were enhanced by applying a uniform background subtraction to the entire image; subsequent adjustments to brightness and contrast were applied as necessary.

2.3.6 Measurement and analysis of cell migration

Cells were plated on fibronectin-conjugated substrates at a subconfluent density of 1×10^3 cells/cm^2 at least 10 hours prior to the start of imaging in at least three independent experiments. In each experiment, 10x phase contrast time-lapse images were acquired every 15 minutes over a 12 hour period for at least 10 representative fields of view per substrate and at least 2 substrates per condition. A representative subset of these time-lapse videos was analyzed using the SimplePCI software package, where the periphery of each cell in each frame was used to define an object, and the Motion Tracking and Analysis module of the SimplePCI software was used to track the centroid of each object throughout the time sequence.

2.3.7 Measurement of cell proliferation

Cells were seeded on fibronectin-conjugated substrates at a subconfluent density of 7000 cells/cm^2. 50 µM 5-bromodeoxyuridine (BrdU, Sigma-Aldrich) was added to the cell culture medium 48 hours after plating and 90 minutes prior to fixation with 4% paraformaldehyde (Fisher Scientific). Cells were permeabilized with 0.1% TritonX-100 (EMD Biosciences), treated with 4 N HCl for 30 minutes, and blocked with 5% goat serum (Gibco) prior to staining with mouse monoclonal anti-BrdU antibody (Sigma-Aldrich), Alexa Fluor 546-labeled goat anti-mouse IgG (H+L) antibody (Invitrogen), and DAPI (Invitrogen).

2.3.8 Inhibition of cellular contractility with Y-27632, Blebbistatin, and Cytochalasin D

Rho-associated kinase (ROCK) inhibitor Y-27632 (Calbiochem, La Jolla, CA), NMMII inhibitor blebbistatin (Sigma-Aldrich), and actin polymerization inhibitor cytochalasin D (Sigma-Aldrich) were added to the cell culture media in relevant timelapse and immunofluorescence experiments at concentrations of 10 or 50 µM, 25 µM, and 1 µM, respectively, after the cells had been given at least 10 hours to adhere. In some migration assays, stage positions were programmed into the microscope software and an initial set or time sequence of images was captured prior to addition of the drugs so that changes in morphology and migration could be observed dynamically.

2.3.9   Statistical Analysis

Data are reported as mean ± standard error unless otherwise noted. Statistical comparisons between three or more sets of data were performed with a one-way analysis of variance (ANOVA) followed by a Tukey-Kramer HSD (honestly significant difference) test for pair-wise comparisons. A student's unpaired t-test was performed if statistical comparisons were made between two sets of data. p-values less than 0.01 denote statistical significance.

2.4   Results

To test the hypothesis that ECM rigidity influences the behavior of cultured glioma cells, we fabricated a series of fibronectin-coated polyacrylamide ECM substrates as we and others have done in the past (34, 37, 61, 197). In this system, ECM stiffness is dictated by the ratio of monomer (acrylamide) to crosslinker (bisacrylamide), and the fibronectin is covalently grafted at a fixed density to the polyacrylamide surface, thus enabling independent control of ECM stiffness and ligand density. Moreover, these polyacrylamide substrates do not support appreciable passive protein adsorption following fibronectin conjugation (198), which permits us to probe effects of ECM rigidity independent of contributions from cell- or serum-derived ECM components. Using this approach, we were able to create a series of ECM platforms whose mechanical compliances range from one order of magnitude below that of normal brain tissue (0.08 kPa) to three orders of magnitude above (119 kPa), as verified by parallel-plate rheometry (see methods).

2.4.1   ECM rigidity alters the morphology and cytoskeletal organization of glioma cells.

We began by asking whether changes in ECM rigidity were sufficient to grossly and systematically alter glioma cell morphology and cytoskeletal organization. To answer this, we cultured glioma cells on fibronectin-coated ECMs of varying rigidity and captured both cell-ECM adhesion area and the organization of cytoskeletal F-actin. The projected cell area of U-373 MG human glioma cells decreased dramatically with decreasing substrate stiffness (Fig. 2.1), a finding that was qualitatively reproducible for several other glioma lines, including U-87 MG, U-251 MG, SNB19, and C6 cells (Fig. 2.2). In all cases, cells cultured on rigid fibronectin-conjugated substrates were typically well-spread with visible actin stress fibers and discrete, elongated vinculin-positive focal adhesions (Fig. 2.1B and C). Importantly, cells cultured on the stiffest substrates formed stress fibers and focal adhesions that were similar to those found in cells cultured on fibronectin-coated glass, suggesting that the conjugation chemistry does not significantly interfere with adhesion-based cytoskeletal assembly. Cells cultured on progressively softer substrates showed a decrease in spreading area, along with a rigidity-dependent dissipation of stress fibers and focal adhesions. Cells on the softest substrates exhibited a uniformly rounded morphology, with cortical rings of F-actin and small and rounded vinculin-positive focal complexes. Interestingly, cell rounding on the softest substrates did not correspond to induction of apoptosis, as evidenced by positive staining for the nuclear antigen Ki67, a marker of passage through the cell cycle (Fig. 2.1A).
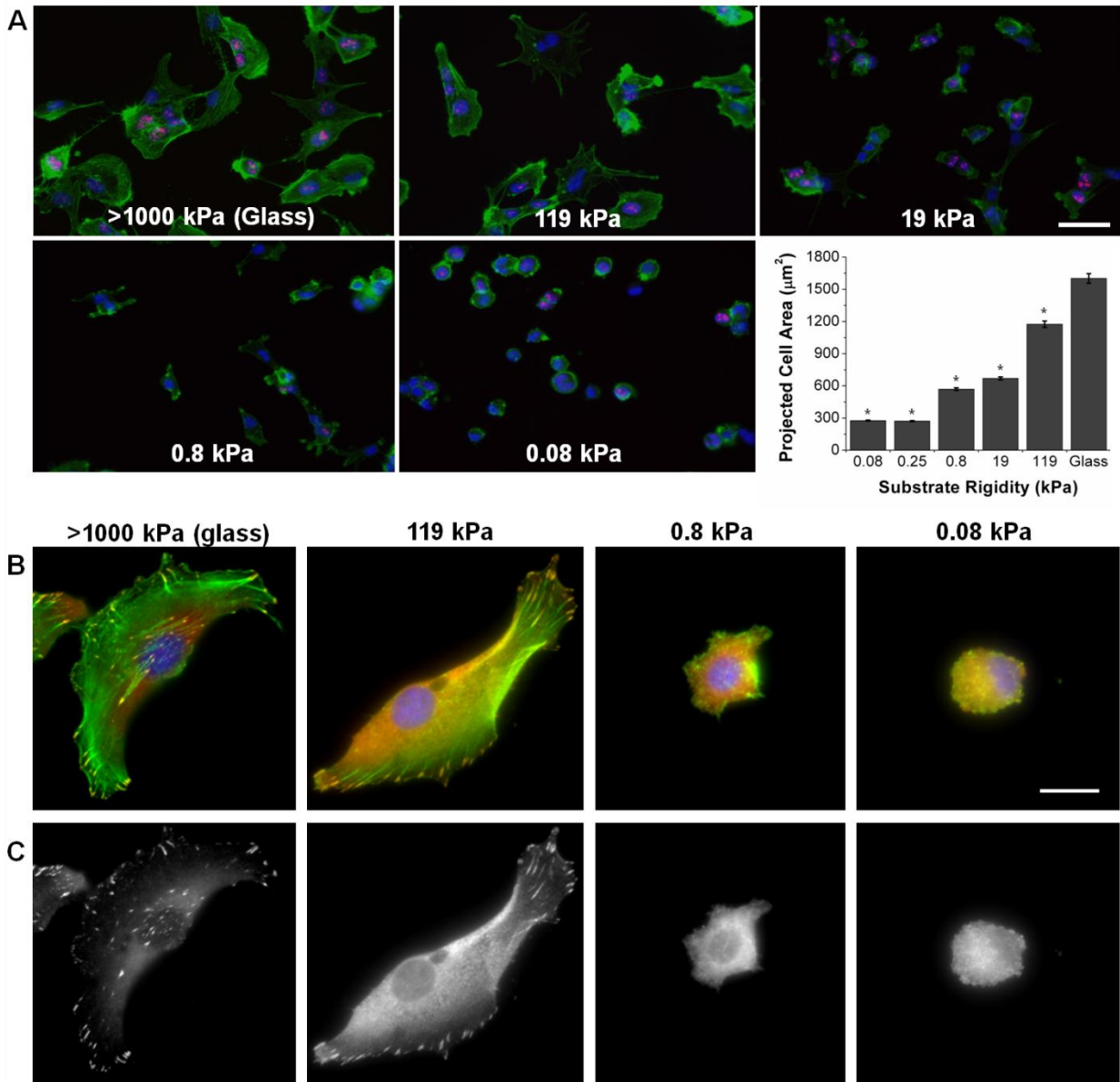
Figure 2.1: **ECM rigidity alters glioma cell morphology and cytoskeletal organization.** (A) Rigidity-dependent changes in cell structure. U373-MG cells cultured on fibronectin-conjugated glass and polyacrylamide gels over a range of stiffnesses were stained for F-actin (green), nuclear DNA (blue) and the nuclear antigen Ki67 (red). Note that a subset of cells on all substrates stained positive for Ki67. Bar is 50 μm. (*p < 0.01 with respect to glass; n > 450 cells for each condition) (B) High-magnification imaging of cytoskeletal and adhesive structures. U87-MG cells were stained for F-actin (green), nuclear DNA (blue), and the focal adhesion protein vinculin (red). Bar is 25 μm. (C) Isolated view of vinculin signal only, showing structure and distributions of cell-ECM adhesions.

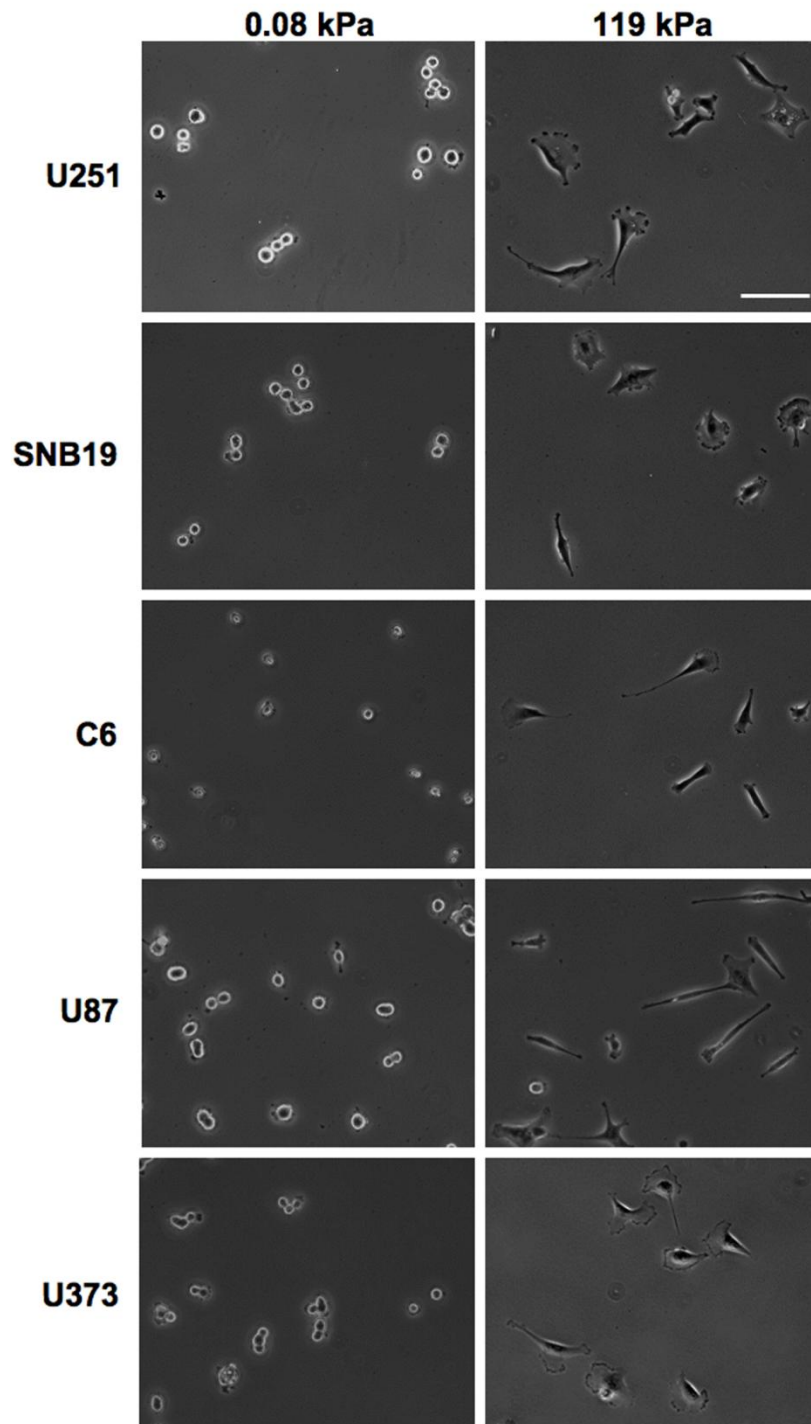**Figure 2.2: Generality of ECM rigidity-dependent changes in glioma cell morphology across multiple cell lines.** U251-MG, SNB19, C6, U87-MG, and U373-MG glioma cells were cultured on 0.08 kPa and 119 kPa fibronectin-coated ECMs as described in Methods and Fig. 2.1. In all cases, cells spread on 119 kPa ECMs and adopt a mutually indistinguishable rounded morphology on 0.08 kPa ECMs. Bar is 100 μm.

2.4.2 ECM rigidity regulates the random motility of glioma cells.

Given that productive cell motility is critical to glioma cell invasion *in vivo*, we next asked whether changes in ECM rigidity could alter migration speed in culture (Fig. 2.3). To address this question, we used time-lapse phase contrast imaging to record the random motility of sparsely-cultured U-373 MG and U-87 MG cells over 12 hours. Mean migration speeds fell dramatically with decreasing substrate rigidity for both U-373 MG and U-87 MG cells, with speeds observed on the most rigid substrates comparable to (or statistically indistinguishable from) those observed on glass (Fig. 2.3A and B; Supplementary Movies 1-4 in (199)). Locomotion was severely limited in all cells plated on the softest substrates (0.08 kPa). For all stiffnesses, cells growing on the surface of the glass coverslips adjacent to polyacrylamide substrates exhibited similar morphology and moved in a qualitatively similar fashion to cells on fibronectin-coated glass substrates (not shown), effectively ruling out the possibility that these rigidity-dependent changes in motility might be due to altered paracrine signaling in the culture.

Concurrent with these reductions in cell speed, we observed a gradual transition in the mode of cell motility (Fig. 2.3C; Supplementary Movies 5-8 in (199)). Cells on glass and the stiffest substrates moved in a smooth, gliding fashion with broad lamellipodia and continuous actin turnover at the leading edge of the cell. On intermediate stiffness ECMs, lamellipodia were much smaller, less well-defined, and less stable, with locomotion following a "stick-slip" pattern in which cells would thin and extend as the leading edge advanced, with the trailing edge of the cell then abruptly detaching and snapping forward to catch up to the cell body. On the most compliant substrates, productive locomotion was abrogated, with cells actively extending small, thin filopodial processes over periods of 6-12 hours but failing to establish stable lamellipodia capable of supporting migration.

Interestingly, while the migration of all cell lines was highly sensitive to ECM rigidity, we observed significant variation between cell lines. Specifically, we observed that on the most rigid substrates, U-373 MG, SNB19, and U-251 MG cells tended to exhibit prominent broad, ruffled lamellipodia and a polygonal morphology, whereas the U-87 MG and C6 cells comparatively lacked prominent lamellipodia and typically exhibited a more elongated spindle morphology (Fig 2.2), as reported by others (200-202). However, all cell lines reduced to a mutually indistinguishable rounded morphology with largely non-productive filopodial extension when cultured on the most compliant substrates (0.08 kPa).

2.4.3 ECM rigidity regulates the proliferation rate of glioma cells.

The above results demonstrate that ECM rigidity can substantially regulate the morphology, cytoskeletal organization, and motility of cultured glioma cells. Given that alterations in shape and motility have been previously correlated with alterations in tumor growth (203), we reasoned that ECM rigidity might concurrently alter cell proliferation. Our first clue that this might be the case came from our observation that in long-term cultures of all five glioma cell lines, cells on stiff substrates bore a propensity to reach confluency and overgrow their substrates more rapidly than cells on soft substrates and at a level that could not be solely attributed to differences in cell spreading area (not shown). To test this connection more rigorously, we used BrdU incorporation to measure percentages of dividing cells as a function of ECM rigidity (Fig. 2.4).
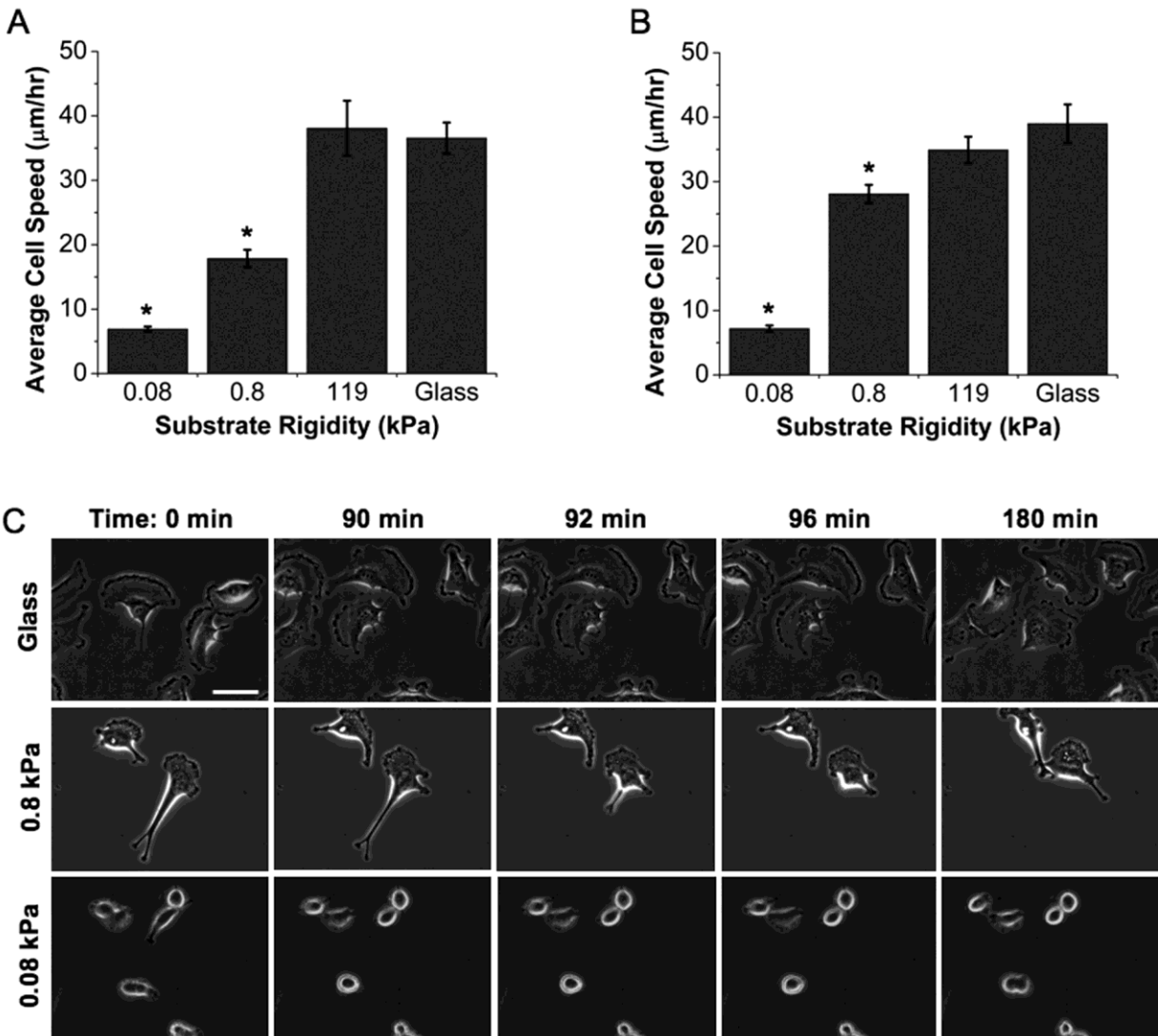
Figure 2.3: ECM rigidity regulates glioma cell motility. Effect of ECM rigidity on the random migration speed of (A) U373-MG and (B) U87-MG cells. Results represent the average migration rate from at least 15 cells per condition over 6-12 hours. Qualitatively similar dependences of migration speed on substrate stiffness were observed for SNB19, U251-MG, and C6 cells. (*p < 0.01 with respect to glass) (C) High-magnification imaging of U373-MG cell migration on ECMs of varying rigidity over both long time scales (columns 1-2 and 4-5) and short time scales (columns 2-4). Cells on glass (top row) migrate quickly, smoothly, and with broad, stable lamellipodia. Cells on 0.8 kPa ECMs (middle row) form smaller, less stable lamellipodia, and migrate in a "stick-slip" fashion, in which the cell thins and extends as it advances and then abruptly contracts as adhesions at the trailing edge rupture. Cells on 0.08 kPa ECMs (bottom row) continuously extend thin filopodia and fail to productively migrate. Bar is 50 μm.

These studies revealed a remarkable correlation between the proliferation rate of U-373 MG and U-87 MG cells and ECM stiffness, with an approximately 5-fold increase in the percentage of BrdU-positive cells on the stiffest substrates (119 kPa) compared to those on the softest substrates (0.08 kPa). Consistent with our previous measurements of cell structure and motility,

BrdU incorporation on the stiffest ECM substrates was comparable to that on fibronectin-coated glass, further suggesting that ECM rigidity, rather than the details of ECM protein conjugation, is the key underlying governing parameter.
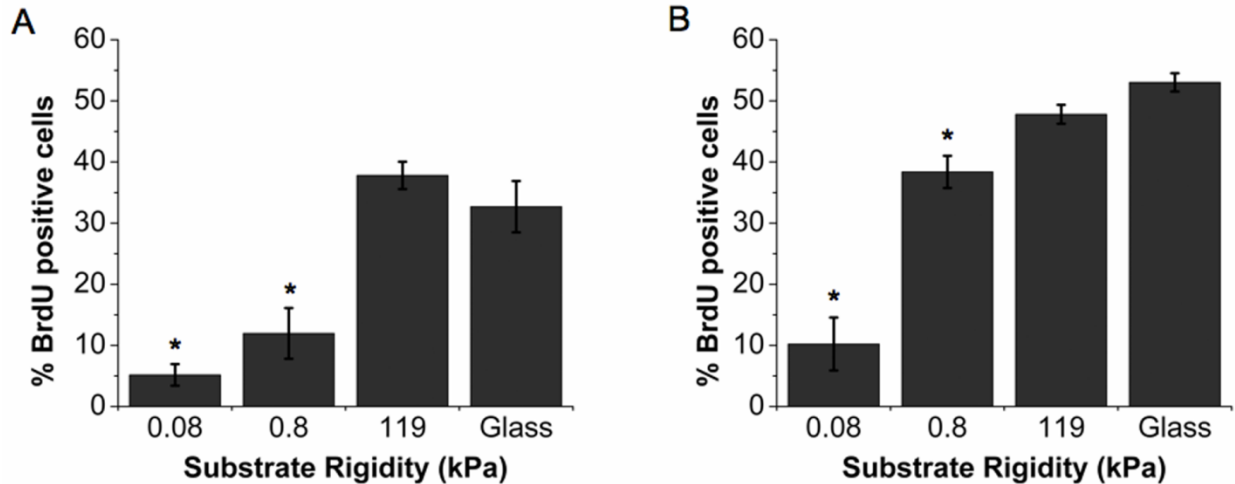

Figure 2.4: **ECM rigidity regulates glioma cell proliferation.** Effect of ECM rigidity on proliferation of (A) U373-MG and (B) U87-MG cells. Results represent quantification of $n > 325$ cells in at least 8 fields of view per substrate for at least five substrates per condition, where the percentage of dividing cells was determined as the average percentage of cells staining positive for BrdU incorporation. (*$p < 0.01$ with respect to glass).

2.4.4 Pharmacologic disruption of intracellular tension tempers mechanical regulation of glioma cell morphology, cytoskeletal architecture, and migration.

Increasing ECM stiffness is associated with increased cell spreading and formation of actomyosin stress fiber bundles (Fig. 2.1), suggesting that ECM rigidity controls NMMII-mediated intracellular contractility. This relationship has been directly observed in other systems (33, 39) and has led to the hypothesis that NMMII and its upstream regulators are critical to processing ECM rigidity-encoded cues. To test this hypothesis in our system, we asked whether glioma cells remained sensitive to ECM rigidity when actin cytoskeletal assembly and contractility are disrupted. Direct pharmacological inhibition of NMMII with blebbistatin or ROCK with Y-27632 blunted sensitivity of cell morphology to ECM rigidity, with cells exhibiting a stellate morphology across all ECM rigidities (Fig 2.5A; Supplementary Movies 9-12 in (199)). Remarkably, inhibition of either NMMII or ROCK on the softest ECMs not only enhanced adhesion but rescued cell motility, with cells spreading and resuming migration within minutes of drug addition (Fig. 2.5B). For all ECMs, ROCK- and NMMII-inhibited cells lacked prominent stress fibers and vinculin-positive focal adhesions (Fig. 2.6). To confirm that this rescue of cell motility requires competent actin polymerization, we treated cells with cytochalasin D, which disrupts F-actin and inhibits new polymerization. Indeed, treatment with cytochalasin D caused cytoskeletal collapse and loss of motility on stiff substrates but failed to induce spreading or rescue migration on the softest substrates (Figs. 2.5, 2.6).
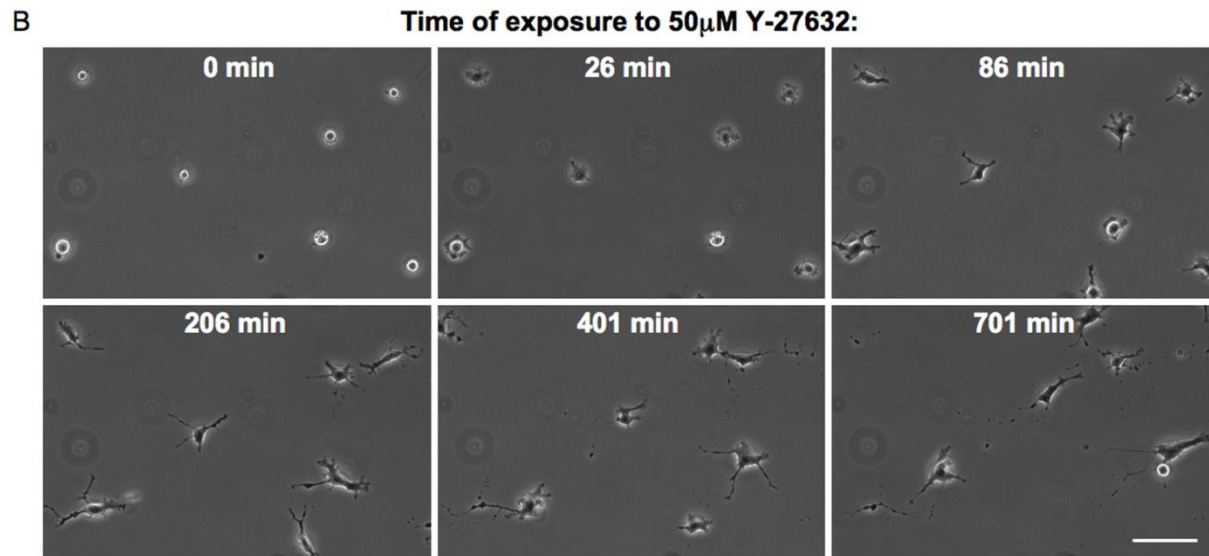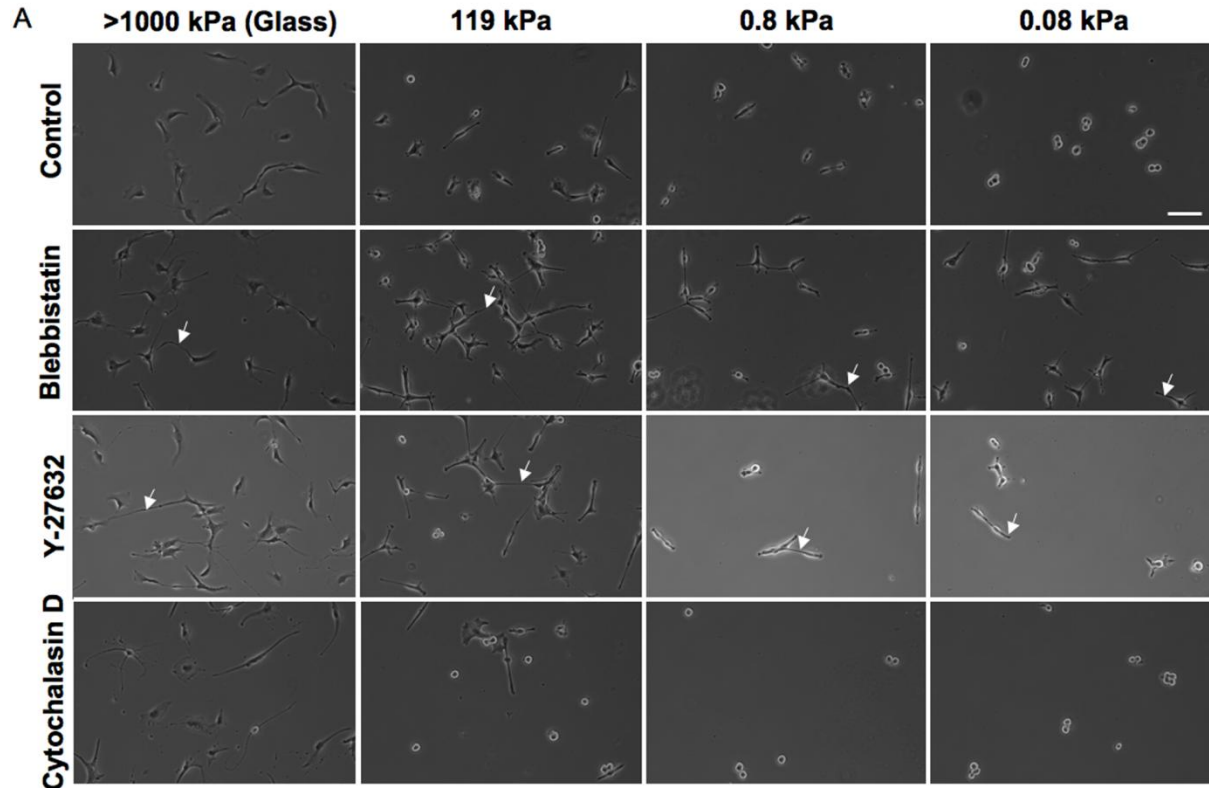
Figure 2.5: **Pharmacologic inhibition of cytoskeletal contractility reduces stiffness-dependent differences in cell morphology.** (A) U87-MG cells cultured on fibronectin-conjugated glass and polyacrylamide substrates in either the absence of drug (control) or 24 hours after addition of 25 μM blebbistatin, 10 μM Y-27632, or 1 μM cytochalasin D. Cells began extending actin-rich processes (arrows) within an hour after addition of Y-27632 or blebbistatin. Cytochalasin D induced stellation and rounding of cells on stiff substrates but had no appreciable effect on the morphology or migration of cells on the softest substrates. Bar is 100 μm. (B) U373-MG cells cultured on 0.08 kPa fibronectin-conjugated polyacrylamide substrates showed enhanced spreading and migration with addition of 50 μM Y-27632. Bar is 100 μm.
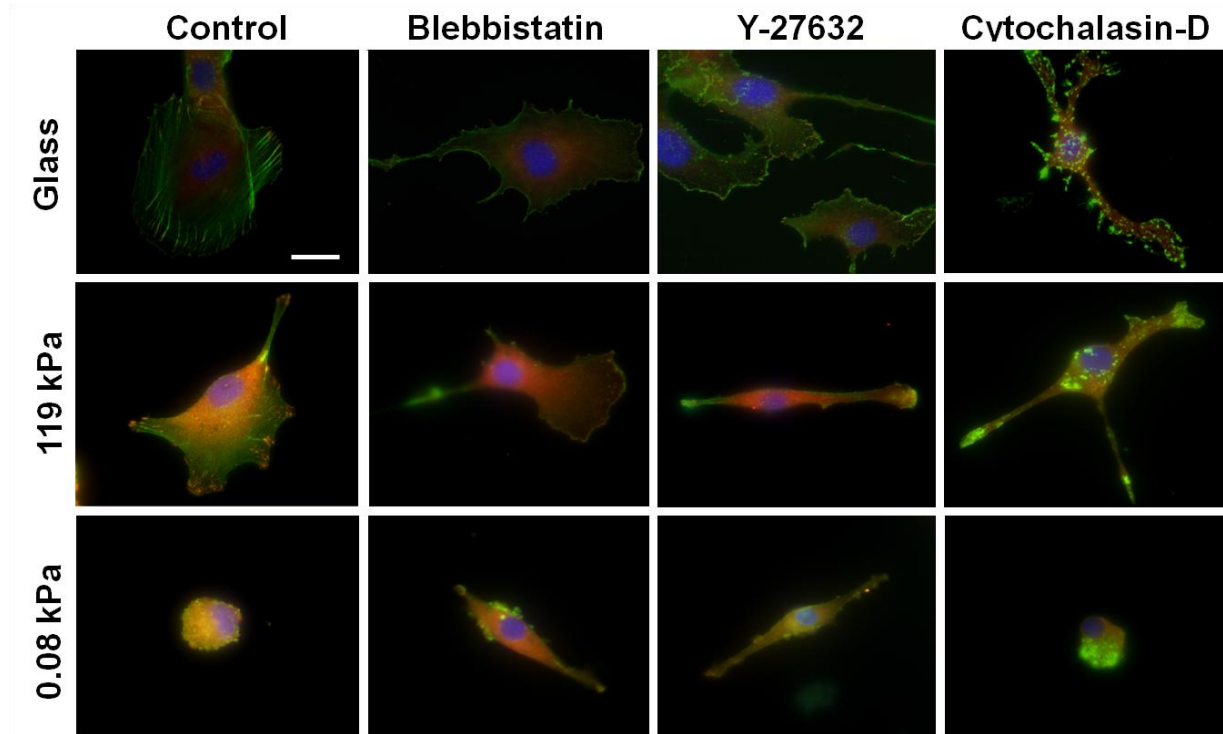
Figure 2.6: **Pharmacologic inhibition of cell tension reduces stiffness-dependent differences in cytoskeletal and adhesive architecture.** U87-MG cells cultured on fibronectin-coated glass and polyacrylamide substrates were treated with 25 µM blebbistatin, 10 µM Y-27632, or 1 µM cytochalasin D for 12-24 hours before fixation and staining for nuclear DNA (blue), F-actin (green), and vinculin (red). In all cases, the number and size of vinculin-positive focal adhesions was reduced with inhibition of cell tension. Blebbistatin and Y-27632 both induced cell spreading on the softest substrates, whereas cytochalasin D induced collapse of the actin cytoskeleton. Bar is 25 µm.

2.5   Discussion

Although mechanistic studies of GBM tumor cell growth and invasion have historically focused on biochemical and genetic factors, numerous studies of other tumorigenic and nontumorigenic cell types have revealed that biomechanical cues presented by the ECM can regulate cell behavior in equally powerful ways. Here, we have begun to explore the role of ECM-based mechanical cues in controlling cell behaviors central to the pathophysiology of GBM. Our studies reveal for the first time striking stiffness-dependent differences in glioma cell structure, migration, and proliferation. This mechanoregulation is especially significant in light of the contrasting mechanical microenvironments associated with normal brain tissue versus tissues associated with gliomagenesis and invasion. Importantly, we were able to temper stiffness-dependent differences in glioma cell structure and migration by pharmacologically inhibiting NMMII-dependent contractility, suggesting that mechanical features of the GBM microenvironment, and the molecular systems that sense and process these features, may serve as informative handles for understanding and manipulating GBM tumor cell physiology *in vitro* and *in vivo*.

The phenomenon of durotaxis (or mechanotaxis) was first defined by Wang and colleagues after they observed that a rigidity gradient could direct the motility of fibroblasts *in vitro* from soft to stiff regions of ECM (36). Subsequent studies have demonstrated that high ECM stiffness enhances the expression and activity of contractility-mediating proteins such as Rho and ROCK (188), a finding that intuitively correlates with the enhanced expression of contractile proteins in many solid tumors (204, 205). In the case of GBM, the role of Rho GTPases in mediating tumor growth and spread *in vivo* is complex and remains incompletely understood. For example, lysophosphatidic acid-mediated NMMII activation can strongly stimulate astrocytoma motility (162), and Rho/ROCK inhibition sensitizes glioma cells to apoptosis induced by radiation (166) and chemotherapy (169). However, RhoA, RhoB, and Rac1 have all been reported to be expressed at reduced levels in primary GBM tumors (196). In our system, we observe stiffness-dependent enhancement in the robustness of cytoskeletal and focal adhesion structures, cell spreading area, and cell migration of glioma cells (Fig. 2.1-2.3), consistent with the predominant model of dynamic mechanical reciprocity in which cells respond to rigidity-encoded cues through "inside-out" signaling that includes reinforcement of contractile and adhesive structures (183). If and how expression levels of contractility-mediating proteins in glioma cells vary with substrate rigidity is an intriguing issue that has not yet been addressed.

Pharmacological inhibition of either NMMII or its upstream regulator ROCK blunts the sensitivity of glioma cells to ECM rigidity, with cells adopting a stellate morphology on and becoming highly motile, even on compliant ECMs (Figs. 4-5). Together, these results suggest that NMMII and its activators form a critical component of the ECM rigidity-sensing pathway in glioma cells, consistent with past observations in other cell types (36, 37, 39, 188). These results are also consistent with recent studies of the contributions of NMMII isoforms (NMMIIA, NMMIIB, and NMMIIC) to cell motility, traction generation and rigidity sensing. Specifically, NMMIIB-null fibroblasts rapidly alter cell shape by extending and retracting unstable protrusions; analogous to our observations of glioma cells under NMMII inhibition, these fibroblasts also migrate faster and are less morphologically sensitive to ECM rigidity than wild-type fibroblasts (206). Moreover, acute depletion of NMMIIA in mouse embryonic fibroblasts speeds cell spreading and slows retrograde flow of actin, suggesting that NMMIIA acts as a brake on cell spreading by globally retarding actin cytoskeletal remodeling (207). Similarly, isoform-specific depletion of NMMIIA but not NMMIIB strongly enhances the spreading of MDA-MB-231 breast cancer cells (208). Additional mechanistic insights are provided by recent observations that glioma cell motility can be stimulated by inhibition of either NMMII (209) or ROCK (167); the latter effect may be blocked by concomitant inhibition of Rac GTPase, implying that it is due to disinhibition of Rac signaling. Importantly, this balance between Rho and Rac activation may also be indirectly disturbed in human glioma cells by pharmacologically inhibiting Ras (163), which offers an unexpected but potentially very important mechanistic connection between Rho GTPase-based mechanosensing and the EGFR/Ras/PI3K pathway. Thus, in our studies, ROCK inhibition may have the dual effect of both releasing NMMII-based restrictions on cell spreading and enhancing Rac-mediated cell motility, which explains why ROCK inhibition rescues motility on compliant substrates much more potently than direct inhibition of NMMII. It remains to be seen if the same relationship between cell motility, Rho family GTPase signaling, and ECM rigidity would hold in 3D ECMs, where NMMII has been demonstrated to play a critical role in facilitating amoeboid migration through narrow pores (159).

Finally, we observe that ECM rigidity strongly regulates glioma cell proliferation, with the most rigid ECM substrates supporting fivefold more robust proliferation than the most compliant ECMs (Fig. 2.4). While the magnitude of this effect is somewhat surprising, ECM rigidity has been previously observed to modulate cell growth in other systems, including cultured fibroblasts (210), hepatocytes (211), and a variety of adult stem cells (40, 42). One potential explanation for this effect is that changes in ECM rigidity might alter the speed of progression through the cell cycle by altering mechanochemical feedback during mitosis. Indeed, direct application of mechanical force can slow cytokinesis and induce shape asymmetries, which cells can actively correct by mobilizing NMMII to produce a restoring force (212). Second, ECM rigidity might regulate mitosis by synergistically triggering mechanotransductive and mitogenic signaling pathways. As described earlier, ECM rigidity can transform cultured breast epithelial cells from a benign, highly-differentiated phenotype into a dysplastic and proliferative one (188, 213). This matrix-driven transformation is accompanied by activation of ERK, Rho GTPase, and NMMII-based contractility, is recreated by overexpressing constitutively active Rho or spontaneously-clustering integrins, and is reversed by pharmacological inhibition of ROCK or ERK. Importantly, many of these pathways also have been implicated in epithelial-mesenchymal transition (214). All of this is consistent with a paradigm in which tumor cells and their pre-malignant progenitors sense matrix rigidification through enhanced integrin clustering, which in turn activates both ERK and mechanosensory signaling, thereby stiffening the cell and inducing proliferation. Suppression of these mitogenic pathways on compliant matrices may also explain why we fail to observe high proliferation in the face of low motility, as would be predicted by the "go or grow" hypothesis (203). The relationship between ECM rigidity, cellular mechanics, and EGFR/Ras/ERK signaling remains largely unexplored in GBM and other non-epithelial tumors. Given that 88% of clinical GBM tumors in the TCGA group were recently discovered to bear mutations in the EGFR/Ras/PI3K pathway (179), it would be intriguing to ask if rigidity-dependent proliferation is accompanied by alterations in EGFR-based signaling or could be indirectly modulated by EGFR pathway manipulation.

2.6 Conclusions

In summary, we have shown that increasing ECM rigidity can induce a suite of phenotypic changes in human glioma cells that includes increased cell spreading, more rapid motility, and enhanced proliferation. As described earlier, bulk human brain tissue has an elastic compliance of 0.5-1 kPa, approximately the same order of magnitude as the most compliant matrices considered in this study. While we are unaware of systematic and definitive measurements of the mechanical rigidity of explanted GBM tumor tissue, intraoperative ultrasound clearly demonstrates that both GBM tumors and their surrounding stroma are substantially stiffer than the surrounding normal brain parenchyma. Placed in context of the notion that invasive glioma cells actively remodel their surroundings from a brain-like to a tumor-like microenvironment (215), this raises the intriguing hypothesis that GBM tumor cells stiffen their surroundings as they invade. We envision that this remodeling could occur through a combination of proteolytic degradation of existing matrix components, secretion of matrix components *de novo*, induction of strain-stiffening, and contractility-dependent bundling and alignment of ECM fibrils, as was recently observed for invading breast cancer cells (216, 217). The resulting microenvironmental

stiffening, in turn, may deliver reciprocal mechanobiological signals to tumor cells that act through integrins, focal adhesion proteins, Rho GTPases, and the cytoskeleton to promote shape plasticity, motility, and ultimately proliferation. If this is the case, then pharmacologic interventions that either interfere with mechanotransductive signaling or mechanical remodeling may hold value in slowing or arresting GBM invasion, analogous to the use of integrin and FAK inhibitors (153, 158). Though challenging, revisiting these ideas in the setting of 3D ECMs or *in vivo* platforms that allow precise tracking of cell-mediated mechanical remodeling during invasion should permit more direct evaluation of this hypothesis.

2.7   Acknowledgements

Chapter 3. Probing cellular mechanobiology in 3-dimensional culture with collagen-agarose matrices

3.1   Abstract

The study of how cell behavior is controlled by the biophysical properties of the extracellular matrix (ECM) is limited in part by the lack of three-dimensional (3D) scaffolds that combine the biofunctionality of native ECM proteins with the tunability of synthetic materials. Here, we introduce a biomaterial platform in which the biophysical properties of collagen I are progressively altered by adding agarose. We find that agarose increases the elasticity of 3D collagen ECMs over two orders of magnitude with modest effect on collagen fiber organization. Surprisingly, increasing the agarose content slows and eventually stops invasion of glioma cells in a 3D spheroid model. Electron microscopy reveals that agarose forms a dense meshwork between the collagen fibers, which we postulate slows invasion by structurally coupling and reinforcing the collagen fibers and introducing steric barriers to motility. This is supported by time lapse imaging of individual glioma cells and multicellular spheroids, which shows that addition of agarose promotes amoeboid motility and restricts cell-mediated remodeling of individual collagen fibers. Our results are consistent with a model in which agarose shifts ECM dissipation of cell-induced stresses from non-affine deformation of individual collagen fibers to bulk-affine deformation of a continuum network.

3.2 Introduction

The behavior of many mammalian cell types is exquisitely sensitive to biophysical signals from the extracellular matrix (ECM), including those encoded within matrix mechanical properties (2). The robust mechanosensitivity of mammalian cells has been extensively probed in vitro using two-dimensional (2D) biomaterial platforms that feature full-length ECM proteins covalently conjugated to polymeric hydrogels of defined stiffness (182), thus allowing independent modulation of ECM mechanical and biochemical properties. We and others have used these platforms to demonstrate that cellular structure, motility, and proliferation can be strongly regulated by the mechanical rigidity of the ECM (182, 199). However, many cells reside in a three-dimensional (3D) ECM in vivo, and it is now well-established that culture dimensionality strongly impacts gene expression, cell adhesion and migration, and assembly into multicellular structures (218, 219).

Although there is increasing interest in investigating cellular mechanobiological properties in 3D culture systems, the development of matrices for this purpose has proven challenging. One common strategy is based on incorporation of cell adhesion peptides (e.g., RGD) into synthetic polymer networks (220-222); while this frequently offers robust and independent control of ECM ligand density and mechanics, it necessarily sacrifices the rich biochemical and topological information encoded in networks of full-length matrix proteins. Conversely, strategies that control 3D matrix properties by varying the concentration of a native ECM formulation (e.g., collagen, Matrigel) access a fairly narrow stiffness range due to the intrinsically low elasticity of most of these materials and concurrently change ECM mechanics, ligand density, microstructure, and other potentially confounding biophysical parameters (46, 189).

Collagen I is both the most abundant ECM protein in mammalian tissues and one of the most widely-used scaffolds for three-dimensional cell culture and tissue engineering applications,

which is partly derived from the ability of purified collagen I monomers to self-assemble into stable, three-dimensional gels at physiological temperature and pH (218). Gelation begins with the entropy-driven nucleation of triple-helical collagen monomers into small aggregates, which subsequently self-assemble into thin filaments that laterally crosslink into collagen fibers. A three-dimensional matrix is then formed via non-covalent entanglement of the fibers (218). As a consequence of this entanglement, reconstituted collagen networks typically exhibit non-affine mechanical properties; i.e., applied stresses are dissipated non-uniformly throughout the gel via the sliding, slipping, bending, and buckling of individual collagen fibers (223). Indeed, this non-affine stress dissipation is a near-universal property of native ECM formulations and contributes to the strongly nonlinear elastic properties of these matrices in bulk, which may provide an important source of mechanical reinforcement when these matrices are loaded in vivo (32, 224).

The fiber diameter, pore size, and bulk elasticity of reconstituted collagen gels can be tuned within modest ranges by changing collagen concentration, ionic strength, pH, and the temperature of gelation (218, 225). Although matrix stiffness is most commonly varied by changing collagen concentration, even modest changes in the concentration of collagen monomers can significantly influence gelation kinetics, fiber diameter, fiber number, and porosity, in addition to increasing the number of integrin-binding sites, as described earlier (225). To circumvent these limitations, a variety of approaches have been developed to crosslink collagen ECMs, including UV or gamma irradiation (226, 227), enzymatic or chemical crosslinking (228-231), and nonenzymatic glycation or nitration (232, 233). More recently, crosslinking mechanisms utilizing the plant extract genipin (234) or multifunctional dendrimers (235) have been used to stiffen collagen matrices. However, speed, cost, and cytotoxicity continue to pose significant experimental limitations; for example, irradiation and chemical crosslinking can be highly cytotoxic, glycation often requires weeks, and the use of enzymes such as lysyl oxidase or transglutaminase can be prohibitively expensive (234).

Agarose, a neutral, galactopyranose-based linear polysaccharide, is a biocompatible and readily-available material that potentially offers a much wider dynamic range of biophysical properties than collagen (236). Gelation of a homogeneous agarose solution occurs according to a coil-helix transition that begins when the solution is cooled to the ordering temperature (typically ~35ºC) where random coils of agarose begin forming single or double helices in solution. These helices aggregate to form an ordered structure of bundled double helices connected by flexible chains (237). The physical and mechanical properties of agarose gels have been studied in considerable detail over the past 30 years, showing that the final gel structure tends to be isotropic with an average porosity of approximately 100-300 nm (238, 239). Agarose also has a number of attractive properties for biomaterial applications, in that it is inexpensive, non-toxic, inert to mammalian cell adhesion and degradation, and stiffens over several orders of magnitude for only modest increases in concentration (236). Indeed, 3D agarose hydrogels have proven valuable as a culture scaffold for a variety of tissue engineering applications that do not require provision of a bioactive ECM (43, 240). Moreover, recent studies have suggested that agarose can be incorporated into networks of collagen I, which has generated interest in the potential utility of these composites in tissue engineering and 3D cell culture applications (241-244).

Given these properties, and given the need for 3D matrix systems that combine the biofunctionality of native ECM formulations with the tunability and dynamic range of synthetic

scaffolds, we asked whether we might be able to vary the biophysical properties of collagen I matrices in a graded fashion by adding defined concentrations of agarose. In this study, we systematically vary the agarose content of collagen-agarose scaffolds in order to create a simple, inexpensive material platform in which ECM biophysical properties can be tuned independently of collagen content in 3D. We measure gel elasticity using parallel plate rheometry and characterize matrix structure using a combination of light and electron microscopy. We then use a series of collagen-agarose gels with increasing stiffness to study the mechanosensitivity of glioblastoma multiforme (GBM) cells, a system we showed to be highly sensitive to ECM-based biophysical cues in 2D culture in Chapter 2 of this dissertation (199).

3.3   Materials and Methods

3.3.1   Preparation of collagen-agarose gels

Stock 1.5 mg/ml collagen solutions were prepared on ice immediately prior to use by diluting PureCol (3 mg/ml sterile pepsin-solubilized bovine collagen in solution, ~97% collagen I, 3% collagen III; Advanced Biomatrix, San Diego, CA) in Dulbecco's Modified Eagle Medium (DMEM, Life Technologies, Grand Island, NY); 1 M NaOH was added to bring the pH to 7.4. Stock agarose solutions were prepared by dissolving 2% w/v low melting temperature agarose (A9414 supplied with sulfate content <0.1%; Sigma-Aldrich, St. Louis, MO) in DMEM and adjusting the pH to 7.4; the solution was then brought to 95ºC in a water bath prior to use. Collagen-agarose gels were prepared by combining collagen and agarose stock solutions with additional DMEM in appropriate volumes to create 0.5 mg/ml collagen gels with agarose concentrations ranging from 0-1% w/v. Solutions were mixed thoroughly prior to dispensing into cell culture or rheology dishes. Substrates were incubated at 37°C for 1 hour prior to addition of a superlayer of cell culture medium.

3.3.2   Characterization of mechanical properties

All rheology measurements were taken with an Anton Paar Physica MCR-300 or 301 rheometer (Anton Paar USA, Temecula, CA) at 37ºC and high humidity using a 25 mm parallel plate geometry and Rheoplus software. Preliminary amplitude sweeps over the range γ=0.1-10% were used to identify the linear regime; frequency sweeps at 5% strain over the range 0.1-10 Hz were then used to extract the storage modulus, loss modulus, and complex modulus of each sample. At least five independent samples were measured for each gel formulation; reported storage moduli represent mean ± SEM at 0.4 Hz. Representative amplitude and frequency sweeps for different gel formulations are provided in Fig. 3.1.

3.3.3   Cell culture and preparation of glioma spheroids

U373-MG human glioma cells were obtained from the Tissue Culture Facility at the University of California, Berkeley and cultured in DMEM supplemented with 10% Calf Serum Advantage (J.R. Scientific, Woodland, CA) and 1% penicillin/streptomycin, MEM nonessential amino acids, and sodium pyruvate (Life Technologies). Multicellular tumor spheroids were created using the hanging drop method (195, 245). Briefly, droplets of cell suspension containing ~500

cells were plated on the lid of a petri dish, inverted, and cultured over a dish of cell culture medium for 3 days. Spheroids of ~150 µm in diameter were manually collected using a micropipette and implanted in collagen-agarose substrates prior to gelation.

3.3.4   Microscopy and measurement of spheroid invasion

Simultaneous confocal reflectance and second harmonic generation (SHG) images were obtained using a Zeiss LSM 510/NLO META by exciting the sample with 800 nm from a Spectra-Physics MaiTai HP laser at a power of <25% of the maximum power as well as 488 nm from an argon ion laser at a power of <1% of total power (~0.3mW). The META detector of the instrument was used in the emission pathway, where the detector range was set to 390 nm-410 nm to obtain the SHG signal while the Zeiss was operated with no band pass filter so that all the light reflected was detected by the photomultiplier tube. We employed a 63x oil objective with NA 1.3 to obtain images of 512 x 512 pixels (133.6 µm x 133.6 µm) at a scan speed of ~1 sec/frame. DIC and phase contrast microscopy were performed using an inverted Nikon TE2000-E2 microscope equipped with a motorized, programmable stage (Prior Scientific, Inc, Rockland, MA), an incubator chamber to maintain constant temperature, humidity, and CO_2 levels (In Vivo Scientific, St. Louis, MO), a digital camera (Photometrics CoolSNAP HQ II, Roper Scientific, Tucson, AZ), and SimplePCI software (Hamamatsu Corporation, Sewickley, PA). Quantification of spheroid invasion was performed in SimplePCI by quantifying the total area occupied by cells in time lapse 10x phase contrast images captured through the mid-plane of each spheroid. Values were normalized to the initial area, such that the area is 100% for t=0.

3.3.5   Scanning electron microscopy

Collagen-agarose solutions were incubated at 37°C at high humidity for 1 hour on silicon wafers. Gels were fixed in 2% glutaraldehyde overnight at 4°C and 1% osmium tetroxide for 1 hour at room temperature (both in 0.1M sodium cacodylate buffer, pH 7.2) prior to dehydration in an ethanol series, critical-point drying (AutoSamdri 815, Tousimis, Rockville, MD), sputter coating with 1-2 nm of gold and palladium (Tousimis), and examination with a Hitachi S-5000 scanning electron microscope at 3000x, 10,000x and 30,000x magnification.

3.4   Results

3.4.1   Gel elasticity and structure

We began by synthesizing a series of collagen-agarose hydrogels in which we fixed the collagen concentration at 0.5 mg/ml and varied the agarose concentration from 0 to 1% w/v, and we asked whether addition of agarose could progressively alter gel elastic properties while preserving collagen fiber architecture. Parallel-plate rheometry revealed that the macroscopic storage modulus of collagen increased by over two orders of magnitude as the agarose concentration was increased from 0-1% w/v (Figs. 3.1 and 3.2), with the highest agarose concentrations yielding storage moduli approaching 1 kPa. This value is more than an order of magnitude greater than we could achieve with pure collagen gels, even by tripling the collagen concentration to 1.5 mg/ml (Fig 3.3A). Visualization of collagen-agarose gels using Nomarski DIC imaging,
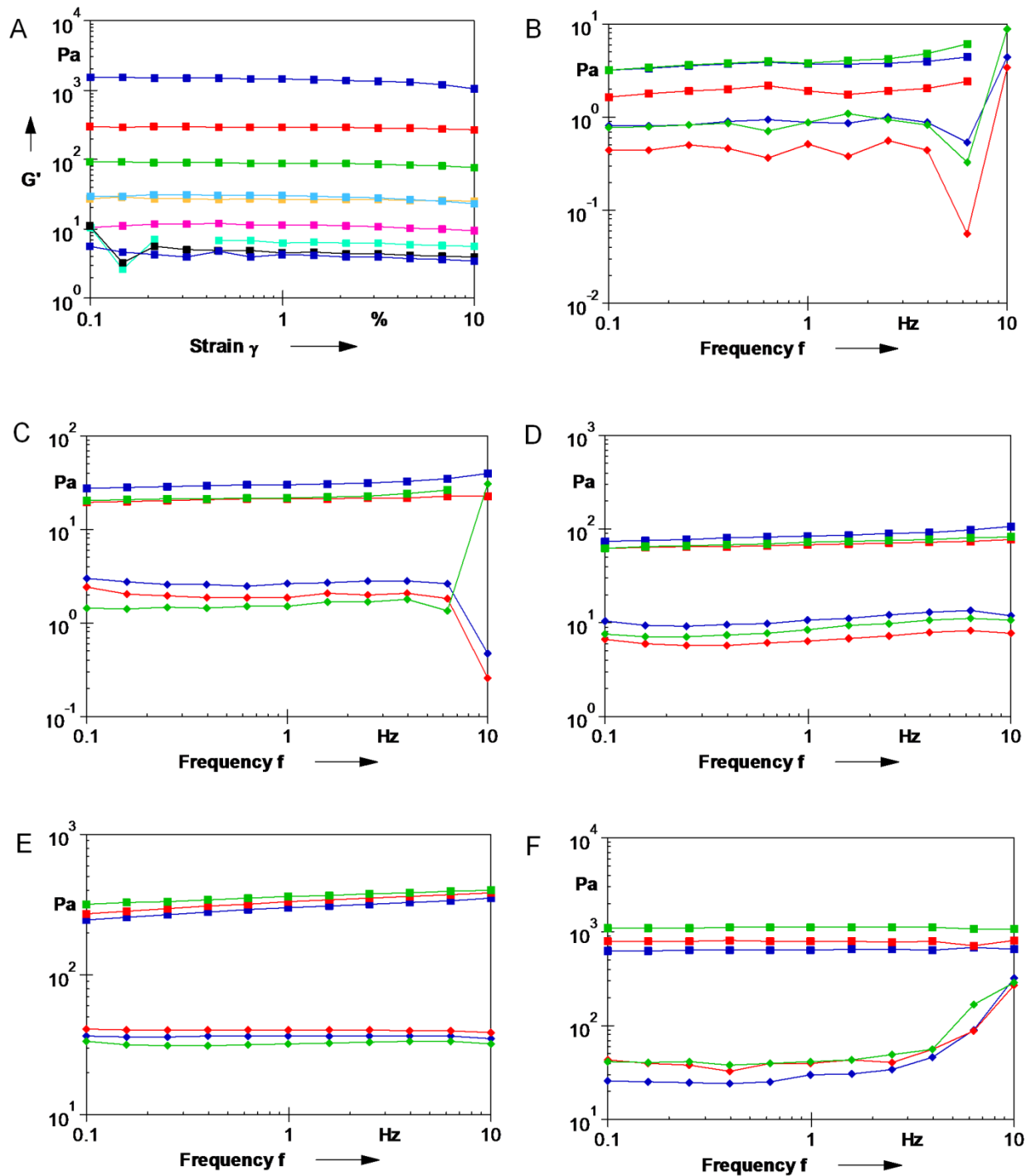
Figure 3. 1. Rheometry of collagen-agarose gels. A. Typical amplitude sweeps of collagen and collagen-agarose gels at 37°C and 0.4 Hz. Gel formulations ranged from 0.5-1.5 mg/ml collagen (0.5-1.5 C) and 0-1 % w/v agarose (0-1 A). From the top, curves represent: 0.5 C /1 A ; 0.5 C/0.5 A; 0.5 C/0.25 A; 0.5 C/0.125 A; 1 C/0 A; 0.75 C/0 A; 0.5 C/0.01 A; 0.5 C/0 A. B.-F. Typical frequency sweeps of collagen/agarose gels at 5% strain for the following gel formulations: B. 0.5 C; C. 0.5 C/0.125% A; D. 0.5 C/0.25% A; E. 0.5 C/0.5 A; F. 0.5 C/1 A. Red, blue, and green curves represent independent samples of each gel formulation. Data are representative of n ≥ 5 samples per condition.

confocal reflectance microscopy, and SHG imaging all failed to reveal gross alterations in apparent collagen fiber diameter or architecture up to 0.25% w/v agarose, with moderate differences becoming clear only for gels with agarose content of 0.5% w/v or higher (Fig. 3.4). This is in stark contrast to pure collagen gels stiffened by increasing collagen concentration from 0.5 mg/ml to 1.5 mg/ml (Fig. 3.3B; (225, 246-248)).
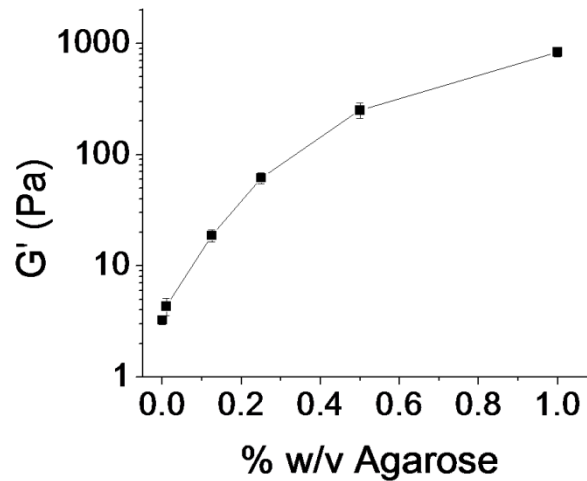

Figure 3.2. Effect of agarose on storage modulus of collagen gels. Parallel-plate rheometric measurements of the bulk storage (elastic) modulus (G') of 0.5 mg/ml collagen gels in the presence of 0-1% w/v agarose. Each data point represents mean ± SEM for n ≥ 5 samples.

3.4.2 Glioma cell invasion

Previously, we have shown that increasing ECM elasticity in 2D could speed the random motility of a panel of glioma cell lines, including U373-MG cells. Therefore, we next used our collagen-agarose gel platform to ask how variation in the agarose content of 0.5 mg/ml collagen gels might influence glioma cell invasion in the context of 3D ECMs. For these studies, we used a spheroid invasion model in which cells are grown as multicellular spheroids in hanging-drop culture and implanted into the gel during the gelation process, such that the gel forms around the spheroid (195). Over time, cells migrate away from the spheroid into the surrounding matrix, and invasion may be tracked by measuring the total projected area occupied by cells throughout the matrix. Time lapse phase contrast microscopy revealed a dramatic inhibition of spheroid invasion as the concentration of agarose was increased, including complete abolition of invasion in gels containing 1% w/v agarose (Fig. 3.5; also see Supplementary Movies 1-3 in (249)). This is in stark contrast to pure collagen gels stiffened by increasing collagen concentration, where gel stiffness did not directly correlate with invasiveness (Fig. 3.3C and D), as has been reported by others (195). Importantly, pure agarose gels did not support cellular invasion at any concentration in the absence of collagen, demonstrating that adhesive cues from the collagen are both necessary and sufficient for motility (Fig. 3.6). Based on these results, we surmised that
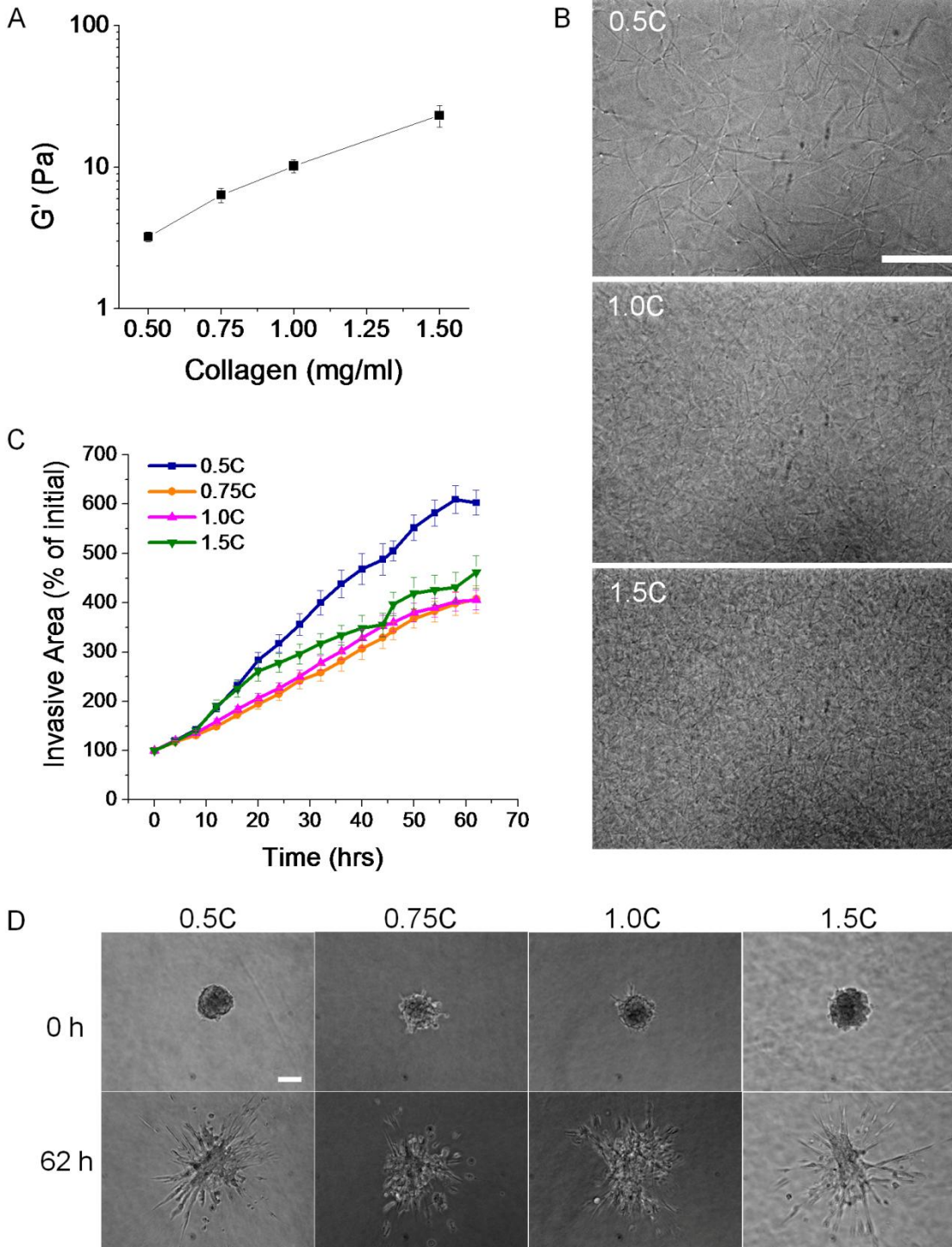
Figure 3.3. Rheological, microstructural and cell invasive properties of pure collagen matrices. A. Storage moduli of pure-collagen gels. The storage modulus of pure collagen gels varies modestly as protein concentration is increased from 0.5-1.5 mg/ml collagen (0.5-1.5 C). Each data point represents mean ± SEM for n ≥ 4 samples. B. Microstructure of pure collagen gels. DIC imaging of pure collagen gels shows large differences in collagen microstructure as the concentration is varied from 0.5-1.5 C. Bar = 25 μm. C, D. Spheroid invasion assays. Spheroid invasion in pure collagen gels does not correlate cleanly with gel stiffness, possibly due to the competing effects of gel stiffness, ligand availability and collagen microstructure.

38
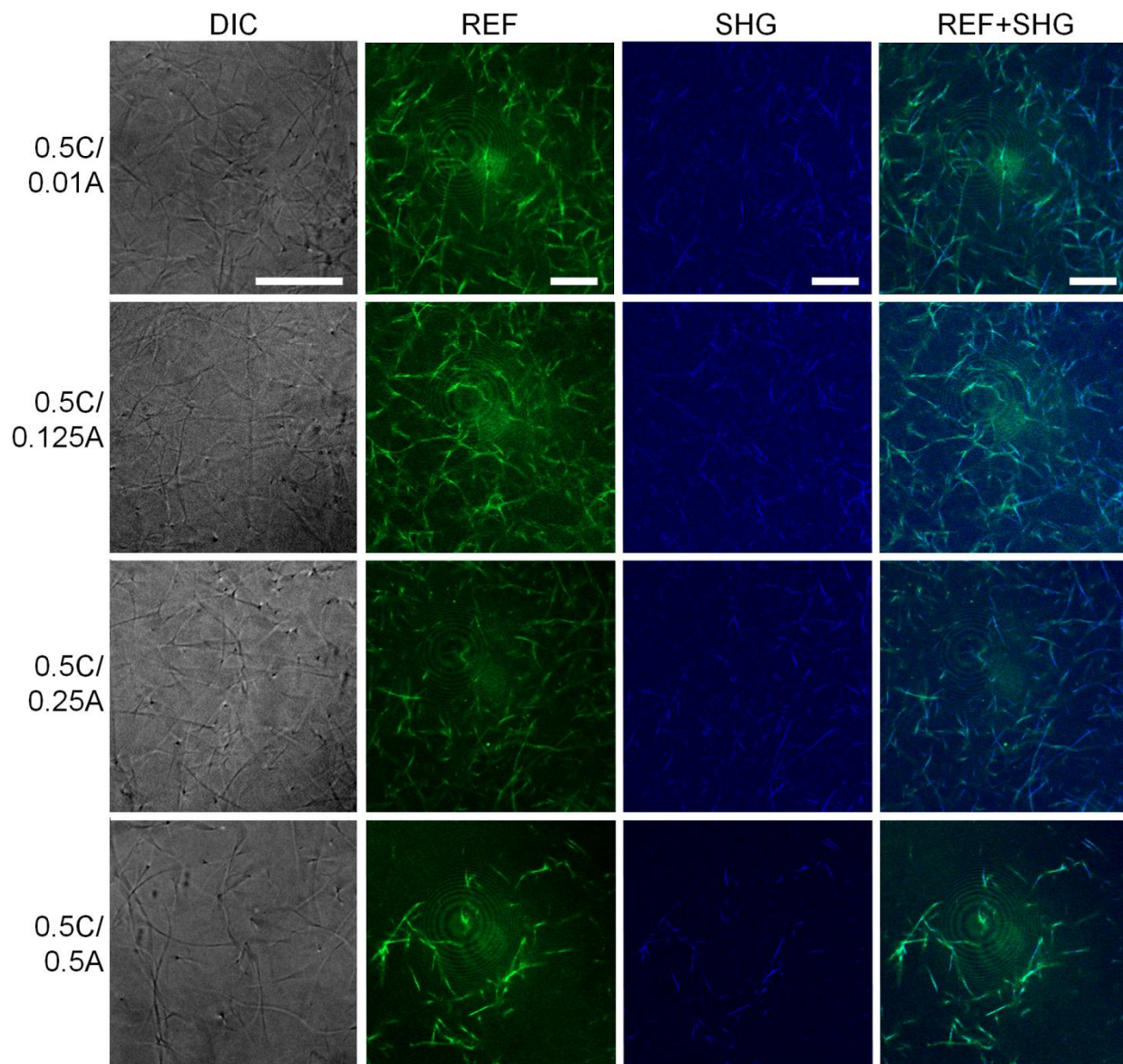
Figure 3.4. Effect of agarose on collagen fibril architecture. High-magnification differential interference contrast (DIC), confocal reflectance (REF) and second harmonic generation (SHG) imaging of collagen fiber microarchitecture within collagen-agarose composite gels containing 0.5 mg/ml collagen (0.5C) and 0.01-0.5% w/v agarose (0.01A - 0.5A). DIC and REF images are representative of n ≥ 3 samples per condition; REF+SHG images were captured simultaneously and are representative of multiple images acquired from within a single gel sample. Bar = 25 μm.
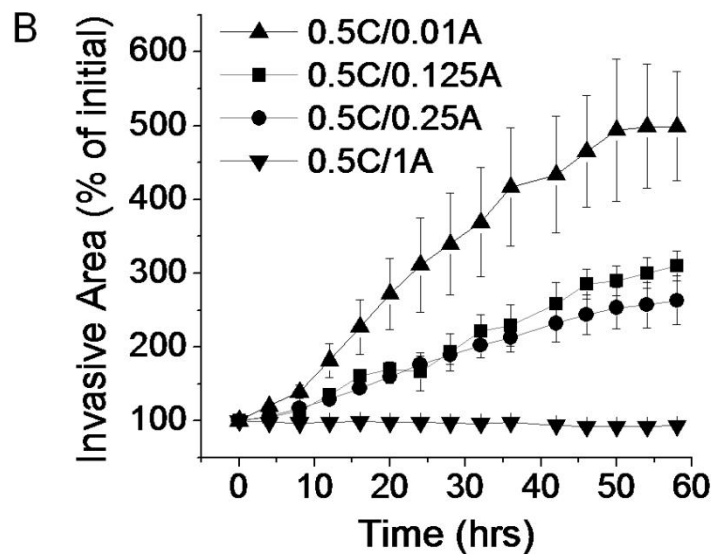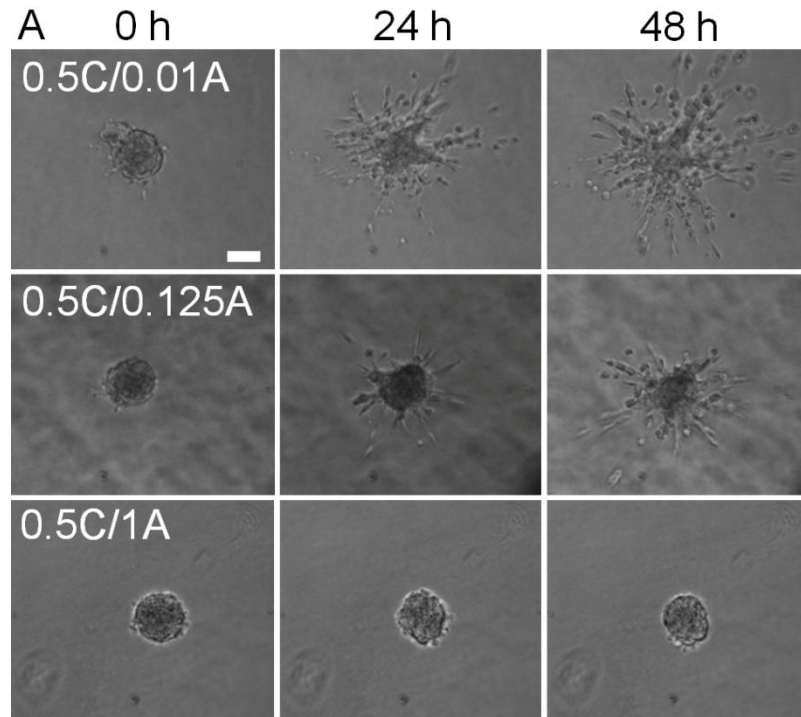
Figure 3.5. Control of 3D cell motility by agarose content. Glioma cell invasion from spheroids into collagen-agarose gels is progressively restricted by the presence of agarose. **A.** Time lapse images of spheroid invasion in gels composed of 0.5 mg/ml collagen (0.5C) and 0.01-1% w/v agarose (0.01A - 1A). Images depict the gel/spheroid sample with the median final invasive area for a given gel formulation. Bar = 100 μm. **B.** Quantification of the total spheroid cross-sectional area as a function of time. Data represent mean ± SEM for n ≥ 3 spheroids per condition.
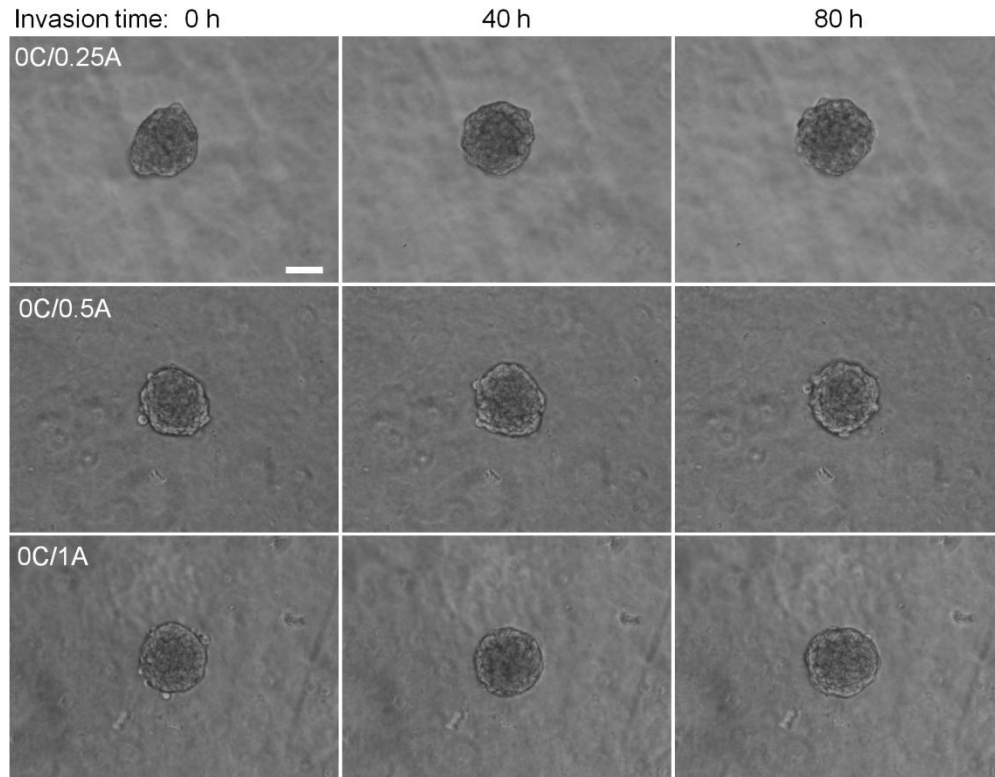
Figure 3.6. Spheroid invasion in pure agarose matrices. Spheroids implanted into pure agarose gels ranging between 0.25-1% w/v agarose (0.25-1 A) failed to invade the surrounding matrix over 80 hours. Images are representative of n ≥ 4 spheroids per condition. Note that we were unable to form gels in the absence of collagen for 0.01 and 0.125% w/v agarose gels (0 C/0.01 A and 0 C/0.125 A, respectively), consistent with previous reports that the critical concentration of agarose is typically between 0.1-0.2% w/w. Bar = 100 μm.

increasing ECM rigidity apparently exerted the opposite effect in 2D and 3D, enhancing motility in the former case and inhibiting it in the latter.

3.4.3 Gel porosity

The above results imply that addition of agarose to collagen I matrices increases stiffness and reduces cell motility in 3D, but does so through a mechanism that does not primarily involve substantial changes in collagen ligand density or fiber architecture. Given that agarose had only a modest influence on collagen fiber organization, we hypothesized that the dramatic inhibition of glioma invasion might result from steric hindrance, where the increasing agarose content reduced the mesh size of the ECM, which would in turn progressively restrict the movement of both individual collagen fibers and glioma cells. This would also help reconcile the disparity between rigidity effects in 2D and 3D, as cells migrating in 2D culture need not overcome steric barriers in order to migrate. To test this hypothesis and gain additional insight into potential microstructural effects, we used SEM imaging to directly visualize the collagen and agarose. These studies revealed that agarose forms an intercalating matrix between the collagen fibers with a fine web-like architecture (Fig. 3.7) similar to the agarose structure reported by others (250) and consistent with the notion that agarose creates steric barriers to motility. Moreover,

collagen fiber diameters observed by SEM were in good agreement with those observed by DIC, reflectance, and SHG imaging (Fig. 3.4; (246-248)) and provided further confirmation that fiber diameter is largely independent of agarose concentration.
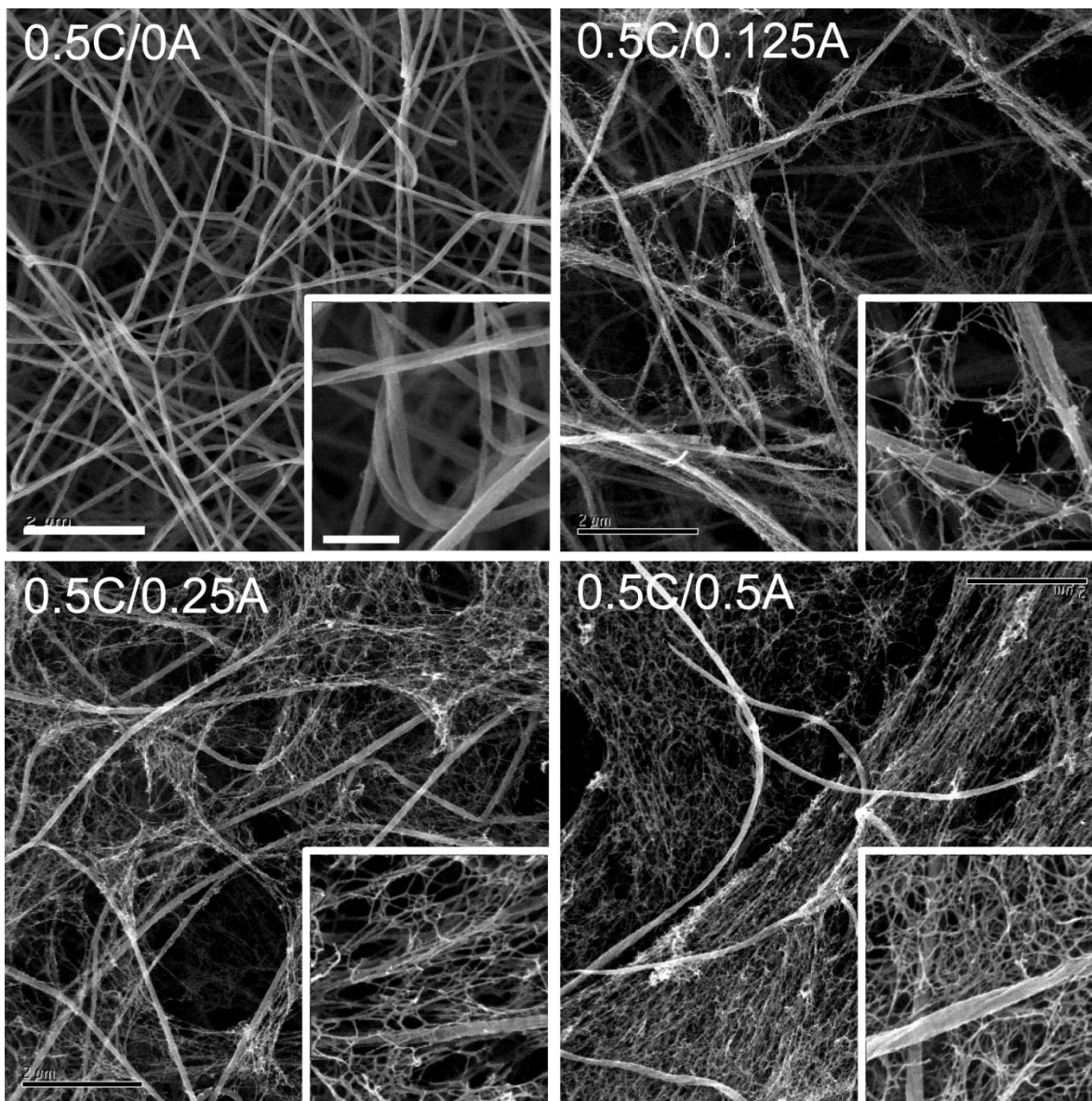
Figure 3.7. Scanning electron microscopy imaging of collagen-agarose gels. SEM reveals that agarose forms an intercalating web-like network between the entangled collagen fibers that becomes progressively denser as the concentration of agarose is increased from 0-0.5% w/v agarose (0A - 0.5A) in a 0.5 mg/ml collagen gel (0.5C). Note that dehydration during SEM sample processing can give rise to an artifactual variation in the apparent density of collagen fibers at the surface of each gel sample. Bar = 2 μm (main panels) and 500 nm (insets).

3.4.4 Mesenchymal-amoeboid transition

Such dramatic changes in gel porosity would be expected to trigger a mesenchymal-amoeboid transition (MAT), in which cell migration transforms from a "mesenchymal" mode of motility characterized by an elongated morphology with established cell polarity and proteolytic degradation of the surrounding matrix to an "amoeboid" mode of motility characterized by a rounded morphology and propulsive, contractility-dependent squeezing through pre-existing pores in the matrix (251-253). Indeed, high-resolution time lapse imaging of single glioma cells migrating through 3D collagen-agarose matrices showed strong evidence for a progressive MAT as the agarose content was increased (Fig. 3.8; also see Supplementary Movies 4-6 in (249)). Cells in agarose-poor gels were often elongated and moved in a directionally persistent fashion, whereas cells in agarose-rich gels extended thin projections in many directions at the leading edge and exhibited multiple constriction rings along the cell body as the cells squeezed through pores in the matrix.
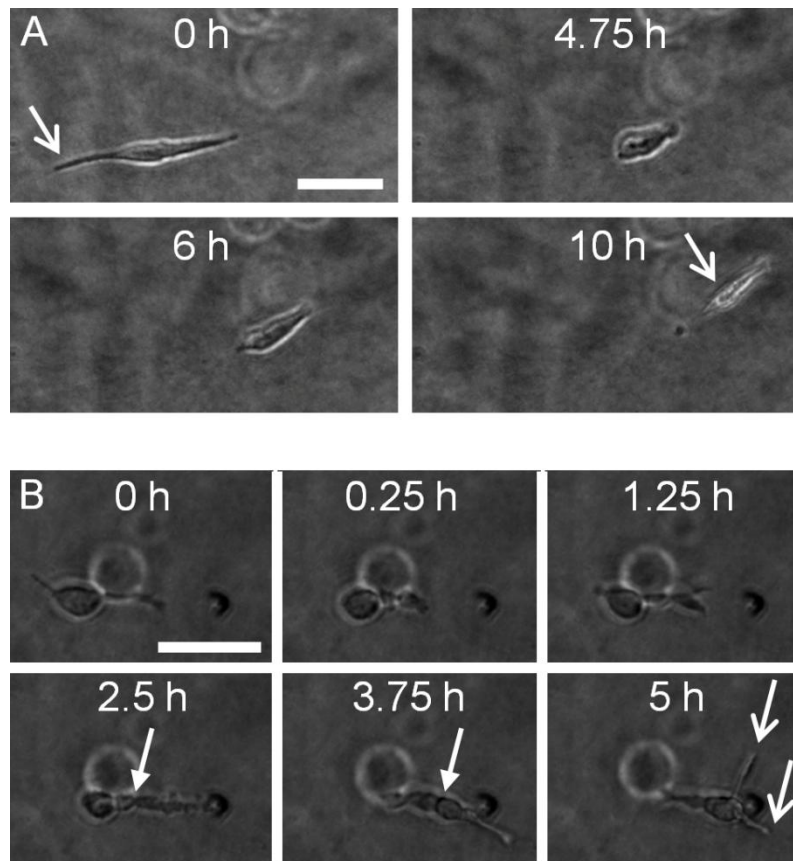
Figure 3.8. Agarose-induced mesenchymal-to-amoeboid transition in cell motility. A. Motility in pure-collagen gels. Cells in pure collagen gels are elongated (arrows) and migrate in a directionally-persistent, mesenchymal fashion. Similar motility was observed in agarose-poor gels (data not shown). B. Motility in agarose-rich gels. Cells embedded in 0.5 mg/ml collagen supplemented with 0.25% agarose exhibit a more rounded morphology and migrate in an amoeboid fashion, indicated by the presence of constriction rings (solid arrows) and active exploration of multiple migration paths at the leading edge (open arrows). Bar = 50 μm in both cases.

3.4.5   Collagen fiber deformability

Mesenchymal motility in collagen matrices is associated with successive deformation and relaxation of individual collagen fibers (251). Thus, we reasoned that an additional mechanistic origin of the observed MAT might be that addition of agarose restricts the deformability of individual collagen fibers. To visualize these potential differences directly and in the complete absence of 3D steric barriers, we next cultured glioma cells on the surface of collagen-agarose gels and obtained phase contrast and DIC time lapse images of cell motility. After 24 hours, cells plated on the surface of relatively thick gels (> 1 mm) showed dramatic differences in cell morphology and organization (Fig. 3.9A). Specifically, cells plated on agarose-poor gels were elongated and visibly aligned with collagen fiber bundles, whereas cells plated on agarose-rich gels were rounded and tended to form spherical aggregates, consistent with a restricted ability to access and remodel the collagen fibers into larger bundles.

Additional insight into this phenomenon came from high-magnification time lapse DIC imaging of cells plated on the surface of thin gels (50-100 µm), which allowed visualization of the dramatic differences in collagen fiber bundling (Fig. 3.9B) and revealed intriguing differences in the mechanisms through which cells interact with collagen fibers as the agarose content of the gels is increased (Fig. 3.9C and D; also see Supplementary Movies 7 and 8 in (249)). In pure collagen or agarose-poor matrices, we primarily observed non-affine bending and slipping of individual collagen fibers in response to cell-induced stresses. In contrast, cells on agarose-rich gels appeared to deform the matrix as a continuum structure, with deformations of individual collagen fibers very strongly coupled to the deformations of surrounding fibers.

Revisiting the effects of agarose on microscale matrix remodeling in 3D spheroidal culture, we found that we could observe these differences particularly clearly by obtaining time lapse imaging of spheroid pairs that were fortuitously implanted in close proximity to one another (Fig. 3.10). In pure collagen gels, spheroids initially located over a millimeter apart were capable of mutually remodeling the ECM between them, ultimately creating bundles of fibers that served as contact guidance cues for trans-spheroid motility. Both the ECM remodeling and directional motility were significantly reduced in collagen/agarose matrices and completely absent in pure agarose matrices, even for spheroids initially located < 300 µm (in this case, less than one spheroid diameter) from one another. In other words, addition of agarose inhibits the ability of cells to communicate mechanical signals to one another through the gel via remodeling of intervening matrix fibers.

3.5   Discussion

We have developed a strategy for modulating the biophysical properties of collagen gels in a graded fashion based on the incorporation of agarose, and we have shown that this approach is capable of fortifying the elasticity of weak collagen gels over two orders of magnitude without grossly disrupting fiber architecture. The addition of agarose also substantially inhibits cell invasion into the matrix and induces a transition from mesenchymal to amoeboid motility. This is consistent with a model in which agarose creates steric barriers to adhesion and motility and restricts cell-induced deformation and remodeling of the matrix, thus converting matrix rheology
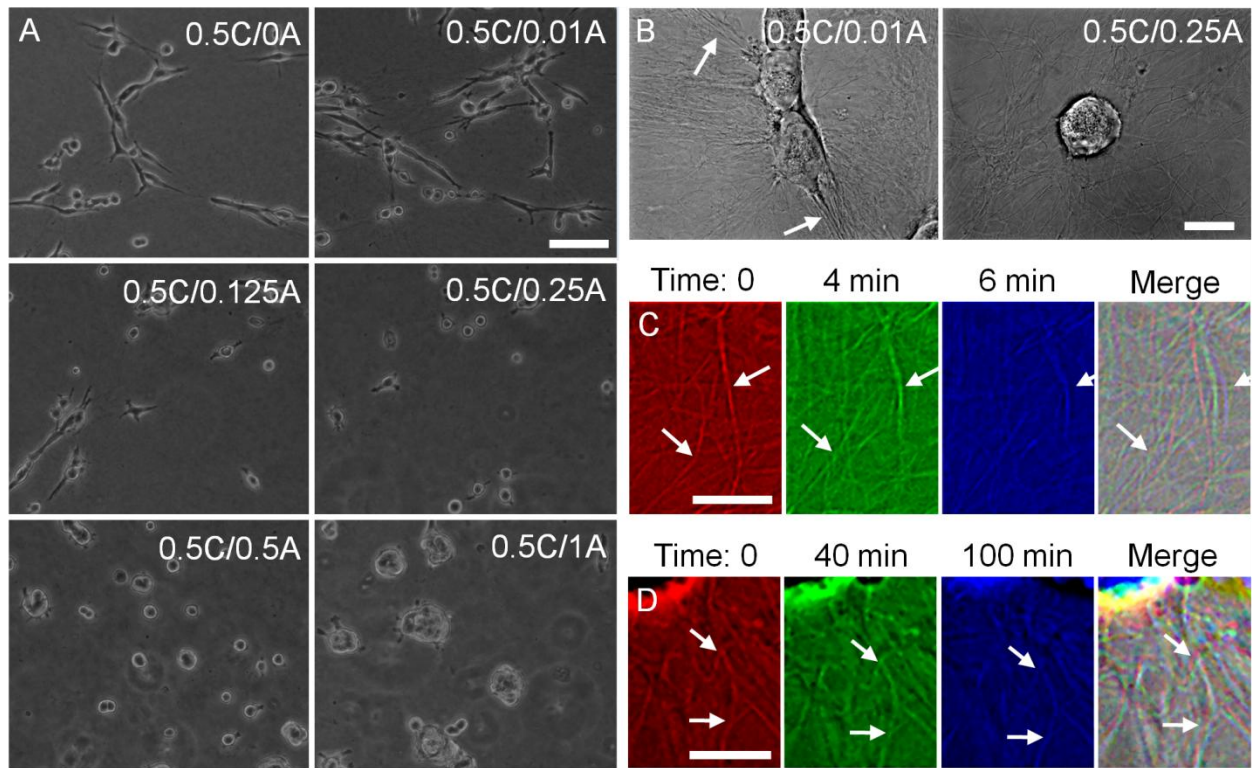
Figure 3.9. Agarose-induced alterations in time-scale and mechanism of stress dissipation. A. Phase contrast imaging of glioma cells on thick 2D collagen/agarose gels. Glioma cells cultured on the surface of 0.5 mg/ml collagen gels (0.5C; gels are >1 mm in thickness) for 24 hours are elongated and often organized into linear (end-to-end) patterns. As the concentration of agarose is increased from 0-1% w/v agarose (0A - 1A), cells become more rounded and form aggregates more readily. Bar =100 μm. B. DIC imaging of cells on thin collagen/agarose gels. Glioma cells cultured on the surface of thin collagen-agarose gels (50-100 μm in thickness) are able to remodel the surrounding matrix to create bundles of aligned collagen fibers (arrows) when the matrix is agarose-poor. In contrast, even after 48 hours, the collagen fibers in agarose-rich matrices are randomly aligned and resemble unseeded substrates. Bar = 25 μm. C, D. Differential matrix deformation dynamics in agarose-poor and agarose-rich gels. The images on the right (merge) depict a color overlay of DIC images obtained at the three time points on the left (red, green, and blue images) during high-magnification DIC time lapse imaging of the collagen fiber deformation generated by glioma cells cultured on the surface of thin collagen-agarose matrices (50-100 μm in thickness). C. Non-affine deformation in agarose-poor matrices. Individual collagen fibers in a 0.5 mg/ml collagen gel bear cell-imposed contractile stresses by slipping and bending (arrows) in divergent directions over short time scales. D. Bulk-affine deformation in a 0.5 mg/ml collagen gel supplemented with 0.25% w/v agarose. Individual collagen fibers appear to be coupled and deform over long time scales as a continuum substrate rather than a network of discrete entangled fibers, consistent with the expected decrease in the organizational entropy of individual collagen fibers. Bar = 10 μm for C and D.

from a non-affine regime in which cell-induced loads are dissipated via the bending and slipping of individual collagen fibers to a bulk-affine regime in which the available degrees of freedom for individual fiber deformation is restricted and the movement of neighboring fibers appears coupled. One consequence of the cells' reduced ability to deform and remodel individual ECM fibrils is abrogation of topological communication between multicellular spheroids separated by only hundreds of micrometers.
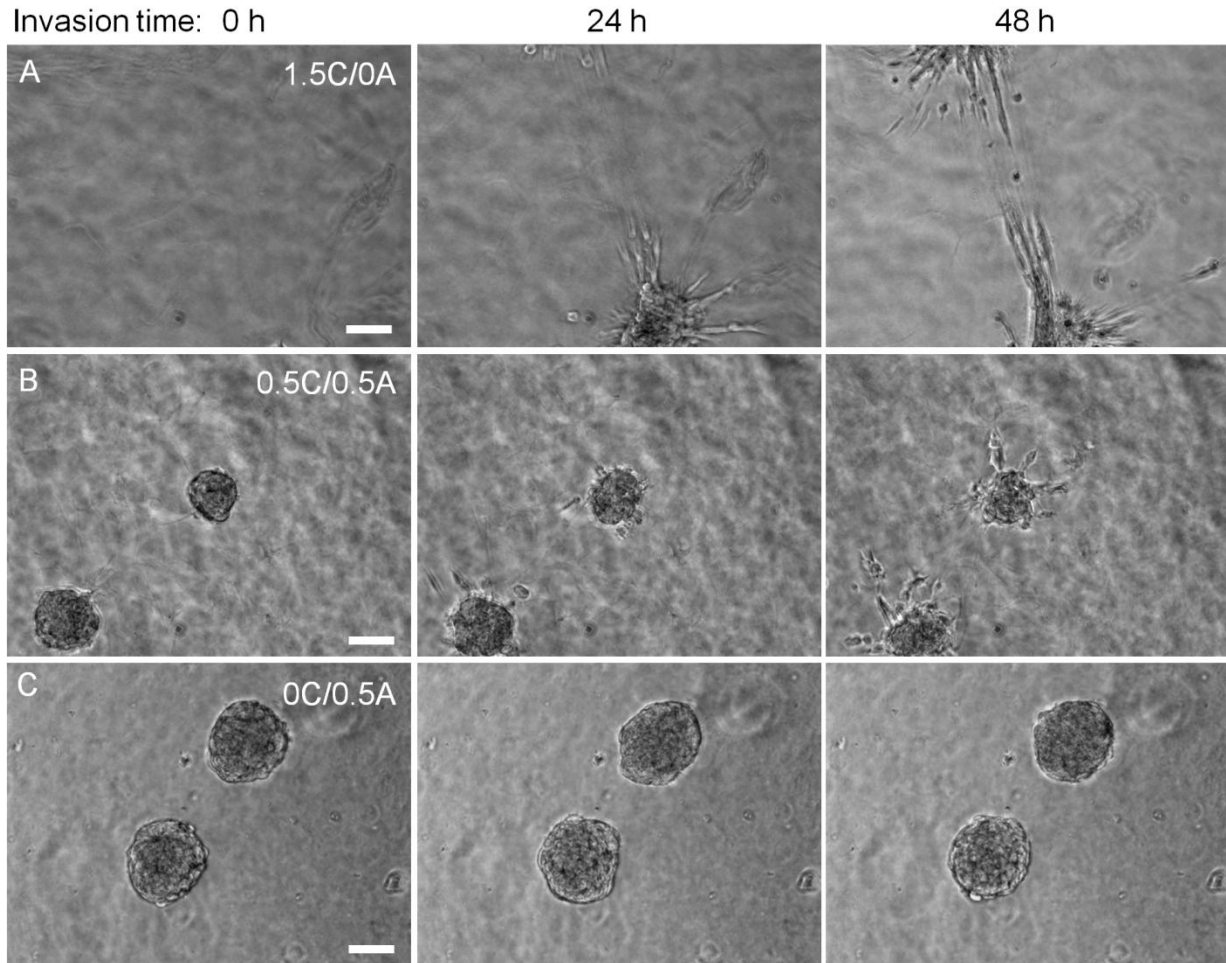
Figure 3.10. Topological communication between adjacent spheroids: Selected time lapse images. A. Pure collagen. Spheroids implanted into pure collagen or agarose-poor collagen gels are capable of generating large matrix deformations and transmitting forces across long distances, as evidenced by the propensity of spheroids that were fortuitously placed close together to grow towards one another while creating visible lines of tension in the matrix. B. Collagen/agarose. Spheroids implanted into agarose-rich collagen gels are not capable of generating large matrix deformations, but are capable of limited invasion, as evidenced by the behavior of two spheroids that were placed anomalously close together. C. Pure agarose. Spheroids implanted into pure agarose gels are unable to deform or invade the surrounding matrix in the absence of collagen, even when placed within close proximity. In all cases, bar = 100 μm.

Our findings bear at least two levels of significance. First, our material system combines the rich topological and biochemical information encoded in full-length, native ECM proteins with the wide biophysical dynamic range of agarose, which offers an alternative to the common practice of controlling the biophysical properties of native ECM formulations simply by varying ECM concentration. In doing so, our work adds to the small but growing repository of such hybrid materials (254-258) without requiring chemical conjugation of component precursors. Second, our results illustrate the inherent challenge – and instructiveness – of translating biophysical regulatory principles from 2D ECMs to 3D ECMs, in the sense that scaffold parameters not widely considered central to 2D motility, such as mesh size and fiber deformation, ultimately play critical roles in governing 3D motility. This lesson comes in the context of a surge of

interest among cell biologists in dissecting the relative contributions of 3D ECM biophysical parameters to cell motility (43, 243, 259, 260) and supports the notion that these parameters are sometimes intimately coupled; in this case, for example, a change in elasticity is accompanied by a concurrent change in microstructure, and both appear to govern cell-matrix interactions during motility.

To expand on the latter point, the rigidity-dependence of cell spreading and motility in glioma cells on the surface of our collagen-agarose gels contrast with the rigidity-dependent behaviors we previously observed on polyacrylamide (pAA) gels in Chapter 2 of this dissertation (199). Specifically, the high levels of glioma cell spreading and motility observed on the stiffest pAA gels (G'~40 kPa) were severely restricted as matrix rigidity was decreased, where cells on the softest (G'~27 Pa) pAA gels were uniformly rounded with limited motility. In contrast, glioma cell spreading and motility was restricted on the stiffest collagen-agarose gels (G'~835 Pa) and progressively increased as matrix rigidity was decreased, where cells on the softest (G'~3 Pa) gels were elongated and highly motile. This apparent contradiction is a consequence of the contrasting material properties of collagen and pAA. Collagen gels are comprised of entangled fibers that are known to impart non-affine mechanical properties (32, 223); as a result, we would expect cells in collagen matrices to generate long-range nonlinear matrix deformations and localized strain stiffening via non-uniform transmission of forces along individual collagen fibers or bundles. In contrast, pAA gels are linearly elastic; as a result, transmission of cell-generated forces should be homogeneous and therefore spatially limited. This phenomenology is in good agreement with recently-reported associations between the linear and nonlinear elastic properties of pAA and fibrin substrates, respectively, and differences in cell spreading, motility, and matrix deformability (224). Finally, we would expect the presence of agarose in our collagen-agarose matrices to couple the collagen fibers together while restricting the available degrees of freedom for fiber bending, buckling and slipping. As a result, we expect that dissipation of cell-generated forces should transition from non-affine deformation of individual collagen fibers towards the bulk-affine deformation of a continuum network. This is consistent with the bulk-affine behavior that would be expected when the fibers in a non-affine matrix are made more resistant to bending (218).

We may also place our study in the context of earlier in vitro studies of glioma cell invasion and spheroid expansion (193, 195, 261). In particular, Gordon et al. observed that expanding glioma spheroids exert both significant outward mechanical pressure and inward traction forces on the surrounding matrix (193). In our system, we speculate that agarose may interfere with both of these processes; for example, the reduced mesh size of these gels prevents the intimate adhesion and spreading along collagen fibrils that would be needed to generate tractional forces, and the increased elastic modulus and conversion to bulk-affine mechanics may retard transmission of spheroid-generated compressive forces. This is strongly supported by our observation that reduction of agarose concentration promotes both invasion and apparent transmission of mechanical information through the matrix.

Our findings also have interesting connections to the recent work of Rosenfeld, Canoll, and colleagues, who found that under some conditions, glioma cell migration is rate-limited by the size of 3D matrix pores, and that below a critical pore size, these cells recruit nonmuscle myosin II (NMMII) to deform the nucleus and allow pore traversal (159). This notion is consistent with

our observation of MAT with increasing agarose concentration, because amoeboid motility is also accompanied by recruitment of myosin motors (262). Thus, we would predict that repetition of these studies in the setting of NMMII inhibition would abrogate amoeboid motility and impair cellular invasion into agarose-rich gels. Also, it is noteworthy that cellular invasion is abrogated in the absence of collagen at all agarose concentrations (Fig. 3.6), suggesting that U373-MG cells cannot transition to a ligand-independent mode of motility as has been reported for other cell types (262). Finally, the MAT we observe in agarose-rich gels is strikingly similar to a recent report of MAT in U87-MG glioma cells, in which Yamazaki et al. examined the roles of RhoA and Rac1 signaling in cell migration through 3D collagen gels (252). In this system, Rac1 signaling promoted mesenchymal motility via WAVE/Arp2/3-dependent formation of cellular protrusions and adhesions, whereas RhoA signaling promoted amoeboid motility via Rho/ROCK pathway-mediated actomyosin contractility. This is consistent with the classically-observed antagonistic relationship between Rho and Rac GTPases in 2D cell migration and begs the question of whether RhoA and Rac1 play similar regulatory roles in our system. Biochemical studies and live-cell cytoskeletal imaging should help to clarify this issue.

3.6 Conclusions

In summary, we have introduced a materials platform in which we can modulate the biophysical properties of collagen I matrices in a simple, straightforward, and cost-effective manner. By combining multiple ultrastructural characterization methods with high-resolution live-cell imaging, we have used this system to explore the interplay between mechanics, microstructure and motility in human glioma cells. We anticipate that the approaches described in this study may prove valuable for probing the invasive behavior of a wide variety of tumor cell systems and, more generally, for investigating the effect of biophysical signals encoded in 3D matrices on cellular mechanobiology.

3.7 Acknowledgements

Chapter 4. Glioma cell-extracellular matrix interactions in collagen-agarose matrices: Microscale mechanisms of agarose-induced disruption of collagen remodeling

4.1   Abstract

Cells are strongly influenced by the local structure and mechanics of the extracellular matrix (ECM). In Chapter 3 of this dissertation, we showed that adding agarose to soft collagen ECMs can mechanically stiffen these hydrogels by two orders of magnitude while limiting 3D cell motility, which we speculated might derive from agarose-mediated inhibition of collagen fiber deformation and remodeling. Here, we directly address this hypothesis by investigating the effects of agarose on cell-collagen interactions at the microscale. Addition of agarose progressively restricts cell spreading, reduces stress fiber and focal adhesion assembly, and inhibits macroscopic gel compaction. While time-of-flight secondary ion mass spectrometry and scanning electron microscopy fail to reveal agarose-induced alterations in collagen ligand presentation, the latter modality shows that agarose strongly impairs cell-directed assembly of large collagen bundles. Agarose-mediated inhibition of cell spreading and cytoarchitecture can be rescued by β-agarase digestion or by covalently crosslinking the matrix with glutaraldehyde. Based on these results, we argue that cell spreading and motility on collagen requires local matrix stiffening, which can be achieved via cell-mediated fiber remodeling or by chemically crosslinking the fibers. These findings provide new mechanistic insights into the regulatory function of agarose and bear general implications for cell adhesion and motility in fibrous ECMs.

4.2 Introduction

The ability of the extracellular matrix (ECM) to present localized biomechanical and biochemical cues to resident cell populations is as critical to proper cell and tissue function as the structural support it provides. Indeed, it is now well established that the geometry, elasticity, and dimensionality of the ECM can act through specific cell-matrix adhesion receptors to control a wide variety of cell behaviors central to tissue homeostasis (263-267). However, it has only recently begun to emerge that the microscale context of this signaling plays a critical role in modulating these interactions. For example, native ECMs are often structurally and mechanically anisotropic on the cellular length scale, and cells may locally remodel ECM fibers and other microcomponents to create microenvironments that instruct or permit cell behavior in ways that are not intuitively predictable from the bulk properties of the matrix (224, 268, 269). Thus, the development of biomaterial systems that facilitate detailed interrogation of cell-ECM interactions at the microscale have the potential to yield fundamental insight into the nature of normal and perturbed crosstalk between cells and the surrounding ECM. This in turn could inform the design of material scaffolds that manipulate these interactions in tissue engineering and regenerative medicine applications.

A growing number of biomaterial systems allow manipulation of one or more microscale, matrix-linked cell-instructive cues, including microenvironmental mechanics, topography, and biochemistry (221, 222, 254, 255, 259, 270, 271). Reconstituted collagen hydrogels have become one of the most commonly used 3D cell culture models for studying the effect of these cues, largely because type I collagen is the most abundant protein in the human body and can be readily reconstituted to form a 3D scaffold in vitro (218). Importantly, the nonlinear elasticity of collagen and other fibrillar ECMs can render cellular responses to matrix biophysical properties dramatically different from those observed when similar matrix-linked cues are presented in

linearly elastic biomaterial systems such as polyacrylamide and other highly crosslinked polymer networks (32, 199). For example, the strain-stiffening behavior of 3D collagen gels can allow mammalian cells to spread on the surface of ECMs of low bulk elastic moduli that would otherwise only be expected to support a rounded cell morphology (224, 249). This occurs because as cells deform individual collagen fibers by even modest amounts, the fibers stiffen dramatically and present an effective high-elasticity microenvironment even though the bulk elasticity of the material remains relatively low. Understanding cellular remodeling in these matrices is of particular physiological relevance given the ubiquity of type I collagen and other fibrous proteins in connective tissue matrices. Moreover, many if not most soft tissues in the body are comprised of fibrillar collagen meshed with non-fibrillar collagens and other components such as laminin and fibronectin; while our understanding of how cells interact with single-component fibrous matrices is slowly beginning to advance, relatively little is understood about how cell-ECM interactions and resulting cell behaviors are modified by the presence of both fibrillar and non-fibrillar ECM components.

Composite collagen-agarose hydrogels have recently been developed in which fibrillar collagen is co-assembled with the linear marine polysaccharide agarose, which is biocompatible but bioinert to mammalian cells (241, 244, 249, 272). In Chapter 3 of this dissertation, we described the creation of a collagen-agarose composite hydrogel system in which the mechanical properties of 0.5 mg/mL native collagen I hydrogels are directly modulated via incorporation of agarose (249). We showed that adding agarose to soft collagen ECMs can mechanically stiffen these hydrogels by two orders of magnitude while limiting 3D cell motility, which we speculated might derive in part from agarose-mediated inhibition of collagen fiber deformation and remodeling. Through a combination of single-cell immunofluorescence and electron microscopy imaging, mass spectrometric analysis, and measurements of cell contraction, we now provide direct mechanistic support for these ideas. Our results support a model in which agarose restricts local matrix stiffening by interfering with collagen fiber deformation and bundling, despite the fact that agarose increases matrix stiffness in bulk. In addition to providing new insights into agarose-induced disruptions of collagen remodeling, our findings have general implications for the micromechanics of composite fibrillar-nonfibrillar ECMs in vivo and the use of such matrices in tissue engineering and regenerative medicine applications.

4.3   Materials and Methods

4.3.1   Synthesis and characterization of ECM substrates

Collagen and collagen-agarose matrices were prepared as previously described (249), except PBS was used for matrix reconstitution instead of DMEM as noted. Pre-digestion of molten 2% agarose in PBS was accomplished via incubation with β-agarase (Lonza, Rockland, ME) for 2 h at 45°C according to manufacturer's instructions; the solution was heated to 95°C to fully inactivate the β-agarase prior to synthesis of collagen-agarose hydrogels. Matrix crosslinking was accomplished following full gelation via overnight incubation with a superlayer of 0.2% glutaraldehyde (Electron Microscopy Sciences, Hatfield, PA). Glutaraldehyde-treated hydrogels were washed extensively with PBS and soaked in 8% L-glutamic acid, pH 7.4, for 48 h to

quench residual glutaraldehyde (273) prior to extensive washing and cell seeding on the gel surface.

4.3.2   Cell culture

U373-MG human glioma cells were obtained from the Tissue Culture Facility at the University of California, Berkeley and cultured in Dulbecco's Modified Eagle medium (DMEM, Life Technologies, Grand Island, NY) supplemented with 10% Calf Serum Advantage (J.R. Scientific, Woodland, CA) and 1% penicillin/streptomycin, MEM nonessential amino acids, and sodium pyruvate (Life Technologies).

4.3.3   Electron microscopy

Silicon wafers were functionalized with 0.1 N NaOH, 3'aminopropyltriethoxysilane, and 0.5% glutaraldehyde and washed extensively with deionized water prior to sterilization with 70% ethanol. Collagen-agarose solutions were dispensed onto treated silicon wafers prior to gelation, and incubated at 37°C at high humidity for at least 45 minutes prior to cell seeding. Cells were cultured for 48 hours prior to fixation, dehydration, and sputter-coating for electron microscopy as previously described (249). We note that β-agarase-digested agarose oligomers are alcohol-soluble, as per manufacturer's information; therefore, when imaging ethanol-dehydrated SEM samples from our digestion studies, we selected regions of the gels in which the agarose oligomers were not completely washed away during sample processing.

4.3.4   Time-of-Flight Secondary Ion Mass Spectrometry (ToF-SIMS) measurements and Principal Component Analysis (PCA)

Collagen-agarose solutions were prepared in PBS, polymerized as thin films on glass slides and dried at 37°C. ToF-SIMS measurements were carried out with a TOF-SIMS V instrument (ION-TOF GmbH, Germany), by using 25 keV Bi_3^{2+} primary ions. The analysis area of 150 x 150 μm^2 was randomly rastered by the primary ions and was charge-compensated for glass-slide samples by low-energy electron flooding. The primary ion dose density was maintained below 1.0×10^{12} ions/cm^2 to ensure static SIMS conditions. Mass resolution was higher than 5000 at $m/z < 500$ in both positive and negative modes. To conduct PCA analysis, 3 positive and 3 negative spectra were acquired from each sample, respectively. For internal mass calibration, CH_3^+, $C_2H_3^+$ and $C_3H_5^+$ peaks were used for positive spectra and CH^-, C_2H^- and C_3H^- peaks were used for negative spectra. PCA analysis was performed on SIMS spectra using a PLS_Toolbox (version 5.2, Eigenvector Research, Manson, WA) for MATLAB (version 7.1, MathWorks Inc., Natick, MA). Each peak was selected by using the auto-peak searching algorithm in the Ion-Specs software (ION-TOF GmbH, Germany) and normalized by using the summation of the intensity of the selected peaks to eliminate systematic differences between the spectra, and then mean-centered before PCA (274, 275).

4.3.5   Phase contrast and fluorescence microscopy

All phase contrast and fluorescence imaging was performed using an inverted Nikon TE2000-E2 microscope equipped with a motorized, programmable stage (Prior Scientific, Inc, Rockland,

MA), an incubator chamber to maintain constant temperature, humidity, and CO_2 levels (In Vivo Scientific, St. Louis, MO) during live-cell imaging, a digital camera (Photometrics Coolsnap HQ II, Roper Scientific, Tucson, AZ), and SimplePCI software (Hamamatsu Corporation, Sewickley, PA). Immunofluorescence staining for F-actin, nuclear DNA, and the focal adhesion protein vinculin was accomplished as previously described in detail (199).

4.3.6   Hydrogel contraction assays

Collagen-agarose matrices were prepared with U373-MG cells fully embedded in 3D or plated on the 2D surface of fully polymerized gels as noted. After 24 hours of culture, gels were carefully detached from the edges of each well with a thin, sterile blade and allowed to contract for at least 48 hours prior to imaging with a handheld Canon PowerShot SD780 IS digital camera set in macro mode. Percentage gel contraction was measured using ImageJ software to manually identify the edge of the well and contracted gel, respectively (276). Data reported are mean ± standard deviation for 4 gels per condition in one experiment. Experiments were repeated in triplicate with qualitatively consistent results.

4.3.7 Parallel plate rheometry

Collagen-agarose matrices were prepared in PBS and gelled at 37ºC and high humidity for at least 2 h prior to rheological analysis. All measurements were taken with an Anton Paar Physica MCR-301 rheometer (Anton Paar USA, Temecula, CA) at 37ºC and high humidity using a 25 mm parallel plate geometry and Rheoplus software. Frequency sweeps at 5% strain over the range 0.1–10 Hz were used to extract the storage modulus, loss modulus, and complex modulus of each sample as previously described (249). At least five samples were measured for each gel formulation; reported shear moduli represent mean ± standard deviation at 1 Hz.

4.4 Results

4.4.1   Cell-mediated bundling of collagen fibers

We began by directly visualizing associations between cells and collagen fibers in the presence of varying concentrations of agarose. In Chapter 3 of this dissertation, we used live-cell Nomarski differential interference contrast (DIC) microscopy to image glioma cells and surrounding collagen fibers simultaneously, and saw evidence of enhanced collagen bundling in low-agarose content gels (249). However, the limited spatial resolution of DIC imaging makes it difficult to visualize all but the largest collagen bundles or to colocalize bundles with cellular migratory processes. Thus, to investigate this finding more deeply, we began here by imaging glioma cells on collagen and collagen-agarose matrices using scanning electron microscopy (SEM). SEM of glioma cells adherent to the surface of native 0.5 mg/mL collagen I hydrogels revealed clear cell-directed bundling of collagen into large fibers, which was especially pronounced at the tips of cell protrusions into the matrix (Fig. 4.1). When agarose was introduced at low concentrations, the intercalating agarose network modestly restricted glioma cell spreading and collagen fiber bundling (Fig. 4.2). However, at high agarose concentrations, cells on the gel surface were rounded and appeared to have restricted capacity for remodeling, as

evidenced by a decrease in the number of collagen fiber bundles oriented radially away from the cell body (Fig. 4.3). In these cases, the random orientation of collagen fibers located on the gel surface a short distance away from the cell body supports our previous speculation that the presence of agarose restricts long-range transmission of cell-generated forces through collagen matrices (249). We note that the apparent change in the surface density of collagen fibers as agarose content is increased can be partially attributed to incidental compaction of the gels during SEM sample preparation (277) and partially attributed to apparent differences in localized cell-mediated compaction of collagen fibers during culture, a process that is strongly regulated by the pericellular microenvironment (278). We also note that our previous in situ imaging studies of cell-free matrices revealed no appreciable difference in collagen microstructure between 0.5 mg/mL collagen gels containing 0% and 0.25% w/v agarose (249).
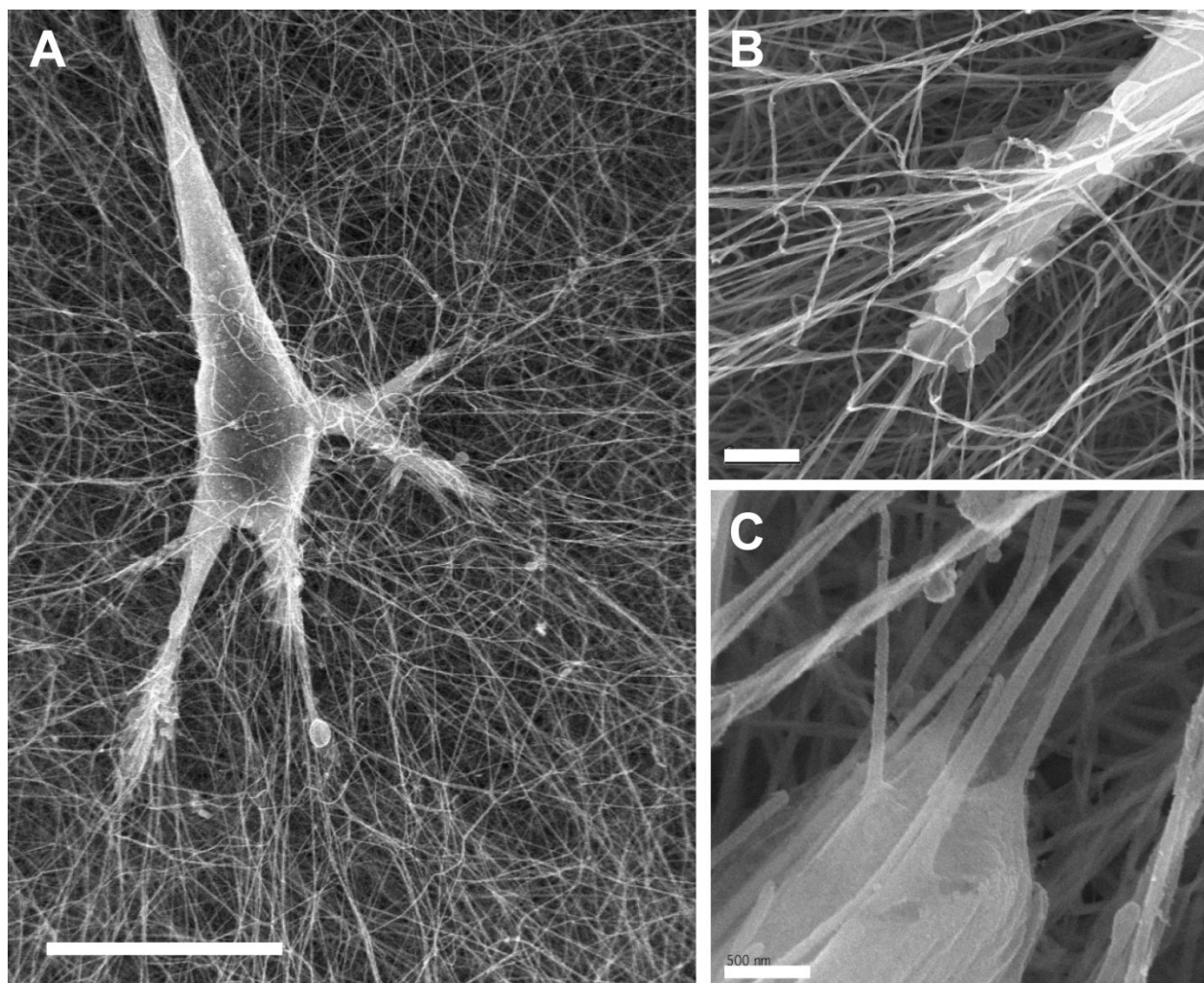

Figure 4.1. Scanning electron microscopy images of a U373-MG glioma cell on a 0.5 mg/mL collagen matrix. A. Low magnification image of a single cell. Bar is 20 μm. B. High magnification image of a cell protrusion in the collagen matrix. Bar is 2 μm. C. The tip of a cell protrusion with bound collagen fibers. Bar is 500 nm.

Figure 4.2. Scanning electron microscopy images of a U373-MG glioma cell on a 0.5 mg/mL collagen matrix containing 0.125% w/v agarose. A. Low magnification image of a single cell. Bar is 10 μm. B. High magnification image of a cell protrusion in the matrix. Bar is 2 μm. C. The tip of a cell protrusion with bound collagen fibers. Bar is 1 μm.

4.4.2 Molecular structure of collagen

Cell adhesion and remodeling of collagen-agarose matrices can be affected not only by matrix mechanics but also by the surface chemistry of exposed collagen binding motifs in the matrices. Thus, we investigated changes in the molecular conformation of collagen fibers at the surface of dried collagen-agarose matrices with time-of-flight secondary ion mass spectrometry (ToF-SIMS). ToF-SIMS can characterize the surface chemistry of protein films because of its chemical selectivity and surface sensitivity with a sample depth of ~1 nm (279). We obtained ToF-SIMS positive spectra from collagen-agarose matrices of varying composition (Fig. 4.4A). As described previously (274, 275), by applying the multivariate principal component analysis (PCA) technique, we were able to reduce a complex set of ToF-SIMS spectra to quantitatively interpretable scores and loading plots, which reflect the relationship among samples as well as the relationship between original variables (spectral peaks) and new variables (principal components), respectively.

We completed PCA for peak lists selected by an auto peak search of the positive ToF-SIMS spectra acquired from collagen-agarose hydrogels, as well as pure collagen and pure agarose. Scores and loadings for the first principal component (PC 1) from this analysis show that the
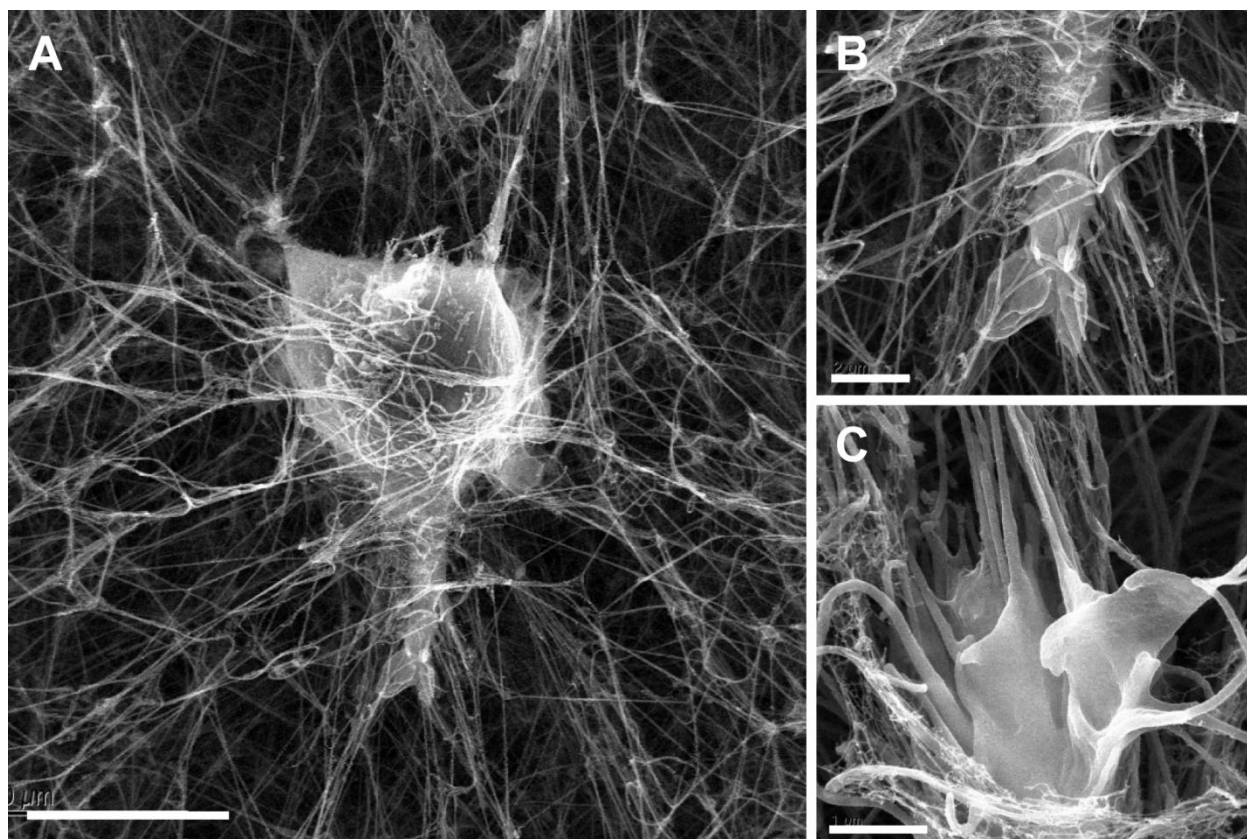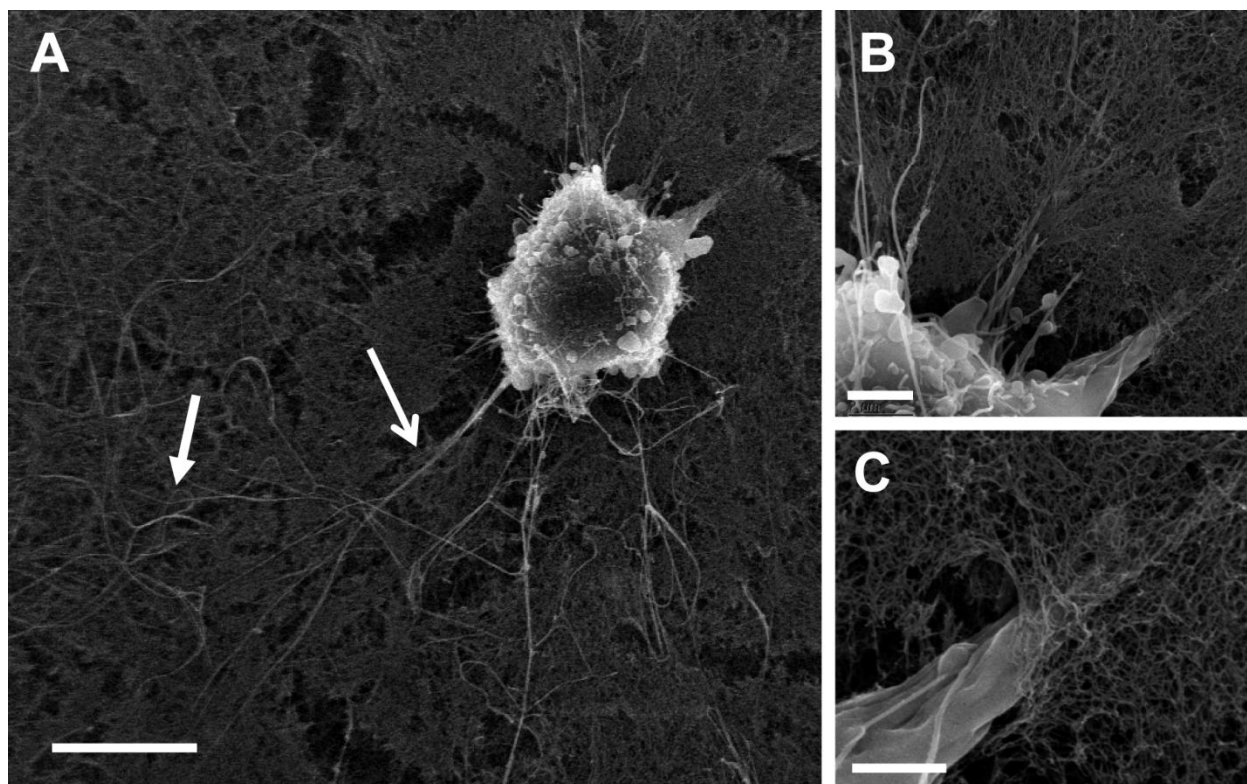
Figure 4.3. Scanning electron microscopy images of a U373-MG glioma cell on a 0.5 mg/mL collagen matrix containing 0.5% w/v agarose. A. Arrows highlight randomly oriented native collagen fibers in the matrix (closed), in contrast to the aligned collagen fibers found near glioma cells (open). Bar is 10 μm. B. Aligned collagen fibers extending into the matrix at the cell edge. Bar is 2 μm. C. A cell protrusion extends through the agarose matrix. Bar is 1 μm.

surface chemistry of 0.5 mg/mL collagen gels does not vary significantly across matrix formulations as the agarose content is increased to 0.4% w/v (Fig. 4.4B and C). The loading plots for PC 1 reveal differences in the compositions of the outer surface of the matrices. For peaks loading positively on PC 1 such as 30 (cysteine), 44 (alanine/cysteine/lysine), 70 (arginine/leucine/proline/threonine) and S containing SO_3H, C_2SO_2, and C_3SO_2 peaks, the intensities contribute to positive PC 1 scores. Thus, the relative concentrations corresponding to these peaks should be higher in samples with positive PC 1 scores. Conversely, for peaks loading negatively on PC 1 such as Na containing C_2HNa and $HSNa_2$ peaks and agarose fragment peaks of m/z 165, 180, 186, 196, 289, and 305, the corresponding surface species should be more prevalent in agarose. The scores on PC 1 of collagen and agarose mixture gels with agarose content up to 0.4% w/v (0.5C/0.4A) are similar to that of pure collagen fibers. This suggests that the addition of agarose does not modify the surface composition or molecular configuration of collagen fibers in 0.5 mg/mL collagen matrices up to 0.4% w/v agarose.

4.4.3 Cellular adhesion and contractility

Our imaging and ToF-SIMS data suggest that the observed differences in glioma cell spreading and bundling of collagen fibers are not attributable to initial differences in exposed collagen as the concentration of agarose is increased. Because engagement of ECM fibers by adhesion
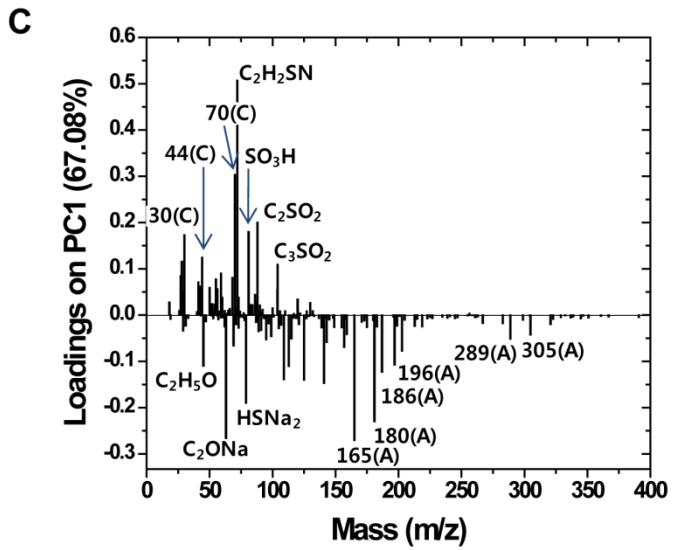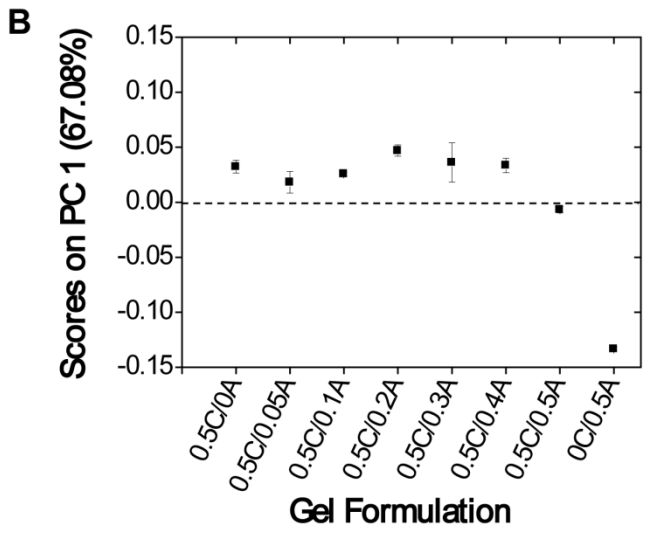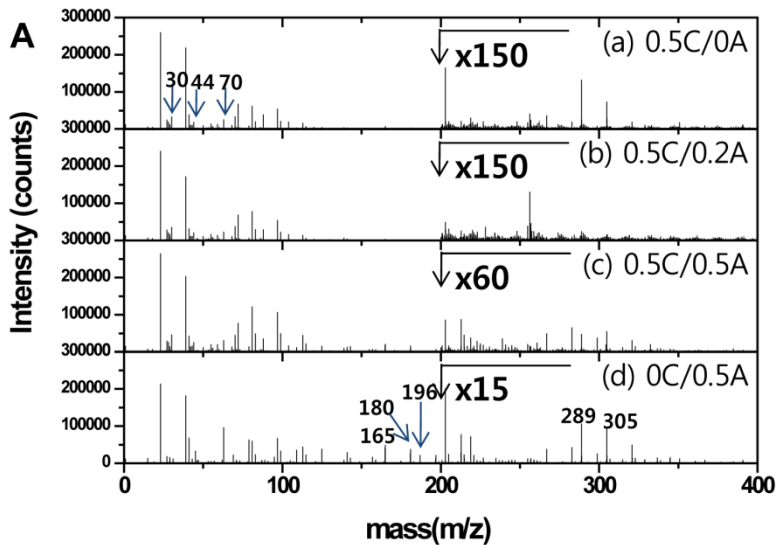
Figure 4.4. Effect of agarose content on the molecular conformation of collagen fibers in matrices containing 0.5 mg/mL collagen (0.5C) and 0 – 0.5% w/v agarose (0A – 0.5A).

A. Positive ToF-SIMS spectra obtained from samples containing (a) 0.5C, (b) 0.5C/0.2A, (c) 0.5C/0.5A, and (d) 0C/0.5A. B,C. Plots of PC 1 (B) scores and (C) loadings from PCA of positive ion spectra obtained from collagen-agarose gels with indicated compositions. Peaks were selected by auto peak searching.

receptors is a necessary first step for generation of contractile forces against these fibers, we next asked whether an increasing agarose concentration also compromises the ability of cells to mobilize the intracellular adhesive and contractile machinery. To assess microscale cell contractility, we used immunofluorescence imaging to visualize actin cytoskeletal assembly and focal adhesion maturation. We found that glioma cells on low-agarose content gels form actomyosin stress fibers and robust vinculin-positive focal adhesions, and that these structures become progressively less prominent as the agarose content of the matrix is increased (Fig. 4.5A and B). We then evaluated macroscale contractility by conducting bulk gel contraction assays in which U373-MG cells were fully embedded inside gels with varying agarose content. Here, measurements of projected gel area were taken 48 h after the gels were detached from the edges of the wells as a macroscopic measure of the ability of embedded cells to remodel and contract the ECM. We found that gel contraction is inversely related to agarose content, with cells compacting gels by 40-50% at low agarose concentrations and <5% at high agarose concentrations (Fig. 4.5C). Together, these two data sets support the notion that cells on agarose-poor gels are in a more highly contractile state and are able to deform and remodel individual collagen fibers to a much greater extent than cells in agarose-rich gels.

4.4.4   Chemical crosslinking and agarose digestion

The above results indicate that incorporation of agarose into collagen ECMs reduces cell contractility. This is somewhat surprising given that we previously showed that agarose increases the elasticity of entangled 0.5 mg/mL collagen networks by several orders of magnitude without appreciably altering the collagen microstructure (249); traditionally, one would expect increasing matrix stiffness to be associated with increased cell spreading and contractility (199). We reasoned that this apparent contradiction could be explained by considering the non-affine mechanical properties of fibrillar matrices, where the non-linear propagation of applied stresses in collagen gels stands in stark contrast to the propagation of stresses through linearly elastic culture materials such as polyacrylamide (224, 249). In other words, even though agarose increases the *bulk* stiffness of collagen hydrogels, it reduces *microscale* stiffness because it interferes with the strain-stiffening and remodeling properties of collagen. To directly test this hypothesis, we investigated the effects of two additional modifications to our collagen matrices: disruption of collagen fiber remodeling via covalent crosslinking and partial disruption of the agarose network via enzymatic digestion. We reasoned that because covalent crosslinking stiffens the matrix on all length scales but reduces the ability of cells to remodel and compact the collagen network, it should rescue cell spreading and elaboration of stress fibers and focal adhesions without rescuing collagen bundling or bulk gel contraction. Conversely, partial digestion of the agarose should rescue both cell spreading and cell-mediated matrix remodeling for all gel formulations because it disrupts the intercalating agarose network, restores the collagen to a nonlinearly elastic regime, and liberates it for cell-directed remodeling.
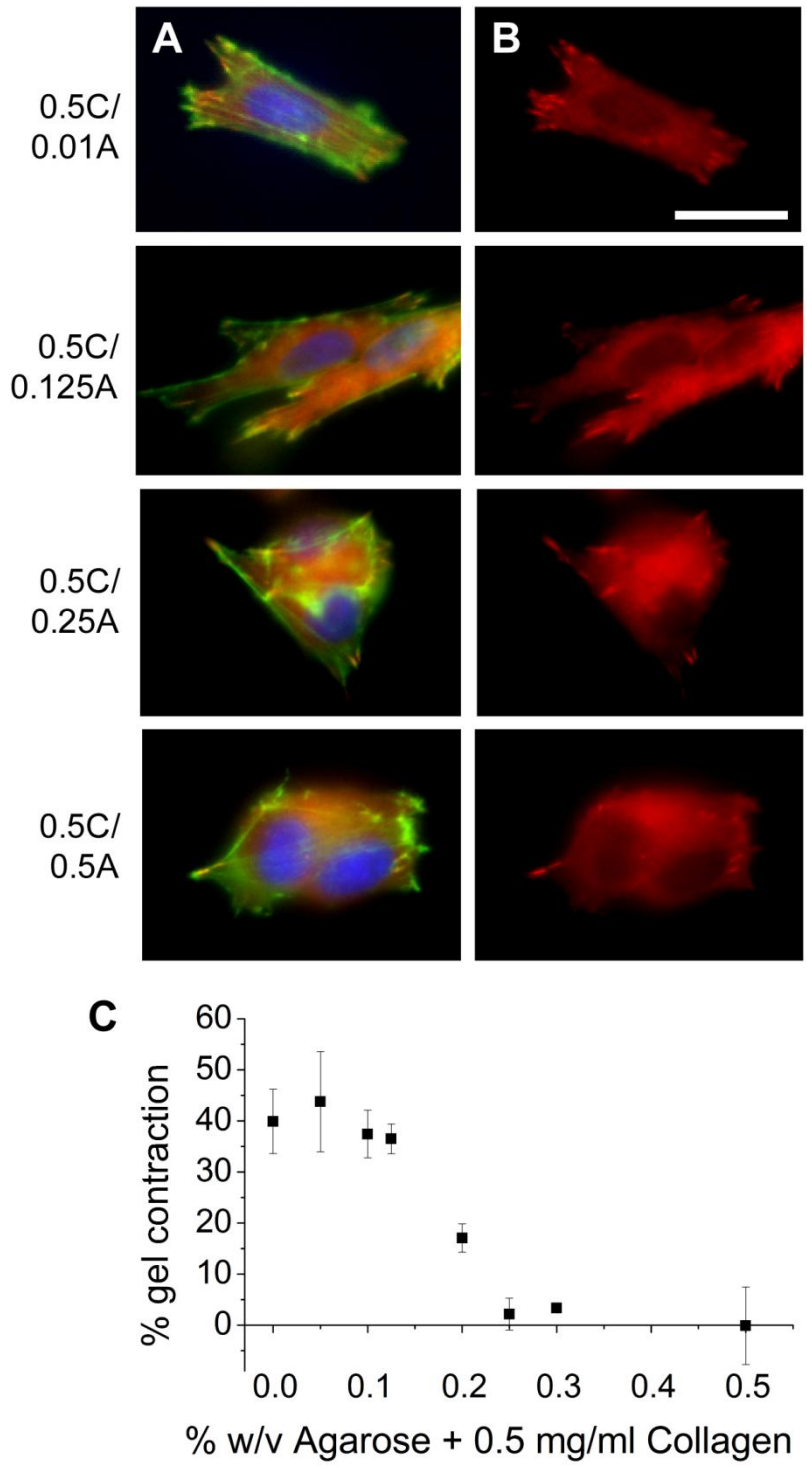
Figure 4.5. Effect of agarose content on cellular contractility. A. Fluorescence imaging of cytoskeletal and adhesive structures of U373-MG cells cultured on the surface of 0.5 mg/mL collagen gels (0.5C) containing 0 − 0.5% w/v agarose (0A − 0.5A). Cells were stained for F-actin (green), nuclear DNA (blue) and the focal adhesion protein vinculin (red). B. Isolated view of vinculin signal only. Bar is 25 μm. C. Percentage gel contraction for U373-MG glioma cells cultured within the 3D matrix, measured 48 hours after detachment.

Indeed, we found that cells are able to spread on the surface of glutaraldehyde-crosslinked collagen-agarose matrices, including gels containing 0.5% w/v agarose that would otherwise result in cell rounding (Fig. 4.6). Importantly, these glutaraldehyde-crosslinked gels lack the prominent cell-directed fiber bundles characteristic of pure collagen gels, showing that cells can spread on these matrices without requiring substantial matrix remodeling (Fig. 4.7). It also confirms that the agarose does not simply act by sterically blocking adhesion sites on collagen, as glutaraldehyde crosslinking should in principle be unable to overcome such barriers. Similarly, we find that partial enzymatic pre-digestion of agarose with β-agarase rescues cell spreading and matrix reorganization on high-agarose content matrices (Fig. 4.6). Under these digestion conditions, the agarose still lightly coats the collagen fibers without forming a continuous network throughout the hydrogel (Fig. 4.8), indicating that the presence of an intact agarose network, and not merely the constituent agarose oligomers, is required to induce the cell rounding and decrease in cell contractility observed in high-agarose content matrices. We note that doubling the collagen concentration to 1 mg/mL also enhances cell spreading on the surface of gels containing 0.5% w/v agarose (Fig. 4.6), illustrating that a substantial increase in initial ligand availability can also rescue cell spreading on high-agarose content matrices.

To gain additional insight into the mechanism governing the observed rescue of cell spreading on these modified matrices, we first used parallel plate rheology to evaluate the bulk shear modulus of each gel formulation. As expected, we found that glutaraldehyde crosslinking stiffens low-agarose content gels; with increasing agarose content, the elastic moduli of crosslinked and non-crosslinked matrices converge, presumably as the gels transition from a regime in which gel mechanics are dominated by the collagen network to one in which the agarose network is the main determinant of gel mechanics (Fig. 4.9A). Likewise, β-agarase digestion abrogated agarose-induced gel stiffening in all gel formulations. We note that a decrease in measured shear moduli here compared to our previous measurements (249) is not unexpected since these samples were subjected to more extensive handling and washing over multiple days following glutaraldehyde and L-glutamic acid treatment, and the slightly higher ionic strength of PBS (0.193) than that of DMEM (0.169) (280) would be expected to result in softer gels as well (281). Finally, we evaluated the effect of collagen crosslinking and agarose digestion on cell-mediated matrix remodeling. To do so while avoiding glutaraldehyde cytotoxicity, we modified our contraction assay to plate cells on the 2D surface of fully polymerized gels. We found that glutaraldehyde restricts the ability of cells to contract gels at all agarose concentrations, whereas β-agarase digestion rescues this ability (Fig. 4.9B). Immunofluorescence imaging of cellular cytoskeletal and adhesive structures on glutaraldehyde-crosslinked 0.5C-0.5A gels reveals actomyosin stress fibers, indicating that cells are in a highly contractile state despite their inability to contract the gels (Fig. 4.9C).

4.5   Discussion

We demonstrated in Chapter 3 of this dissertation that incorporation of agarose can increase the shear modulus of soft 0.5 mg/mL type I collagen ECMs by two orders of magnitude while limiting 3D glioma cell invasion, which we speculated might be partly derived from agarose-mediated inhibition of collagen fiber deformation and remodeling (249). Here, we have provided direct mechanistic support for this hypothesis. Despite the fact that agarose does not
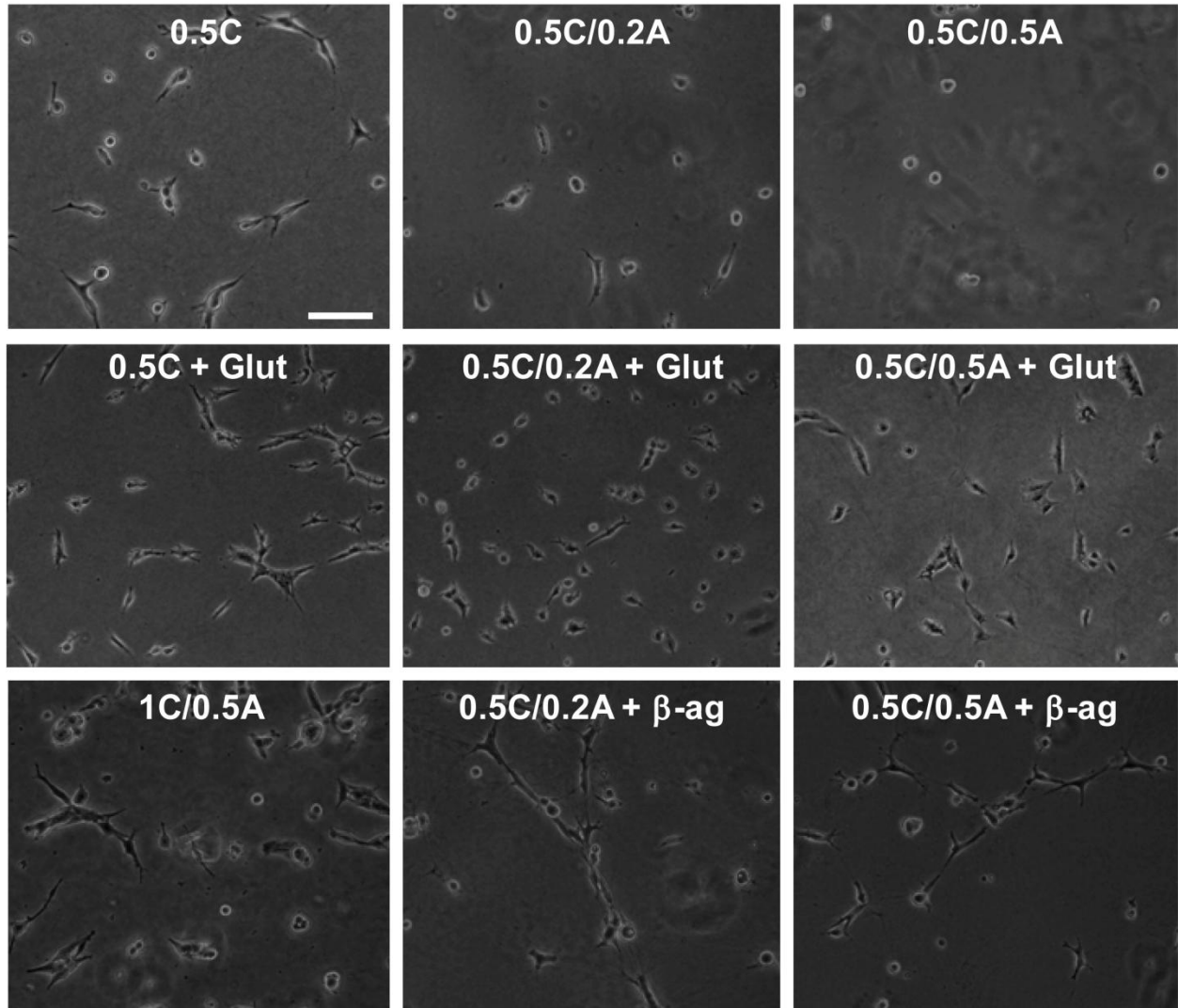
Figure 4.6. Effect of agarose degradation or collagen crosslinking on glioma cell morphology. Live-cell phase contrast imaging of U373-MG cells cultured for 24-48 hours on the surface of matrices containing 0.5 – 1 mg/mL collagen (0.5C – 1C) and 0 – 0.5% w/v agarose (0A – 0.5A). Crosslinking was accomplished via overnight incubation with 0.2% glutaraldehyde following gel polymerization (+Glut). β-agarase was used for pre-digestion of agarose prior to gel synthesis (+β-ag). Scalebar is 100 μm.

affect collagen presentation in matrices containing up to 0.4% w/v agarose, it strongly decreases glioma cell contractility and matrix remodeling. Either chemical crosslinking of these composite matrices with glutaraldehyde or enzymatic digestion with β-agarase rescues agarose-induced inhibition of cell spreading and cytoarchitecture, whereas only β-agarase digestion (but not glutaraldehyde crosslinking) rescues cell-mediated bulk matrix contraction. Thus, cell spreading and motility on collagen requires local matrix stiffening, which can be achieved either by chemically crosslinking the fibers or by allowing the cells to remodel the fibers into large bundles. Agarose precludes this local stiffening because it prevents bundling while also failing to mechanically couple the fibers and offer resistance to cellular contractile forces. However, whereas cell-mediated bundling is a local phenomenon that cumulatively leads to gel contraction
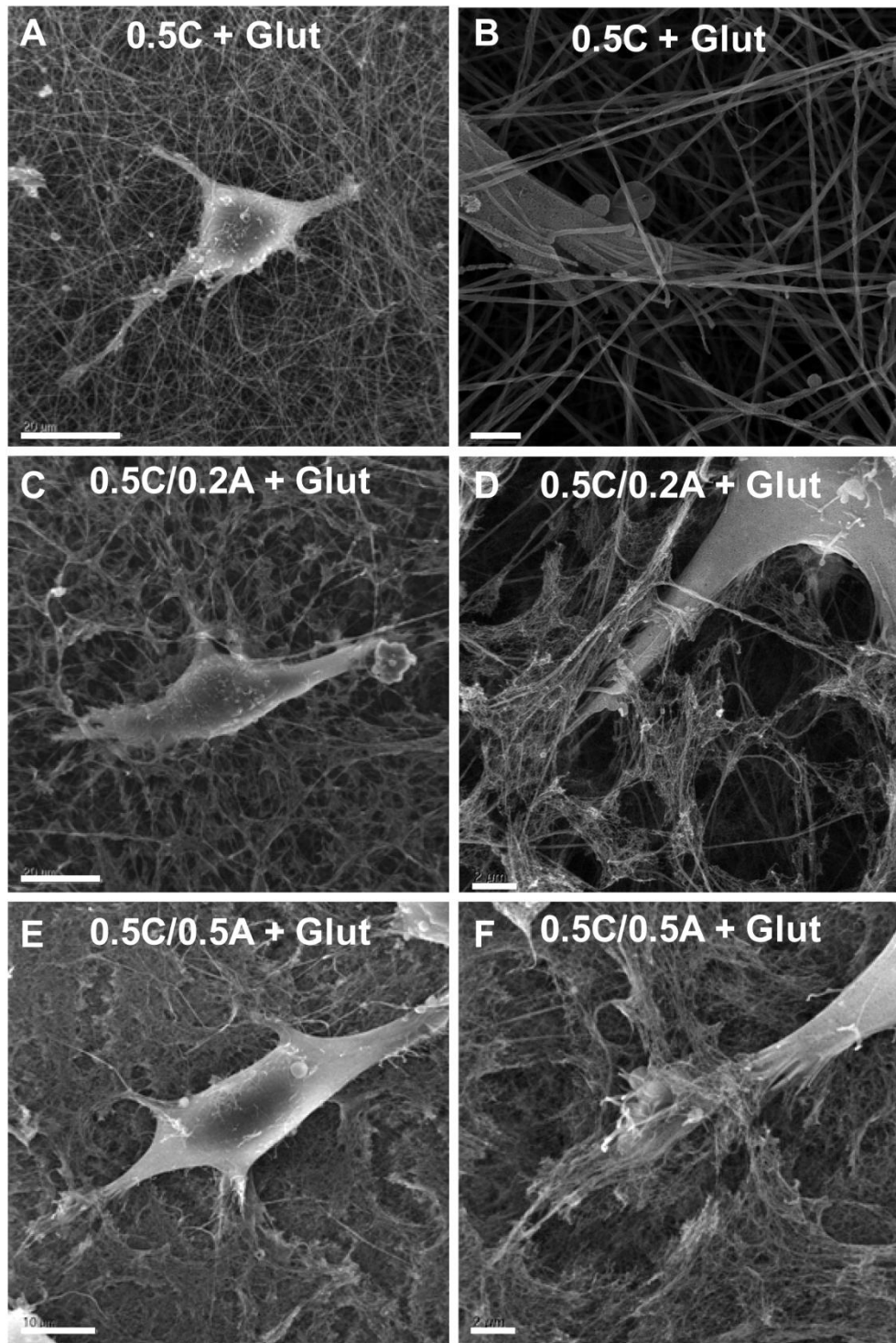
Figure 4.7. **Scanning electron microscopy images of U373-MG glioma cells on glutaraldehyde-crosslinked collagen-agarose matrices.** A. Low magnification image of a single cell on a 0.5 mg/mL crosslinked collagen matrix. Bar is 20 μm. B. High magnification image of a cell protrusion in the crosslinked collagen matrix. Bar is 1 μm. C. Low magnification image of a single cell on a 0.5 mg/mL crosslinked collagen matrix containing 0.2% w/v agarose. Bar is 20 μm. D. High magnification image of a cell protrusion in the crosslinked collagen-agarose matrix. Bar is 2 μm. E. Low magnification image of a single

cell on a 0.5 mg/mL crosslinked collagen matrix containing 0.5% w/v agarose. Bar is 10 μm. F. High magnification image of a cell protrusion in the crosslinked collagen-agarose matrix. Bar is 2 μm.

on the macroscale, chemical crosslinking stiffens the gel globally and therefore makes the gel resistant to macroscopic contraction. In other words, progressive incorporation of agarose increases the macroscale stiffness of collagen hydrogels while interfering with the ability of embedded cells to locally stiffen their environment, resulting in an effective *softening* of the cell-scale microenvironment in high agarose-content gels.

In addition to providing new insight into the mechanisms by which agarose interferes with cell-mediated collagen remodeling, our findings have general implications for the micromechanics of composite fibrillar-nonfibrillar ECMs and the use of such matrices in tissue engineering and regenerative medicine applications. First, our results indicate that cell spreading, local matrix remodeling, bulk matrix contraction, and cellular contractility are not necessarily correlated in matrices containing both fibrillar and non-fibrillar components. This disparity underscores the inherent complexity of 3D culture systems; as engineered biomaterial platforms become increasingly sophisticated in an effort to recapitulate the complexity of native tissues, associated design principles must anticipate and account for incongruities across length scales in cellular responses to fibrillar, nonfibrillar, and hybrid fibrillar-nonfibrillar matrix components. Second, these findings lend insight into the function of collagen and other fibrillar ECM components in defining matrix mechanics in vivo and in 3D culture systems. Specifically, it is important to understand the degree to which non-fibrillar components facilitate or interfere with microscale cell-directed remodeling of fibrillar components, as this remodeling may critically underlie establishment of polarity, migration, and other behaviors. Similarly, these nonfibrillar components may alter bulk matrix properties in ways that are uninformative or even misleading with respect to predicting cell responses; microscale matrix properties are much more relevant. A contemporaneous and independent study involving high-resolution rheological and optical characterization of cell-free collagen-agarose hydrogels seems broadly supportive of these ideas and specifically supports the notion that although collagen is traditionally thought of as the primary load-bearing element in most tissues, nonfibrillar ECM components can play a significant role in modulating cell-fiber interactions and overall tissue mechanics (282). With this in mind, additional methods will be needed to quantify microscale matrix mechanics in three-dimensional systems, such as those based on particle tracking microrheology (283) and inference of collagen fiber mechanics from image correlation spectroscopy (247).

To expand upon this last point, our observation that agarose can increase the bulk stiffness of collagen networks while effectively decreasing the local stiffness of the cell-scale microenvironment corresponds quite well to a theoretical study by Chandran and Barocas in which the underlying affine mechanics of a collagen network model was seen to be markedly different than a model of individual collagen fibril kinematics, which was instead found to be non-affine in nature (223). Because cells interact with collagen ECMs on the length-scale of individual fibers or bundles of fibers, it seems intuitive that cellular behavior should be correlated more with individual fiber mechanics than with macroscale hydrogel mechanics. This concept is also consistent with the recent observation that cellular compaction of collagen gels is limited to a zone that extends only tens of micrometers from the cell surface, which strongly

implies that cell-directed remodeling produces a local microenvironment with dramatically different mechanical properties than the macroscale material (278).

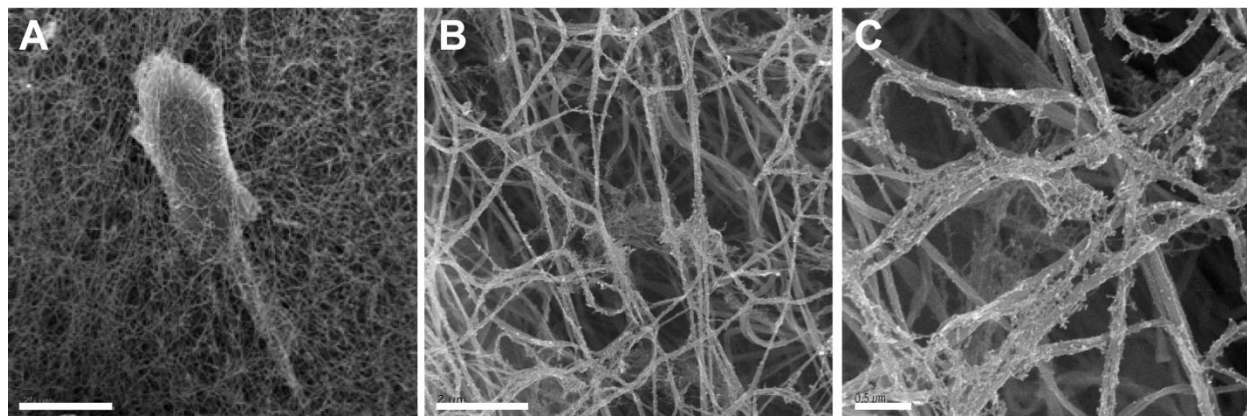**Figure 4.8. Scanning electron microscopy images showing the effect of agarose degradation on collagen-agarose matrices.** A. Low magnification image of a single U373-MG glioma cell cultured on the surface of a gel containing 0.5 mg/mL collagen and 0.2% agarose that had been pre-digested with Beta-agarase. Bar is 20 μm. B, C. High magnification images of gel structure. B. Bar is 2 μm. C. Bar is 0.5 μm.

We may also place our findings in the context of other recent studies of nonlinear matrix elasticity and its effect on cell-ECM interactions. Our observations of cell spreading and matrix remodeling in nonlinear collagen ECMs are in good agreement with a recent report by Winer et al., in which local strain-stiffening and non-linear propagation of cell-generated forces were seen to give rise to long-distance cell-cell communication and cell-fiber alignment during fibroblast or human mesenchymal stem cell culture on fibrin matrices (224). Importantly, pharmacologic inhibition of cellular contractility was seen to disrupt strain-stiffening behaviors on fibrin gels, underscoring the interdependence of cell mechanics and matrix mechanics, and reinforcing the link between cellular force generation and strain-stiffening of fibrillar matrices. These ideas have important implications for the design of tissue engineering constructs and for our understanding of the relationship between tissue stiffening and disease progression in a variety of contexts. For example, Provenzano and colleagues have observed distinctive patterns of collagen fiber reorganization into radially-oriented bundles at the tumor-stromal interface in vivo and in vitro that have been associated with tumor cell invasion (284). More recently, they have shown that the presence of these "tumor associated collagen signatures" both depends on generation of cellular contractile forces and is necessary to facilitate efficient invasion, suggesting that the ability to manipulate nonlinear ECMs is a critical early step in tumor progression (217). As a second example, the initiation of liver fibrosis has been associated with early-stage tissue stiffening resulting from modifications to the native collagen ECM (285), suggesting that the disease implications of these ideas extend beyond tumorigenesis.

Finally, while our collagen-agarose hydrogel system is not intended to be a physiological mimic of native tissues, we anticipate that this system will be valuable for further interrogation of cell-ECM interactions and the interactions between collagen fibers and nonfibrillar matrix components. Indeed, progress on this problem will depend on the creation of innovative 3D biomaterial systems that are collectively capable of deconstructing the rich biochemical and
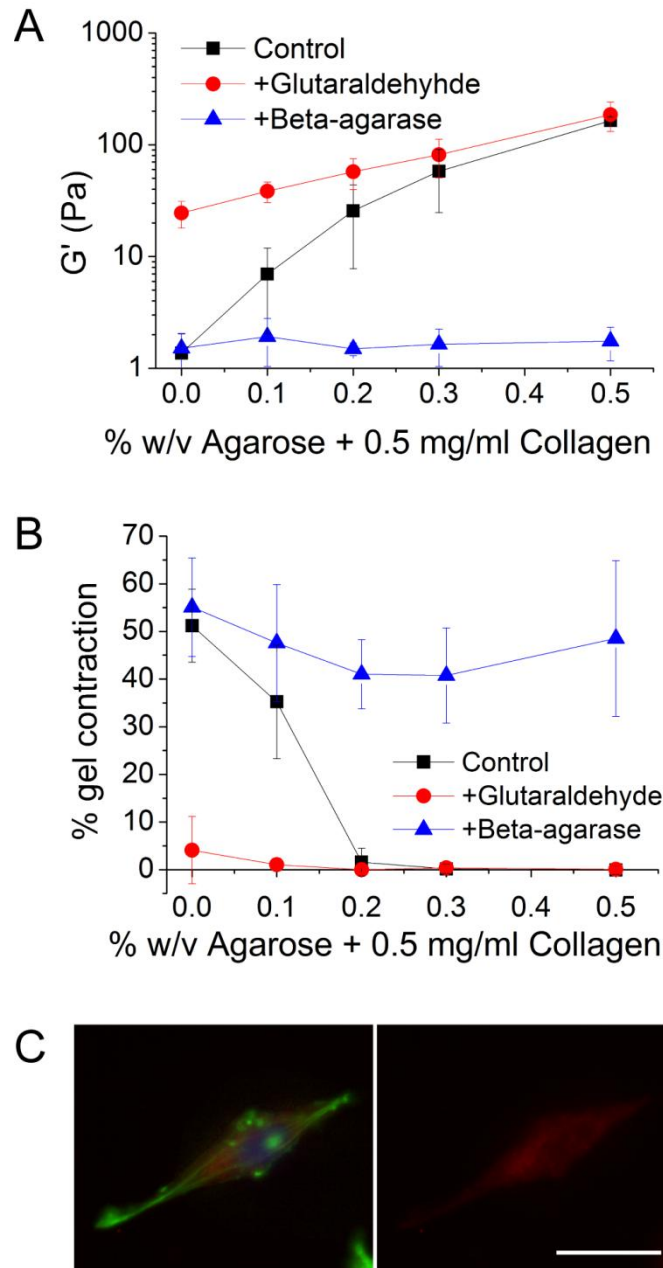
Figure 4.9. Effect of agarose degradation or collagen crosslinking on glioma cell contractility. A. Elastic modulus of 0.5 mg/mL collagen gels containing 0 – 0.5% w/v agarose that were treated with 0.2% glutaraldehyde overnight following gel polymerization (+Glutaraldehyde) or that were created with agarose that had been pre-digested with β-agarase prior to gel synthesis (+Beta-agarase). B. Percentage gel contraction for U373-MG cells cultured on the gel surface, measured 72 hours after gel detachment. C. Fluorescence imaging of cytoskeletal and adhesive structures of U373-MG cells cultured on the surface of 0.5C/0.5A + Glutaraldehyde gels. Cells were stained for F-actin (green), nuclear DNA (blue) and the focal adhesion protein vinculin (red). Bar is 25 μm.

mechanical diversity of the cellular milieu into experimentally tractable numbers of distinct interactions (286). We anticipate that the complementary insights gleaned from such 3D cell culture systems will ultimately bring us closer to the realization of 3D culture methodologies that truly can bridge the gap between current 2D platforms and animal models, as well as a maturation of our understanding of cell-ECM interactions that will facilitate creation of theoretical models with predictive power in complex tissue environments.

4.6   Conclusions

We have evaluated the microscale mechanisms of agarose-induced disruption of collagen remodeling by human glioma cells in composite collagen-agarose matrices. By combining high-resolution and macroscale measures of cellular contractility and matrix remodeling, we have provided direct support for the hypothesis that incorporation of agarose plays dual roles by increasing the bulk stiffness of collagen hydrogels while reducing microscale stiffness via disruption of the strain-stiffening and remodeling properties of collagen. Our results have general significance for the micromechanics of composite fibrillar-nonfibrillar ECMs in vivo and the use of such matrices in tissue engineering and regenerative medicine applications, and we anticipate that the approaches described in this study will prove valuable for detailed investigation of cell-ECM interactions in both fibrillar and composite fibrillar-nonfibrillar matrices.

4.7   Acknowledgements

Chapter 5. Concluding Remarks

This dissertation describes the application and development of technologies in the fields of bioengineering and biomaterials to address fundamental questions in the nascent field of glioma cell mechanobiology. As discussed in Chapter 1, the long history of clinical and biological glioblastoma multiforme research has created an almost desperate need for new perspectives and new approaches to understanding and ultimately therapeutically limiting GBM invasion and recurrence. The work presented in this dissertation demonstrates that microenvironmental mechanics is a critical regulator of glioma cell physiology and invasion in both 2D and 3D culture systems. While this work raises countless more questions than it has answered, the studies described here should help to lay the foundation for a multitude of very promising new research directions related to understanding and controlling cell-ECM interactions, the development of biomaterial systems for basic mechanobiology, tissue engineering, and regenerative medicine applications, and importantly, the pursuit of translational work that seeks to exploit the principles of glioma cell mechanobiology in therapeutic settings. In this chapter, I will summarize the results and significance of the preceding chapters, followed by brief descriptions of several promising ongoing projects that have directly grown out of this work.

5.1 Summary and significance

In Chapter 2, we used a series of biochemically identical 2D polymeric ECM substrates of defined mechanical rigidity (ranging from $0.08 – 119$ kPa) to directly demonstrate that the behavior of human glioblastoma multiforme cell lines is regulated by the mechanical rigidity of the cellular microenvironment. Our studies revealed stark rigidity-dependent differences in cell structure, motility, and proliferation (199). Specifically, tumor cells cultured on highly rigid ECMs spread extensively, formed prominent actomyosin stress fibers and mature focal adhesions, and migrated rapidly, whereas cells cultured on the most compliant ECMs (with rigidities comparable to normal brain tissue) appeared uniformly rounded and failed to productively migrate. Other members of the Kumar Laboratory have subsequently explored related aspects of glioma cell rigidity-sensitivity and mechanotransduction. For example, Sen et al. investigated the role of the focal adhesion protein α-actinin in glioma cell mechanobiology (287), motivated by the observations that α-actinin structurally couples the cellular adhesive and contractile machineries (288) and is significantly upregulated in high-grade astrocytomas (289). These authors found that suppression of either α-actinin isoform (1 and 4) in human glioma reduced cell motility and traction forces and compromised the ability of cells to mechanically adapt to changes in ECM stiffness (287). Importantly, our 2D studies on polyacrylamide ECMs collectively show that glioma cell rigidity-sensitivity can be blunted by direct or indirect pharmacologic inhibition of myosin-based contractility, providing support for a model in which ECM rigidity provides a transformative, microenvironmental cue that acts through actomyosin contractility to regulate the invasive properties of GBM tumor cells.

This model is consistent with the results of the 3D studies presented in Chapters 3 and 4 of this dissertation (249, 290). Here, we explored glioma cell motility and cell-matrix interactions in 3D collagen I matrices that were stiffened through the progressive addition of agarose. We found that the addition of agarose restricted glioma cell invasion by increasing steric barriers to motility and reducing the ability of tumor cells to bundle and remodel the collagen fibers. Consistent with this finding, Kaufman and colleagues recently manipulated pore size in collagen I matrices by controlling the temperature of gelation and showed that pore sizes below 4-6 μm

strongly limited glioma cell invasion speed (291). While microenvironmental mechanics are difficult to control in 3D cell culture models without altering integrin ligand density or microstructure, previous studies by Kaufman and others had also suggested that biophysical and biomolecular factors are both crucial regulators of glioma invasiveness (194, 195). Our studies in Chapters 3 and 4 provide strong, direct support for this idea, and specifically suggest that in collagen-agarose composite matrices, agarose restricts local matrix stiffening by interfering with collagen fiber deformation and bundling, despite the fact that agarose increases matrix stiffness in bulk. In other words, the addition of agarose progressively limits the ability of tumor cells to stiffen their local microenvironment, resulting in an unexpected but important disconnect between the mechanical properties of the macroscale gel and cell-scale microenvironment.

Finally, although our collagen-agarose hydrogel platform is not intended to be a physiological mimic of brain, tumor, or other tissue types, we anticipate that our system will be valuable as a tool for interrogation of cell physiology and matrix mechanics in composite fibrillar-nonfibrillar matrices (290). Although most soft tissues in the body are comprised of fibrillar collagen meshed with non-fibrillar collagens and other components such as laminin and fibronectin, relatively little is currently known about the material interactions that govern the local and bulk mechanical properties of matrices containing both fibrillar and non-fibrillar components or how these properties influence cell behaviors. However, recent work by Lake and Barocas utilized a modified version of our collagen-agarose gels as a simple cell-free experimental model system in which to quantify the material interactions between fibrillar collagen meshed with a non-fibrillar matrix (282). Their study yielded valuable new insights into collagen fiber kinematics in this system in addition to reinforcing the importance of length scale considerations in discussions of gel mechanics. Importantly, this study also suggested that non-fibrillar ECM components may in fact make stronger contributions to gel mechanical responses than the fibrillar proteins traditionally believed to dominate ECM mechanics.

5.2   Future work and final thoughts

The results presented in the preceding chapters of this dissertation directly led to the development of three additional promising projects during my graduate work. I have been extremely fortunate over the last year to have had two very talented and hard-working young bioengineering graduate students, Sophie Wong and Vaibhavi Umesh, join me in this work.

5.2.1   Glioma cell rigidity-sensing at topological interfaces

Our ongoing work examining glioma cell rigidity-sensing at topological interfaces grew naturally out of unpublished observations from experiments related to Chapter 3 of this dissertation, in which we noticed that our glioma cells appeared to invade collagen-agarose gels more efficiently in the presence of interfacial geometries (e.g. ECM configurations in which the cells were essentially "sandwiched" between two 2D surfaces instead of being fully embedded in a 3D gel). As discussed in Chapter 1, pathologists have long noted that malignant gliomas (and indeed, many tumor cell types) frequently invade along anatomical structures in native tissues (e.g. the surface of blood vessels and white matter tracts) that are mechanically and geometrically distinct from the rest of the brain parenchyma. While the 2D and 3D culture

systems that we used in Chapters 2-4 were instructive in elucidating the regulatory role of microenvironmental mechanics in glioma cell physiology and invasion, neither of these systems fully capture the interfacial nature of typical invasion pathways. To address this limitation, we have begun combining our 2D and 3D biomaterial platforms to form "interface" cultures (292), which enable us to probe how ECM rigidity, topology, non-linear elasticity, and ligand density influence cell architecture and motility. Sophie Wong joined me on this project in the last year and has already made some key technical improvements to our culture system. To date, we have found that soft 2D matrices that normally prohibit cell spreading and motility can be converted to pro-motility microenvironments through introduction of dorsal ECM ligands, even if the mechanics of the dorsal ECM would not be compatible with cell spreading or migration in 2D culture. This effect can be eliminated by reducing the ligand density of the dorsal ECM or by restricting the cells' ability to remodel it. These changes in invasiveness appear to be accompanied by changes in the cells' contractile state, suggesting that the contractile mechanisms needed to drive motility are not simply a function of bulk matrix elasticity but also depend on details of ligand distribution. These initial findings suggest that cell behaviors at topological interfaces can be radically different than cellular behaviors in strictly 2D or 3D environments. We expect this work to have implications for both tumor infiltration and for our more general understanding of cell mechanobiology.

5.2.2 Regulation of growth factor-dependent tumor cell proliferation by extracellular matrix mechanics

Additional ongoing work has begun examining the mechanisms by which ECM mechanics regulate growth factor-dependent tumor cell proliferation. This project grew directly out of the work presented in Chapter 2 of this dissertation, where we showed that stiffening the extracellular matrix (ECM) can amplify the proliferation rate of human glioblastoma multiforme cell lines in vitro by more than a factor of five (199). A subsequent study by Assoian and colleagues used a panel of mammary epithelial cells, vascular smooth muscle cells, mouse embryonic fibroblasts, and osteoblasts, and demonstrated that cell-cycle control by matrix stiffness is widely conserved (293). Previous studies have indicated that ECM rigidity can modulate cell growth in other systems as well, including cultured fibroblasts (210), hepatocytes (211), and a variety of adult stem cells (40, 42).

One potential explanation for the correlation between microenvironmental rigidity and cell proliferation is that changes in ECM rigidity might alter the speed of progression through the cell cycle by altering mechanochemical feedback during mitosis. Indeed, direct application of mechanical force has been observed to slow cytokinesis and induce shape asymmetries in *Dictyostelium discoideum* cells, which is actively corrected via mobilization of nonmuscle myosin II (NMMII) to produce a restoring force (212). Second, ECM rigidity might regulate mitosis by synergistically triggering mechanotransductive and mitogenic signaling pathways, as has been suggested by recent studies from the breast cancer community, which reveal that modest increases in ECM rigidity can transform cultured breast epithelial cells from a benign, highly-differentiated phenotype into a dysplastic and proliferative one (188, 213). Importantly, this matrix-driven transformation is accompanied by activation of extracellular signal-regulated kinase (ERK)-mediated proliferative signaling and activation of the contractile markers Rho GTPase and NMMII, which enables enhanced generation of contractile forces. Importantly for

therapeutic applications, this rigidity-dependent phenotype can be reversed by pharmacological inhibition of Rho-associated kinase (ROCK) or ERK activity.

To gain mechanistic insight into rigidity-dependent enhancements of glioma cell proliferation, we began to explore the influence of matrix biomechanics on glioma cell cycle progression and growth factor receptor (EGFR)-dependent signaling. Vaibhavi Umesh joined me on this project as an undergraduate and Master's student, and has brought her knowledge and skill in PCR and Western blotting to bear on these questions. To date, we have found that human glioma cells cultured on soft fibronectin-coated polyacrylamide gels are more likely to be in G0/G1 and less likely to be in S phase of the cell cycle than cells cultured on stiff substrates, consistent with recently published results in other cell systems (293). Importantly, we have found that this gives rise to differential sensitivity to clinical chemotherapeutic agents, such that a fraction of glioma cells cultured in soft environments escape the G2/M arrest normally induced in stiff environments following chemotherapeutic insult. In addition, we find that the expression and phosphorylation of EGFR and its downstream effectors, including Akt and PI3 kinase, depend strongly on ECM rigidity, with EGFR phosphorylation rising with increasing ECM stiffness. Immunostaining reveals that EGFR organization is highly rigidity-dependent, with EGFR co-clustering with focal adhesions on stiff substrates and receding into a diffuse distribution as matrix rigidity falls to physiological levels. We expect that our ongoing work in this area will both strengthen our understanding of the biomechanical regulation of malignant brain tumors and suggest a novel regulatory component to the well-established role of EGFR signaling in governing their proliferation, infiltration, and chemoresistance.

5.2.3 Mechanobiology of primary tumor-initiating glioma cells

Of all of the projects that I have had the privilege to work on in my graduate career, this one is closest to my heart. I began designing this project, which examines the mechanobiology of a subpopulation of primary human glioblastoma multiforme cells called the "tumor-initiating cell" population (also commonly referred to as the "tumor stem cell" population) (294-297), as a class assignment when I was a second year graduate student in Sanjay Kumar's BioE 211 graduate course on cell mechanics. While still an area of vigorous debate in the literature, the tumor stem cell hypothesis suggests that a specific, highly tumorigenic subpopulation of cells called tumor-initiating cells (TICs) promotes therapeutic resistance, invasion, and metastasis in the setting of many human cancers. As discussed in Chapter 1, although GBMs rarely metastasize beyond the CNS, aggressive and highly infiltrative invasion into the surrounding normal brain tissue typically results in tumor recurrence and patient mortality within 12-15 months of diagnosis. GBM TICs have been implicated in a number of malignant behaviors related to tumor progression (including presenting a highly aggressive invasive phenotype and the unique ability to recapitulate the heterogeneity of the original tumor following transplantation), suggesting that therapeutic targeting of this cell population may lead to greater treatment efficacy. Recent work has begun teasing out both the similarities and distinctions between TICs and the normal stem cell population in the brain, providing hope that it might eventually be possible to uniquely target the TIC population in therapeutic settings (298). Essentially nothing is currently known about the mechanobiology of GBM TICs, or indeed, any other tumor stem cell population. However, rapid and exciting progress within the GBM TIC community over the last several years, including a number of key advances in TIC isolation, culture, and characterization techniques

(296, 297), in addition to our own glioma mechanobiology work in Chapters 2-4 of this dissertation, have now provided the strong foundation necessary for initiation and execution of work examining the mechanobiological properties of GBM TICs.

Our results in Chapter 2 had already suggested that the dynamic range of glioma cell mechanosensitivity may differ from that of their nonmalignant counterparts; for example, while highly compliant substrates (~100-500 Pa) have been found to select against the survival and proliferation of astrocytes in both explant studies and adult neural stem cell differentiation studies (42, 49), we found that cultured astrocytoma cell lines survive and proliferate even on 80 Pa polyacrylamide gels (199). Recent work by Tschumperlin, Parsons, and colleagues found that the mechanosensitivity of a panel of tumor cell lines (specifically, their ability to proliferate robustly on soft substrates) could be correlated with their ability to colonize lung tissue in vivo (299). This is an enormously significant result given that the most common sites for the formation of metastatic lesions in human cancers include the softest tissues in the body (e.g. lung, brain, and bone marrow). Importantly, it may also imply that the cells responsible for initiating secondary tumors possess altered mechanobiological characteristics compared to the associated bulk tumor cell populations.

Our initial studies in this area have supported the hypothesis that GBM tumor-initiating cells possess mechanobiological characteristics that are distinct from both the bulk tumor cell population and the non-malignant cell populations in the brain. Sophie Wong joined me on this project several months after we initiated a collaboration with Brent Reynolds' laboratory at the University of Florida and established their culture systems in our laboratory, and Sophie's enthusiasm and hard work have been critical in moving this project forward as I have been occupied by the tasks associated with finishing a Ph.D. and planning my next steps. Our results on this project so far have provided tantalizing evidence that the morphology, structure, random migration speed, and proliferation rate of GBM TIC lines are insensitive to ECM rigidity, even on extremely soft (~80 Pa) ECMs that are normally considered non-permissive for spreading, adhesion maturation, and motility. This rigidity insensitivity correlates well with the reported ability of these cells to evade other traditional inhibitors of cell motility and proliferation, and raises countless very intriguing mechanistic questions with enormous potential significance for both the development of novel therapeutics and also our fundamental understanding of rigidity-sensing and mechanobiological responsiveness in mammalian cells.

5.2.4   Final thoughts

The work presented in this dissertation (and indeed, the vast majority of previous and contemporary work in this area) has focused on understanding the mechanisms by which cells physically invade from tumors into the surrounding tissue. Although much more challenging to address in a laboratory setting, it will be critical to understand and ultimately find ways to limit the subsequent steps in the tumor progression cascade as well in order to begin making therapeutic headway against human cancers that are as yet intractable in the clinic. Two exceptionally important but largely unaddressed issues in this respect are: first, understanding what causes or allows cells to cross tissue boundaries that would normally not be permissive for their translocation (e.g. diapedesis of circulating tumor cells through the vascular

endothelium), and second, understanding what causes or allows cells to aberrantly colonize distant sites.

The issue of colonization is especially significant in the context of GBM tumors but is infrequently discussed in the literature, likely because it is an extraordinarily difficult question to address experimentally. While GBM is often referred to in academic circles as a "disease of cell migration" and is commonly studied as such, the fact remains that there are currently no diagnostic tools that would permit the detection, diagnosis, or initiation of treatment prior to the diffuse infiltration of GBM tumor cells into the surrounding brain parenchyma. As a result, even as my Ph.D. work has sought to answer questions related to pro-motility and invasion cues for GBM tumor cells, I have wondered if the really critical question from a therapeutic perspective may in fact be the inverse question: what causes a small subset of infiltrative tumor cells to *stop* invading and establish a secondary tumor? This question is especially significant in light of the fact that mortality is typically directly related to the formation and growth of secondary tumors (hence indicating that the majority of invasive cells do not directly contribute to the death of the patient). There are tantalizing clues buried within the GBM morbidity and mortality statistics and associated literature that I hope will someday lead to enumeration of the microenvironmental components of the "tumorigenic niche" in the brain. I conclude my graduate work knowing that finding the answers to these GBM-specific questions and related broader questions such as how and why soft tissues preferentially support the formation of metastatic lesions will be a daunting task indeed. However, I am confident that my current and future colleagues in the Kumar Laboratory will continue to make important strides in GBM mechanobiology, and I hope that my own future work will contribute to these important areas as well.

References

1. Suresh S. Biomechanics and biophysics of cancer cells. Acta Biomater 2007; 3: 413-38.
2. Discher D, Dong C, Fredberg JJ, et al. Biomechanics: cell research and applications for the next decade. Ann Biomed Eng 2009; 37: 847-59.
3. Rao JS. Molecular mechanisms of glioma invasiveness: the role of proteases. Nat Rev Cancer 2003; 3: 489-501.
4. Bellail AC, Hunter SB, Brat DJ, Tan C, Van Meir EG. Microregional extracellular matrix heterogeneity in brain modulates glioma cell invasion. Int J Biochem Cell Biol 2004; 36: 1046-69.
5. Jaime Struve PCM, Ya-qin Li, Shawn Kinney, Michael G. Fehlings, Charles Kuntz IV, Larry S. Sherman,. Disruption of the hyaluronan-based extracellular matrix in spinal cord promotes astrocyte proliferation. Glia 2005; 52: 16-24.
6. Greitz D, Franck A, Nordell B. On the pulsatile nature of intracranial and spinal CSF-circulation demonstrated by MR imaging. Acta Radiol 1993; 34: 321-8.
7. Michaela Soellinger AKR, Sebastian Kozerke, Peter Boesiger,. 3D cine displacement-encoded MRI of pulsatile brain motion. Magnetic Resonance in Medicine 2009; 61: 153-62.
8. Wagshul ME, Chen JJ, Egnor MR, McCormack EJ, Roche PE. Amplitude and phase of cerebrospinal fluid pulsations: experimental studies and review of the literature. J Neurosurg 2006; 104: 810-9.
9. Fallenstein GT, Hulce VD, Melvin JW. Dynamic mechanical properties of human brain tissue. Journal of Biomechanics 1969; 2: 217-26.
10. Uftring SJ, Chu D, Alperin N, Levin DN. The mechanical state of intracranial tissues in elderly subjects studied by imaging CSF and brain pulsations. Magnetic Resonance Imaging 2000; 18: 991-6.
11. Elkin BS, Azeloglu EU, Costa KD, Morrison B, 3rd. Mechanical heterogeneity of the rat hippocampus measured by atomic force microscope indentation. J Neurotrauma 2007; 24: 812-22.
12. Prange MT, Margulies SS. Regional, directional, and age-dependent properties of the brain undergoing large deformation. J Biomech Eng 2002; 124: 244-52.
13. Prange MT, Meaney DF, Margulies SS. Defining brain mechanical properties: effects of region, direction, and species. Stapp Car Crash J 2000; 44: 205-13.
14. Hrapko M, van Dommelen JA, Peters GW, Wismans JS. The influence of test conditions on characterization of the mechanical properties of brain tissue. J Biomech Eng 2008; 130: 031003.
15. Cheng S, Clarke EC, Bilston LE. Rheological properties of the tissues of the central nervous system: A review. Medical Engineering & Physics 2008; 30: 1318-37.
16. Janmey PA, Georges PC, Hvidt S. Basic rheology for biologists. Methods Cell Biol 2007; 83: 3-27.
17. Vappou J, Breton E, Choquet P, Willinger R, Constantinesco A. Assessment of in vivo and post-mortem mechanical behavior of brain tissue using magnetic resonance elastography. J Biomech 2008; 41: 2954-9.
18. Kruse SA, Rose GH, Glaser KJ, et al. Magnetic resonance elastography of the brain. Neuroimage 2008; 39: 231-7.

19. Green MA, Bilston LE, Sinkus R. In vivo brain viscoelastic properties measured by magnetic resonance elastography. NMR Biomed 2008; 21: 755-64.
20. Atay SM, Kroenke CD, Sabet A, Bayly PV. Measurement of the dynamic shear modulus of mouse brain tissue in vivo by magnetic resonance elastography. J Biomech Eng 2008; 130: 021013.
21. Manduca A, Oliphant TE, Dresner MA, et al. Magnetic resonance elastography: Non-invasive mapping of tissue elasticity. Medical Image Analysis 2001; 5: 237-54.
22. Vappou J, Breton E, Choquet P, Goetz C, Willinger R, Constantinesco A. Magnetic resonance elastography compared with rotational rheometry for in vitro brain tissue viscoelasticity measurement. MAGMA 2007; 20: 273-8.
23. Gefen A, Margulies SS. Are in vivo and in situ brain tissues mechanically similar? J Biomech 2004; 37: 1339-52.
24. Gefen A, Gefen N, Zhu Q, Raghupathi R, Margulies SS. Age-dependent changes in material properties of the brain and braincase of the rat. J Neurotrauma 2003; 20: 1163-77.
25. Thibault KL, Margulies SS. Age-dependent material properties of the porcine cerebrum: effect on pediatric inertial head injury criteria. Journal of Biomechanics 1998; 31: 1119-26.
26. Metz H, McElhaney J, Ommaya AK. A comparison of the elasticity of live, dead, and fixed brain tissue. Journal of Biomechanics 1970; 3: 453-8.
27. Hrapko M, van Dommelen JA, Peters GW, Wismans JS. The mechanical behaviour of brain tissue: large strain response and constitutive modelling. Biorheology 2006; 43: 623-36.
28. Maikos JT, Elias RA, Shreiber DI. Mechanical properties of dura mater from the rat brain and spinal cord. J Neurotrauma 2008; 25: 38-51.
29. Darvish KK, Crandall JR. Nonlinear viscoelastic effects in oscillatory shear deformation of brain tissue. Med Eng Phys 2001; 23: 633-45.
30. Takhounts EG, Crandall JR, Darvish K. On the importance of nonlinearity of brain tissue under large deformations. Stapp Car Crash J 2003; 47: 79-92.
31. Miller K, Chinzei K, Orssengo G, Bednarz P. Mechanical properties of brain tissue in-vivo: experiment and computer simulation. J Biomech 2000; 33: 1369-76.
32. Storm C, Pastore JJ, MacKintosh FC, Lubensky TC, Janmey PA. Nonlinear elasticity in biological gels. Nature 2005; 435: 191-4.
33. Yeung T, Georges PC, Flanagan LA, et al. Effects of substrate stiffness on cell morphology, cytoskeletal structure, and adhesion. Cell Motil Cytoskeleton 2005; 60: 24-34.
34. Pelham RJ, Jr., Wang Y. Cell locomotion and focal adhesions are regulated by substrate flexibility. Proc Natl Acad Sci U S A 1997; 94: 13661-5.
35. Wang N, Ingber DE. Control of cytoskeletal mechanics by extracellular matrix, cell shape, and mechanical tension. Biophys J 1994; 66: 2181-9.
36. Lo CM, Wang HB, Dembo M, Wang YL. Cell movement is guided by the rigidity of the substrate. Biophys J 2000; 79: 144-52.
37. Peyton SR, Putnam AJ. Extracellular matrix rigidity governs smooth muscle cell motility in a biphasic fashion. J Cell Physiol 2005; 204: 198-209.
38. Halliday NL, Tomasek JJ. Mechanical Properties of the Extracellular Matrix Influence Fibronectin Fibril Assembly in Vitro. Experimental Cell Research 1995; 217: 109-17.

39.   Engler AJ, Sen S, Sweeney HL, Discher DE. Matrix elasticity directs stem cell lineage specification. Cell 2006; 126: 677-89.
40.   Rowlands AS, George PA, Cooper-White JJ. Directing osteogenic and myogenic differentiation of MSCs: interplay of stiffness and adhesive ligand presentation. Am J Physiol Cell Physiol 2008; 295: C1037-44.
41.   Winer JP, Janmey PA, McCormick ME, Funaki M. Bone Marrow-Derived Human Mesenchymal Stem Cells Become Quiescent on Soft Substrates but Remain Responsive to Chemical or Mechanical Stimuli. Tissue Eng Part A 2008.
42.   Saha K, Keung AJ, Irwin EF, et al. Substrate modulus directs neural stem cell behavior. Biophys J 2008; 95: 4426-38.
43.   Balgude AP, Yu X, Szymanski A, Bellamkonda RV. Agarose gel stiffness determines rate of DRG neurite extension in 3D cultures. Biomaterials 2001; 22: 1077-84.
44.   Leach JB, Brown XQ, Jacot JG, Dimilla PA, Wong JY. Neurite outgrowth and branching of PC12 cells on very soft substrates sharply decreases below a threshold of substrate rigidity. J Neural Eng 2007; 4: 26-34.
45.   Flanagan LA, Ju YE, Marg B, Osterfield M, Janmey PA. Neurite branching on deformable substrates. Neuroreport 2002; 13: 2411-5.
46.   Willits RK, Skornia SL. Effect of collagen gel stiffness on neurite extension. J Biomater Sci Polym Ed 2004; 15: 1521-31.
47.   Van Essen DC. A tension-based theory of morphogenesis and compact wiring in the central nervous system. Nature 1997; 385: 313-8.
48.   Zhao C, Deng W, Gage FH. Mechanisms and functional implications of adult neurogenesis. Cell 2008; 132: 645-60.
49.   Georges PC, Miller WJ, Meaney DF, Sawyer ES, Janmey PA. Matrices with compliance comparable to that of brain tissue select neuronal over glial growth in mixed cortical cultures. Biophys J 2006; 90: 3012-8.
50.   Miller WJ, Levental I, Scarsella D, Haydon PG, Janmey PA, Meaney D. Mechanically Induced Reactive Gliosis Causes ATP-Mediated Alterations in Astrocyte Stiffness. J Neurotrauma 2009.
51.   Lam WA, Cao L, Umesh V, Keung AJ, Sen S, Kumar S. Extracellular matrix rigidity modulates neuroblastoma cell differentiation and N-myc expression. Mol Cancer 2010; 9: 35.
52.   Lamoureux P, Buxbaum RE, Heidemann SR. Direct evidence that growth cones pull. Nature 1989; 340: 159-62.
53.   Zheng J, Lamoureux P, Santiago V, Dennerll T, Buxbaum RE, Heidemann SR. Tensile regulation of axonal elongation and initiation. J Neurosci 1991; 11: 1117-25.
54.   Dennerll TJ, Joshi HC, Steel VL, Buxbaum RE, Heidemann SR. Tension and compression in the cytoskeleton of PC-12 neurites. II: Quantitative measurements. J Cell Biol 1988; 107: 665-74.
55.   Bray D. Axonal growth in response to experimentally applied mechanical tension. Dev Biol 1984; 102: 379-89.
56.   Chada S, Lamoureux P, Buxbaum RE, Heidemann SR. Cytomechanics of neurite outgrowth from chick brain neurons. J Cell Sci 1997; 110 (Pt 10): 1179-86.
57.   Fischer TM, Steinmetz PN, Odde DJ. Robust micromechanical neurite elicitation in synapse-competent neurons via magnetic bead force application. Ann Biomed Eng 2005; 33: 1229-37.

58. Fass JN, Odde DJ. Tensile force-dependent neurite elicitation via anti-beta1 integrin antibody-coated magnetic beads. Biophys J 2003; 85: 623-36.
59. Lu YB, Franze K, Seifert G, et al. Viscoelastic properties of individual glial cells and neurons in the CNS. Proc Natl Acad Sci U S A 2006; 103: 17759-64.
60. Dennerll TJ, Lamoureux P, Buxbaum RE, Heidemann SR. The cytomechanics of axonal elongation and retraction. J Cell Biol 1989; 109: 3073-83.
61. Kumar S, Maxwell IZ, Heisterkamp A, et al. Viscoelastic retraction of single living stress fibers and its impact on cell shape, cytoskeletal organization, and extracellular matrix mechanics. Biophys J 2006; 90: 3762-73.
62. Heisterkamp A, Maxwell IZ, Mazur E, et al. Pulse energy dependence of subcellular dissection by femtosecond laser pulses. Opt Express 2005; 13: 3690-6.
63. Puig-De-Morales M, Grabulosa M, Alcaraz J, et al. Measurement of cell microrheology by magnetic twisting cytometry with frequency domain demodulation. J Appl Physiol 2001; 91: 1152-9.
64. Maksym GN, Fabry B, Butler JP, et al. Mechanical properties of cultured human airway smooth muscle cells from 0.05 to 0.4 Hz. J Appl Physiol 2000; 89: 1619-32.
65. Wang N, Ingber DE. Probing transmembrane mechanical coupling and cytomechanics using magnetic twisting cytometry. Biochem Cell Biol 1995; 73: 327-35.
66. Alcaraz J, Buscemi L, Grabulosa M, et al. Microrheology of Human Lung Epithelial Cells Measured by Atomic Force Microscopy. Biophysical Journal 2003; 84: 2071-9.
67. Park S, Koch D, Cardenas R, Käs J, Shih CK. Cell Motility and Local Viscoelasticity of Fibroblasts. Biophysical Journal 2005; 89: 4330-42.
68. Mahaffy RE, Shih CK, MacKintosh FC, Kas J. Scanning probe-based frequency-dependent microrheology of polymer gels and biological cells. Phys Rev Lett 2000; 85: 880-3.
69. Mahaffy RE, Park S, Gerde E, Kas J, Shih CK. Quantitative analysis of the viscoelastic properties of thin regions of fibroblasts using atomic force microscopy. Biophys J 2004; 86: 1777-93.
70. Evans E, Yeung A. Apparent viscosity and cortical tension of blood granulocytes determined by micropipet aspiration. Biophysical Journal 1989; 56: 151-60.
71. Discher DE, Mohandas N, Evans EA. Molecular maps of red cell deformation: hidden elasticity and in situ connectivity. Science 1994; 266: 1032-5.
72. Chien S, Schmid-Schonbein GW, Sung KL, Schmalzer EA, Skalak R. Viscoelastic properties of leukocytes. Kroc Found Ser 1984; 16: 19-51.
73. Mills JP, Qie L, Dao M, Lim CT, Suresh S. Nonlinear elastic and viscoelastic deformation of the human red blood cell with optical tweezers. Mech Chem Biosyst 2004; 1: 169-80.
74. Laurent VM, Henon S, Planus E, et al. Assessment of mechanical properties of adherent living cells by bead micromanipulation: comparison of magnetic twisting cytometry vs optical tweezers. J Biomech Eng 2002; 124: 408-21.
75. Sen S, Kumar S. Cell-matrix de-adhesion dynamics reflect contractile mechanics. Cellular and Molecular Bioengineering 2009; (in press).
76. Janmey P, Schmidt C. Experimental measurements of intracellular mechanics. In: Mofrad MR, Kamm RD, editors. Cytoskeletal Mechanics: Models and Measurements. New York: Cambridge University Press; 2006. p. 18-49.

77.	Bouquet C, Nothias F. Molecular mechanisms of axonal growth. Adv Exp Med Biol 2007; 621: 1-16.
78.	Wen Z, Zheng JQ. Directional guidance of nerve growth cones. Curr Opin Neurobiol 2006; 16: 52-8.
79.	Pak CW, Flynn KC, Bamburg JR. Actin-binding proteins take the reins in growth cones. Nat Rev Neurosci 2008; 9: 136-47.
80.	Kumar S, Hoh JH. Modulation of repulsive forces between neurofilaments by sidearm phosphorylation. Biochem Biophys Res Commun 2004; 324: 489-96.
81.	Kumar S, Yin X, Trapp BD, Hoh JH, Paulaitis ME. Relating interactions between neurofilaments to the structure of axonal neurofilament distributions through polymer brush models. Biophys J 2002; 82: 2360-72.
82.	Kumar S, Yin X, Trapp BD, Paulaitis ME, Hoh JH. Role of long-range repulsive forces in organizing axonal neurofilament distributions: evidence from mice deficient in myelin-associated glycoprotein. J Neurosci Res 2002; 68: 681-90.
83.	Guo X, Rueger D, Higgins D. Osteogenic protein-1 and related bone morphogenetic proteins regulate dendritic growth and the expression of microtubule-associated protein-2 in rat sympathetic neurons. Neurosci Lett 1998; 245: 131-4.
84.	Aranda-Espinoza H, Carl P, Leterrier JF, Janmey P, Discher DE. Domain unfolding in neurofilament sidearms: effects of phosphorylation and ATP. FEBS Lett 2002; 531: 397-401.
85.	Okonkwo DO, Pettus EH, Moroi J, Povlishock JT. Alteration of the neurofilament sidearm and its relation to neurofilament compaction occurring with traumatic axonal injury. Brain Res 1998; 784: 1-6.
86.	Smith DH, Meaney DF. Axonal Damage in Traumatic Brain Injury. Neuroscientist 2000; 6: 483-95.
87.	Mukhopadhyay R, Hoh JH. AFM force measurements on microtubule-associated proteins: the projection domain exerts a long-range repulsive force. FEBS Lett 2001; 505: 374-8.
88.	Linseman DA, Loucks FA. Diverse roles of Rho family GTPases in neuronal development, survival, and death. Front Biosci 2008; 13: 657-76.
89.	Giniger E. How do Rho family GTPases direct axon growth and guidance? A proposal relating signaling pathways to growth cone mechanics. Differentiation 2002; 70: 385-96.
90.	Brown ME, Bridgman PC. Myosin function in nervous and sensory systems. J Neurobiol 2004; 58: 118-30.
91.	Imai K, Tatsumi H, Katayama Y. Mechanosensitive chloride channels on the growth cones of cultured rat dorsal root ganglion neurons. Neuroscience 2000; 97: 347-55.
92.	Jacques-Fricke BT, Seow Y, Gottlieb PA, Sachs F, Gomez TM. Ca2+ influx through mechanosensitive channels inhibits neurite outgrowth in opposition to other influx pathways and release from intracellular stores. J Neurosci 2006; 26: 5656-64.
93.	Sigurdson WJ, Morris CE. Stretch-activated ion channels in growth cones of snail neurons. J Neurosci 1989; 9: 2801-8.
94.	Kamkin A, Kiseleva I, editors. Mechanosensitivity of the Nervous System: Springer Netherlands; 2009.
95.	Bianchi L. Mechanotransduction: touch and feel at the molecular level as modeled in Caenorhabditis elegans. Mol Neurobiol 2007; 36: 254-71.

96.   Tang Y, Yoo J, Yethiraj A, Cui Q, Chen X. Mechanosensitive channels: insights from continuum-based simulations. Cell Biochem Biophys 2008; 52: 1-18.
97.   Barkho BZ, Song H, Aimone JB, et al. Identification of astrocyte-expressed factors that modulate neural stem/progenitor cell differentiation. Stem Cells Dev 2006; 15: 407-21.
98.   Ma DK, Ming GL, Song H. Glial influences on neural stem cell development: cellular niches for adult neurogenesis. Curr Opin Neurobiol 2005; 15: 514-20.
99.   Song H, Stevens CF, Gage FH. Astroglia induce neurogenesis from adult neural stem cells. Nature 2002; 417: 39-44.
100.   Araque A, Sanzgiri RP, Parpura V, Haydon PG. Astrocyte-induced modulation of synaptic transmission. Can J Physiol Pharmacol 1999; 77: 699-706.
101.   Bacci A, Verderio C, Pravettoni E, Matteoli M. The role of glial cells in synaptic function. Philos Trans R Soc Lond B Biol Sci 1999; 354: 403-9.
102.   Wenzel J, Lammert G, Meyer U, Krug M. The influence of long-term potentiation on the spatial relationship between astrocyte processes and potentiated synapses in the dentate gyrus neuropil of rat brain. Brain Res 1991; 560: 122-31.
103.   Araque A, Carmignoto G, Haydon PG. Dynamic signaling between astrocytes and neurons. Annu Rev Physiol 2001; 63: 795-813.
104.   Anderson BJ, Li X, Alcantara AA, Isaacs KR, Black JE, Greenough WT. Glial hypertrophy is associated with synaptogenesis following motor-skill learning, but not with angiogenesis following exercise. Glia 1994; 11: 73-80.
105.   Ullian EM, Sapperstein SK, Christopherson KS, Barres BA. Control of synapse number by glia. Science 2001; 291: 657-61.
106.   Volterra A, Meldolesi J. Astrocytes, from brain glue to communication elements: the revolution continues. Nat Rev Neurosci 2005; 6: 626-40.
107.   Shreiber DI, Hao H, Elias RA. Probing the influence of myelin and glia on the tensile properties of the spinal cord. Biomech Model Mechanobiol 2008.
108.   Mathewson AJ, Berry M. Observations on the astrocyte response to a cerebral stab wound in adult rats. Brain Research 1985; 327: 61-9.
109.   Milos Pekny MN. Astrocyte activation and reactive gliosis. Glia 2005; 50: 427-34.
110.   Cullen DK, Simon CM, LaPlaca MC. Strain rate-dependent induction of reactive astrogliosis and cell death in three-dimensional neuronal-astrocytic co-cultures. Brain Res 2007; 1158: 103-15.
111.   Ostrow LW, Langan TJ, Sachs F. Stretch-induced endothelin-1 production by astrocytes. J Cardiovasc Pharmacol 2000; 36: S274-7.
112.   Cornell-Bell AH, Finkbeiner SM, Cooper MS, Smith SJ. Glutamate induces calcium waves in cultured astrocytes: long-range glial signaling. Science 1990; 247: 470-3.
113.   Charles AC, Merrill JE, Dirksen ER, Sanderson MJ. Intercellular signaling in glial cells: calcium waves and oscillations in response to mechanical stimulation and glutamate. Neuron 1991; 6: 983-92.
114.   Hung J, Colicos MA. Astrocytic Ca(2+) waves guide CNS growth cones to remote regions of neuronal activity. PLoS ONE 2008; 3: e3692.
115.   Agulhon C, Petravicz J, McMullen AB, et al. What is the role of astrocyte calcium in neurophysiology? Neuron 2008; 59: 932-46.
116.   Ostrow LW, Sachs F. Mechanosensation and endothelin in astrocytes--hypothetical roles in CNS pathophysiology. Brain Res Brain Res Rev 2005; 48: 488-508.

117. Cotrina ML, Lin JH, Nedergaard M. Cytoskeletal assembly and ATP release regulate astrocytic calcium signaling. J Neurosci 1998; 18: 8794-804.
118. Abd-El-Basset EM, Fedoroff S. Upregulation of F-actin and alpha-actinin in reactive astrocytes. J Neurosci Res 1997; 49: 608-16.
119. Takamiya Y, Kohsaka S, Toya S, Otani M, Tsukada Y. Immunohistochemical studies on the proliferation of reactive astrocytes and the expression of cytoskeletal proteins following brain injury in rats. Brain Res 1988; 466: 201-10.
120. Abd-el-Basset EM, Fedoroff S. Contractile units in stress fibers of fetal human astroglia in tissue culture. J Chem Neuroanat 1994; 7: 113-22.
121. Parihar MS, Hemnani T. Alzheimer's disease pathogenesis and therapeutic interventions. Journal of Clinical Neuroscience 2004; 11: 456-67.
122. Scholz M, Noack V, Pechlivanis I, et al. Vibrography during tumor neurosurgery. J Ultrasound Med 2005; 24: 985-92.
123. Xu L, Lin Y, Han JC, Xi ZN, Shen H, Gao PY. Magnetic resonance elastography of brain tumors: preliminary results. Acta Radiol 2007; 48: 327-30.
124. Unsgaard G, Rygh OM, Selbekk T, et al. Intra-operative 3D ultrasound in neurosurgery. Acta Neurochir (Wien) 2006; 148: 235-53; discussion 53.
125. Selbekk T, Bang J, Unsgaard G. Strain processing of intraoperative ultrasound images of brain tumours: initial results. Ultrasound Med Biol 2005; 31: 45-51.
126. Bradley WG, Jr., Whittemore AR, Watanabe AS, Davis SJ, Teresi LM, Homyak M. Association of deep white matter infarction with chronic communicating hydrocephalus: implications regarding the possible origin of normal-pressure hydrocephalus. AJNR Am J Neuroradiol 1991; 12: 31-9.
127. Del Bigio MR. Neuropathological changes caused by hydrocephalus. Acta Neuropathol 1993; 85: 573-85.
128. Kalman M, Szabo A. Immunohistochemical investigation of actin-anchoring proteins vinculin, talin and paxillin in rat brain following lesion: a moderate reaction, confined to the astroglia of brain tracts. Exp Brain Res 2001; 139: 426-34.
129. Liesi P, Kauppila T. Induction of Type IV Collagen and Other Basement-Membrane-Associated Proteins after Spinal Cord Injury of the Adult Rat May Participate in Formation of the Glial Scar. Experimental Neurology 2002; 173: 31-45.
130. Hermanns S, Reiprich P, Müller HW. A reliable method to reduce collagen scar formation in the lesioned rat spinal cord. Journal of Neuroscience Methods 2001; 110: 141-6.
131. Spaethling JM, Geddes-Klein DM, Miller WJ, et al. Linking impact to cellular and molecular sequelae of CNS injury: Modeling in vivo complexity with in vitro simplicity. Progress in Brain Research: Elsevier; 2007. p. 27-39.
132. Furnari FB, Fenton T, Bachoo RM, et al. Malignant astrocytic glioma: genetics, biology, and paths to treatment. Genes Dev 2007; 21: 2683-710.
133. Dandy WE. Removal of right cerebral hemisphere for certain tumors with hemiplegia: preliminary report. JAMA 1928; 90: 823-5.
134. Fisher PG, Buffler PA. Malignant gliomas in 2005: where to GO from here? JAMA 2005; 293: 615-7.
135. Holland EC. Glioblastoma multiforme: the terminator. Proc Natl Acad Sci U S A 2000; 97: 6242-4.

136. Stupp R, Hegi ME, van den Bent MJ, et al. Changing paradigms--an update on the multidisciplinary management of malignant glioma. Oncologist 2006; 11: 165-80.

137. Charles AC, Naus CC, Zhu D, Kidder GM, Dirksen ER, Sanderson MJ. Intercellular calcium signaling via gap junctions in glioma cells. J Cell Biol 1992; 118: 195-201.

138. Zhang W, Couldwell WT, Simard MF, Song H, Lin JH, Nedergaard M. Direct gap junction communication between malignant glioma cells and astrocytes. Cancer Res 1999; 59: 1994-2003.

139. Yamasaki T, Enomoto K, Moritake K, Maeno T. Analysis of intra- and intercellular calcium signaling in a mouse malignant glioma cell line. J Neurosurg 1994; 81: 420-6.

140. Fry T, Evans JH, Sanderson MJ. Propagation of intercellular calcium waves in C6 glioma cells transfected with connexins 43 or 32. Microsc Res Tech 2001; 52: 289-300.

141. Lin JH, Takano T, Cotrina ML, et al. Connexin 43 enhances the adhesivity and mediates the invasion of malignant glioma cells. J Neurosci 2002; 22: 4302-11.

142. Scherer HJ. The forms of growth in gliomas and their practical significance. Brain 1940; 63: 1-35.

143. Rutka JT, Muller M, Hubbard SL, et al. Astrocytoma adhesion to extracellular matrix: functional significance of integrin and focal adhesion kinase expression. J Neuropathol Exp Neurol 1999; 58: 198-209.

144. Friedlander DR, Zagzag D, Shiff B, et al. Migration of brain tumor cells on extracellular matrix proteins in vitro correlates with tumor type and grade and involves alphaV and beta1 integrins. Cancer Res 1996; 56: 1939-47.

145. Paulus W, Baur I, Schuppan D, Roggendorf W. Characterization of integrin receptors in normal and neoplastic human brain. Am J Pathol 1993; 143: 154-63.

146. Lefranc F, Brotchi J, Kiss R. Possible future issues in the treatment of glioblastomas: special emphasis on cell migration and the resistance of migrating glioblastoma cells to apoptosis. J Clin Oncol 2005; 23: 2411-22.

147. Belot N, Rorive S, Doyen I, et al. Molecular characterization of cell substratum attachments in human glial tumors relates to prognostic features. Glia 2001; 36: 375-90.

148. Hehlgans S, Haase M, Cordes N. Signalling via integrins: implications for cell survival and anticancer strategies. Biochim Biophys Acta 2007; 1775: 163-80.

149. Aoudjit F, Vuori K. Integrin signaling inhibits paclitaxel-induced apoptosis in breast cancer cells. Oncogene 2001; 20: 4995-5004.

150. Cordes N, Seidler J, Durzok R, Geinitz H, Brakebusch C. beta1-integrin-mediated signaling essentially contributes to cell survival after radiation-induced genotoxic injury. Oncogene 2006; 25: 1378-90.

151. Hikawa T, Mori T, Abe T, Hori S. The ability in adhesion and invasion of drug-resistant human glioma cells. J Exp Clin Cancer Res 2000; 19: 357-62.

152. Yuan L, Siegel M, Choi K, et al. Transglutaminase 2 inhibitor, KCC009, disrupts fibronectin assembly in the extracellular matrix and sensitizes orthotopic glioblastomas to chemotherapy. Oncogene 2007; 26: 2563-73.

153. Reardon DA, Nabors LB, Stupp R, Mikkelsen T. Cilengitide: an integrin-targeting arginine-glycine-aspartic acid peptide with promising activity for glioblastoma multiforme. Expert Opin Investig Drugs 2008; 17: 1225-35.

154. Maglott A, Bartik P, Cosgun S, et al. The small alpha5beta1 integrin antagonist, SJ749, reduces proliferation and clonogenicity of human astrocytoma cells. Cancer Res 2006; 66: 6002-7.

155. Akabani G, Reardon DA, Coleman RE, et al. Dosimetry and radiographic analysis of 131I-labeled anti-tenascin 81C6 murine monoclonal antibody in newly diagnosed patients with malignant gliomas: a phase II study. J Nucl Med 2005; 46: 1042-51.

156. Leins A, Riva P, Lindstedt R, Davidoff MS, Mehraein P, Weis S. Expression of tenascin-C in various human brain tumors and its relevance for survival in patients with astrocytoma. Cancer 2003; 98: 2430-9.

157. Ying H, Biroc SL, Li WW, et al. The Rho kinase inhibitor fasudil inhibits tumor progression in human and rat tumor models. Mol Cancer Ther 2006; 5: 2158-64.

158. Shi Q, Hjelmeland AB, Keir ST, et al. A novel low-molecular weight inhibitor of focal adhesion kinase, TAE226, inhibits glioma growth. Mol Carcinog 2007; 46: 488-96.

159. Beadle C, Assanah MC, Monzo P, Vallee R, Rosenfeld SS, Canoll P. The Role of Myosin II in Glioma Invasion of the Brain. Mol Biol Cell 2008; 19: 3357-68.

160. Gillespie GY, Soroceanu L, Manning TJ, Jr., Gladson CL, Rosenfeld SS. Glioma migration can be blocked by nontoxic inhibitors of myosin II. Cancer Res 1999; 59: 2076-82.

161. Lepley D, Paik JH, Hla T, Ferrer F. The G protein-coupled receptor S1P2 regulates Rho/Rho kinase pathway to inhibit tumor cell migration. Cancer Res 2005; 65: 3788-95.

162. Manning TJ, Jr., Parker JC, Sontheimer H. Role of lysophosphatidic acid and rho in glioma cell motility. Cell Motil Cytoskeleton 2000; 45: 185-99.

163. Goldberg L, Kloog Y. A Ras inhibitor tilts the balance between Rac and Rho and blocks phosphatidylinositol 3-kinase-dependent glioblastoma cell migration. Cancer Res 2006; 66: 11709-17.

164. Zhai GG, Malhotra R, Delaney M, et al. Radiation enhances the invasive potential of primary glioblastoma cells via activation of the Rho signaling pathway. J Neurooncol 2006; 76: 227-37.

165. Chan AY, Coniglio SJ, Chuang YY, et al. Roles of the Rac1 and Rac3 GTPases in human tumor cell invasion. Oncogene 2005; 24: 7821-9.

166. Ader I, Delmas C, Bonnet J, et al. Inhibition of Rho pathways induces radiosensitization and oxygenation in human glioblastoma xenografts. Oncogene 2003; 22: 8861-9.

167. Salhia B, Rutten F, Nakada M, et al. Inhibition of Rho-kinase affects astrocytoma morphology, motility, and invasion through activation of Rac1. Cancer Res 2005; 65: 8792-800.

168. Senger DL, Tudan C, Guiot MC, et al. Suppression of Rac activity induces apoptosis of human glioma cells but not normal human astrocytes. Cancer Res 2002; 62: 2131-40.

169. Rattan R, Giri S, Singh AK, Singh I. Rho/ROCK pathway as a target of tumor therapy. J Neurosci Res 2006; 83: 243-55.

170. Demuth T, Berens ME. Molecular mechanisms of glioma cell migration and invasion. J Neurooncol 2004; 70: 217-28.

171. Wells A. Tumor invasion: role of growth factor-induced cell motility. Adv Cancer Res 2000; 78: 31-101.

172. Mahesparan R, Tysnes BB, Read TA, Enger PO, Bjerkvig R, Lund-Johansen M. Extracellular matrix-induced cell migration from glioblastoma biopsy specimens in vitro. Acta Neuropathol 1999; 97: 231-9.

173. Zagzag D, Friedlander DR, Dosik J, et al. Tenascin-C expression by angiogenic vessels in human astrocytomas and by human brain endothelial cells in vitro. Cancer Res 1996; 56: 182-9.

174.   Deryugina EI, Bourdon MA. Tenascin mediates human glioma cell migration and modulates cell migration on fibronectin. J Cell Sci 1996; 109 (Pt 3): 643-52.

175.   Monferran S, Skuli N, Delmas C, et al. Alphavbeta3 and alphavbeta5 integrins control glioma cell response to ionising radiation through ILK and RhoB. Int J Cancer 2008; 123: 357-64.

176.   Koul D, Shen R, Bergh S, et al. Targeting integrin-linked kinase inhibits Akt signaling pathways and decreases tumor progression of human glioblastoma. Mol Cancer Ther 2005; 4: 1681-8.

177.   Natarajan M, Hecker TP, Gladson CL. FAK signaling in anaplastic astrocytoma and glioblastoma tumors. Cancer J 2003; 9: 126-33.

178.   Magro AM, Magro AD, Cunningham C, Miller MR. Down-regulation of vinculin upon MK886-induced apoptosis in LN18 glioblastoma cells. Neoplasma 2007; 54: 517-26.

179.   Comprehensive genomic characterization defines human glioblastoma genes and core pathways. Nature 2008; 455: 1061-8.

180.   Ritch PA, Carroll SL, Sontheimer H. Neuregulin-1 enhances motility and migration of human astrocytic glioma cells. J Biol Chem 2003; 278: 20971-8.

181.   Dey N, Crosswell HE, De P, et al. The protein phosphatase activity of PTEN regulates SRC family kinases and controls glioma migration. Cancer Res 2008; 68: 1862-71.

182.   Discher DE, Janmey P, Wang YL. Tissue cells feel and respond to the stiffness of their substrate. Science 2005; 310: 1139-43.

183.   Paszek MJ, Weaver VM. The tension mounts: mechanics meets morphogenesis and malignancy. J Mammary Gland Biol Neoplasia 2004; 9: 325-42.

184.   Chen CS, Mrksich M, Huang S, Whitesides GM, Ingber DE. Geometric control of cell life and death. Science 1997; 276: 1425-8.

185.   McBeath R, Pirone DM, Nelson CM, Bhadriraju K, Chen CS. Cell shape, cytoskeletal tension, and RhoA regulate stem cell lineage commitment. Dev Cell 2004; 6: 483-95.

186.   Bissell MJ, Radisky DC, Rizki A, Weaver VM, Petersen OW. The organizing principle: microenvironmental influences in the normal and malignant breast. Differentiation 2002; 70: 537-46.

187.   Provenzano PP, Inman DR, Eliceiri KW, Beggs HE, Keely PJ. Mammary epithelial-specific disruption of focal adhesion kinase retards tumor formation and metastasis in a transgenic mouse model of human breast cancer. Am J Pathol 2008; 173: 1551-65.

188.   Paszek MJ, Zahir N, Johnson KR, et al. Tensional homeostasis and the malignant phenotype. Cancer Cell 2005; 8: 241-54.

189.   Zaman MH, Trapani LM, Sieminski AL, et al. Migration of tumor cells in 3D matrices is governed by matrix stiffness along with cell-matrix adhesion and proteolysis. Proc Natl Acad Sci U S A 2006; 103: 10889-94.

190.   Collin O, Na S, Chowdhury F, et al. Self-Organized Podosomes Are Dynamic Mechanosensors. Curr Biol 2008.

191.   Alexander NR, Branch KM, Parekh A, et al. Extracellular Matrix Rigidity Promotes Invadopodia Activity. Curr Biol 2008.

192.   Thomas TW, DiMilla PA. Spreading and motility of human glioblastoma cells on sheets of silicone rubber depend on substratum compliance. Med Biol Eng Comput 2000; 38: 360-70.

193. Gordon VD, Valentine MT, Gardel ML, et al. Measuring the mechanical stress induced by an expanding multicellular tumor system: a case study. Exp Cell Res 2003; 289: 58-66.

194. Hegedus B, Marga F, Jakab K, Sharpe-Timms KL, Forgacs G. The interplay of cell-cell and cell-matrix interactions in the invasive properties of brain tumors. Biophys J 2006; 91: 2708-16.

195. Kaufman LJ, Brangwynne CP, Kasza KE, et al. Glioma expansion in collagen I matrices: analyzing collagen concentration-dependent growth and motility patterns. Biophys J 2005; 89: 635-50.

196. Forget MA, Desrosiers RR, Del M, et al. The expression of Rho proteins decreases with human brain tumor progression: potential tumor markers. Clin Exp Metastasis 2002; 19: 9-15.

197. Lele TP, Pendse J, Kumar S, Salanga M, Karavitis J, Ingber DE. Mechanical forces alter zyxin unbinding kinetics within focal adhesions of living cells. J Cell Physiol 2006; 207: 187-94.

198. Kandow CE, Georges PC, Janmey PA, Beningo KA. Polyacrylamide hydrogels for cell mechanics: steps toward optimization and alternative uses. Methods Cell Biol 2007; 83: 29-46.

199. Ulrich TA, Juan Pardo EM, Kumar S. The mechanical rigidity of the extracellular matrix regulates the structure, motility, and proliferation of glioma cells. Cancer Res 2009; 69: 4167- 74.

200. Yap CT, Simpson TI, Pratt T, Price DJ, Maciver SK. The motility of glioblastoma tumour cells is modulated by intracellular cofilin expression in a concentration-dependent manner. Cell Motil Cytoskeleton 2005; 60: 153-65.

201. Ito H, Aoki H, Kuhnel F, et al. Autophagic cell death of malignant glioma cells induced by a conditionally replicating adenovirus. J Natl Cancer Inst 2006; 98: 625-36.

202. Tas PW, Gambaryan S, Roewer N. Volatile anesthetics affect the morphology of rat glioma C6 cells via RhoA, ERK, and Akt activation. J Cell Biochem 2007; 102: 368-76.

203. Giese A, Loo MA, Tran N, Haskett D, Coons SW, Berens ME. Dichotomy of astrocytoma migration and proliferation. Int J Cancer 1996; 67: 275-82.

204. Somlyo AP, Somlyo AV. Signal transduction by G-proteins, rho-kinase and protein phosphatase to smooth muscle and non-muscle myosin II. J Physiol 2000; 522 Pt 2: 177-85.

205. Itoh K, Yoshioka K, Akedo H, Uehata M, Ishizaki T, Narumiya S. An essential part for Rho-associated kinase in the transcellular invasion of tumor cells. Nat Med 1999; 5: 221-5.

206. Lo CM, Buxton DB, Chua GC, Dembo M, Adelstein RS, Wang YL. Nonmuscle myosin IIb is involved in the guidance of fibroblast migration. Mol Biol Cell 2004; 15: 982-9.

207. Cai Y, Biais N, Giannone G, et al. Nonmuscle myosin IIA-dependent force inhibits cell spreading and drives F-actin flow. Biophys J 2006; 91: 3907-20.

208. Betapudi V, Licate LS, Egelhoff TT. Distinct roles of nonmuscle myosin II isoforms in the regulation of MDA-MB-231 breast cancer cell spreading and migration. Cancer Res 2006; 66: 4725-33.

209. Salhia B, Hwang JH, Smith CA, et al. Role of myosin II activity and the regulation of myosin light chain phosphorylation in astrocytomas. Cell Motil Cytoskeleton 2008; 65: 12-24.

210.   Wang HB, Dembo M, Wang YL. Substrate flexibility regulates growth and apoptosis of normal but not transformed cells. Am J Physiol Cell Physiol 2000; 279: C1345-50.
211.   Semler EJ, Ranucci CS, Moghe PV. Mechanochemical manipulation of hepatocyte aggregation can selectively induce or repress liver-specific function. Biotechnol Bioeng 2000; 69: 359-69.
212.   Effler JC, Kee YS, Berk JM, Tran MN, Iglesias PA, Robinson DN. Mitosis-specific mechanosensing and contractile-protein redistribution control cell shape. Curr Biol 2006; 16: 1962-7.
213.   Huang S, Ingber DE. Cell tension, matrix mechanics, and cancer development. Cancer Cell 2005; 8: 175-6.
214.   Turley EA, Veiseh M, Radisky DC, Bissell MJ. Mechanisms of disease: epithelial-mesenchymal transition--does cellular plasticity fuel neoplastic progression? Nat Clin Pract Oncol 2008; 5: 280-90.
215.   Nakada M, Nakada S, Demuth T, Tran NL, Hoelzinger DB, Berens ME. Molecular targets of glioma invasion. Cell Mol Life Sci 2007; 64: 458-78.
216.   Wolf K, Wu YI, Liu Y, et al. Multi-step pericellular proteolysis controls the transition from individual to collective cancer cell invasion. Nat Cell Biol 2007; 9: 893-904.
217.   Provenzano PP, Inman DR, Eliceiri KW, Trier SM, Keely PJ. Contact guidance mediated three-dimensional cell migration is regulated by Rho/ROCK-dependent matrix reorganization. Biophys J 2008; 95: 5374-84.
218.   Pedersen JA, Swartz MA. Mechanobiology in the third dimension. Ann Biomed Eng 2005; 33: 1469-90.
219.   Pampaloni F, Reynaud EG, Stelzer EH. The third dimension bridges the gap between cell culture and live tissue. Nat Rev Mol Cell Biol 2007; 8: 839-45.
220.   Kim S, Healy KE. Synthesis and characterization of injectable poly(N-isopropylacrylamide-co-acrylic acid) hydrogels with proteolytically degradable cross-links. Biomacromolecules 2003; 4: 1214-23.
221.   Peyton SR, Raub CB, Keschrumrus VP, Putnam AJ. The use of poly(ethylene glycol) hydrogels to investigate the impact of ECM chemistry and mechanics on smooth muscle cells. Biomaterials 2006; 27: 4881-93.
222.   Seliktar D, Zisch AH, Lutolf MP, Wrana JL, Hubbell JA. MMP-2 sensitive, VEGF-bearing bioactive hydrogels for promotion of vascular healing. J Biomed Mater Res A 2004; 68: 704-16.
223.   Chandran PL, Barocas VH. Affine versus non-affine fibril kinematics in collagen networks: theoretical studies of network behavior. J Biomech Eng 2006; 128: 259-70.
224.   Winer JP, Oake S, Janmey PA. Non-linear elasticity of extracellular matrices enables contractile cells to communicate local position and orientation. PLoS ONE 2009; 4: e6382.
225.   Yang YL, Kaufman LJ. Rheology and confocal reflectance microscopy as probes of mechanical properties and structure during collagen and collagen/hyaluronan self-assembly. Biophys J 2009; 96: 1566-85.
226.   Hamed G, Rodriguez F. Gelation of dilute collagen solutions by ultraviolet light. Journal of Applied Polymer Science 1975; 19: 3299-313.
227.   Inoue N, Bessho M, Furuta M, Kojima T, Okuda S, Hara M. A novel collagen hydrogel cross-linked by gamma-ray irradiation in acidic pH conditions. J Biomater Sci Polym Ed 2006; 17: 837-58.

228. Orban JM, Wilson LB, Kofroth JA, El-Kurdi MS, Maul TM, Vorp DA. Crosslinking of collagen gels by transglutaminase. J Biomed Mater Res A 2004; 68: 756-62.
229. Olde Damink LHH, Dijkstra PJ, Luyn MJA, Wachem PB, Nieuwenhuis P, Feijen J. Glutaraldehyde as a crosslinking agent for collagen-based biomaterials. Journal of Materials Science: Materials in Medicine 1995; 6: 460-72.
230. Siegel RC. Collagen cross-linking. Synthesis of collagen cross-links in vitro with highly purified lysyl oxidase. J Biol Chem 1976; 251: 5786-92.
231. Sheu MT, Huang JC, Yeh GC, Ho HO. Characterization of collagen gel solutions and collagen matrices for cell culture. Biomaterials 2001; 22: 1713-9.
232. Girton TS, Oegema TR, Tranquillo RT. Exploiting glycation to stiffen and strengthen tissue equivalents for tissue engineering. J Biomed Mater Res 1999; 46: 87-92.
233. Paik DC, Dillon J, Galicia E, Tilson MD. The nitrite/collagen reaction: non-enzymatic nitration as a model system for age-related damage. Connect Tissue Res 2001; 42: 111-22.
234. Sundararaghavan HG, Monteiro GA, Lapin NA, Chabal YJ, Miksan JR, Shreiber DI. Genipin-induced changes in collagen gels: correlation of mechanical properties to fluorescence. J Biomed Mater Res A 2008; 87: 308-20.
235. Duan X, Sheardown H. Crosslinking of collagen with dendrimers. J Biomed Mater Res A 2005; 75: 510-8.
236. Normand V, Lootens DL, Amici E, Plucknett KP, Aymard P. New insight into agarose gel mechanical properties. Biomacromolecules 2000; 1: 730-8.
237. Arnott S, Fulmer A, Scott WE, Dea IC, Moorhouse R, Rees DA. The agarose double helix and its function in agarose gel structure. J Mol Biol 1974; 90: 269-84.
238. Barrangou LM, Daubert CR, Allen Foegeding E. Textural properties of agarose gels. I. Rheological and fracture properties. Food Hydrocolloids; 20: 184-95.
239. Griess GA, Moreno ET, Easom RA, Serwer P. The sieving of spheres during agarose gel electrophoresis: quantitation and modeling. Biopolymers 1989; 28: 1475-84.
240. Bellamkonda R, Ranieri JP, Aebischer P. Laminin oligopeptide derivatized agarose gels allow three-dimensional neurite extension in vitro. J Neurosci Res 1995; 41: 501-9.
241. Batorsky A, Liao J, Lund AW, Plopper GE, Stegemann JP. Encapsulation of adult human mesenchymal stem cells within collagen-agarose microenvironments. Biotechnol Bioeng 2005; 92: 492-500.
242. Lin PW, Wu CC, Chen CH, Ho HO, Chen YC, Sheu MT. Characterization of cortical neuron outgrowth in two- and three-dimensional culture systems. J Biomed Mater Res B Appl Biomater 2005; 75: 146-57.
243. Cullen DK, Lessing MC, LaPlaca MC. Collagen-dependent neurite outgrowth and response to dynamic deformation in three-dimensional neuronal cultures. Ann Biomed Eng 2007; 35: 835-46.
244. Lund AW, Bush JA, Plopper GE, Stegemann JP. Osteogenic differentiation of mesenchymal stem cells in defined protein beads. J Biomed Mater Res B Appl Biomater 2008; 87: 213-21.
245. Timmins NE, Nielsen LK. Generation of multicellular tumor spheroids by the hanging-drop method. Methods Mol Med 2007; 140: 141-51.
246. Raub CB, Suresh V, Krasieva T, et al. Noninvasive assessment of collagen gel microstructure and mechanics using multiphoton microscopy. Biophys J 2007; 92: 2212-22.

247. Raub CB, Unruh J, Suresh V, et al. Image correlation spectroscopy of multiphoton images correlates with collagen mechanical properties. Biophys J 2008; 94: 2361-73.
248. Mickel W, Munster S, Jawerth LM, et al. Robust pore size analysis of filamentous networks from three-dimensional confocal microscopy. Biophys J 2008; 95: 6072-80.
249. Ulrich TA, Jain A, Tanner K, Mackay JL, Kumar S. Probing cellular mechanobiology in three-dimensional culture with collagen-agarose matrices. Biomaterials 2010; 31: 1875-84.
250. Dillon GP, Yu X, Sridharan A, Ranieri JP, Bellamkonda RV. The influence of physical structure and charge on neurite extension in a 3D hydrogel scaffold. J Biomater Sci Polym Ed 1998; 9: 1049-69.
251. Wolf K, Mazo I, Leung H, et al. Compensation mechanism in tumor cell migration: mesenchymal-amoeboid transition after blocking of pericellular proteolysis. J Cell Biol 2003; 160: 267-77.
252. Yamazaki D, Kurisu S, Takenawa T. Involvement of Rac and Rho signaling in cancer cell motility in 3D substrates. Oncogene 2009; 28: 1570-83.
253. Sahai E, Marshall CJ. Differing modes of tumour cell invasion have distinct requirements for Rho/ROCK signalling and extracellular proteolysis. Nat Cell Biol 2003; 5: 711-9.
254. Gonen-Wadmany M, Oss-Ronen L, Seliktar D. Protein-polymer conjugates for forming photopolymerizable biomimetic hydrogels for tissue engineering. Biomaterials 2007; 28: 3876-86.
255. Almany L, Seliktar D. Biosynthetic hydrogel scaffolds made from fibrinogen and polyethylene glycol for 3D cell cultures. Biomaterials 2005; 26: 2467-77.
256. Dikovsky D, Bianco-Peled H, Seliktar D. The effect of structural alterations of PEG-fibrinogen hydrogel scaffolds on 3-D cellular morphology and cellular migration. Biomaterials 2006; 27: 1496-506.
257. Ghosh K, Pan Z, Guan E, et al. Cell adaptation to a physiologically relevant ECM mimic with different viscoelastic properties. Biomaterials 2007; 28: 671-9.
258. Dutta RC, Dutta AK. Cell-interactive 3D-scaffold; advances and applications. Biotechnology Advances 2009; 27: 334-9.
259. Lutolf MP. Artificial ECM: expanding the cell biology toolbox in 3D. Integr Biol 2009; 1: 234-41.
260. Harley BA, Kim HD, Zaman MH, Yannas IV, Lauffenburger DA, Gibson LJ. Microarchitecture of three-dimensional scaffolds influences cell migration behavior via junction interactions. Biophys J 2008; 95: 4013-24.
261. Deisboeck TS, Berens ME, Kansal AR, Torquato S, Stemmer-Rachamimov AO, Chiocca EA. Pattern of self-organization in tumour systems: complex growth dynamics in a novel brain tumour spheroid model. Cell Prolif 2001; 34: 115-34.
262. Lammermann T, Bader BL, Monkley SJ, et al. Rapid leukocyte migration by integrin-independent flowing and squeezing. Nature 2008; 453: 51-5.
263. Vogel V, Sheetz M. Local force and geometry sensing regulate cell functions. Nat Rev Mol Cell Biol 2006; 7: 265-75.
264. Moore SW, Roca-Cusachs P, Sheetz MP. Stretchy proteins on stretchy substrates: the important elements of integrin-mediated rigidity sensing. Dev Cell 2010; 19: 194-206.
265. Larsen M, Artym VV, Green JA, Yamada KM. The matrix reorganized: extracellular matrix remodeling and integrin signaling. Curr Opin Cell Biol 2006; 18: 463-71.

266. Harjanto D, Zaman MH. Matrix mechanics and receptor-ligand interactions in cell adhesion. Org Biomol Chem 2010; 8: 299-304.
267. Johnson KR, Leight JL, Weaver VM. Demystifying the effects of a three-dimensional microenvironment in tissue morphogenesis. Methods Cell Biol 2007; 83: 547-83.
268. Friedl P, Wolf K. Plasticity of cell migration: a multiscale tuning model. J Cell Biol 2010; 188: 11-9.
269. Sahai E. Mechanisms of cancer cell invasion. Curr Opin Genet Dev 2005; 15: 87-96.
270. Wong JY, Leach JB, Brown XQ. Balance of chemistry, topography, and mechanics at the cell-biomaterial interface: Issues and challenges for assessing the role of substrate mechanics on cell response. Surf Sci 2004; 570: 119-33.
271. Park YD, Tirelli N, Hubbell JA. Photopolymerized hyaluronic acid-based hydrogels and interpenetrating networks. Biomaterials 2003; 24: 893-900.
272. Nomura Y, Ishii Y, Takahashi K. Control of collagen molecular assembly with anionic polysaccharides. Biosci Biotechnol Biochem 2009; 73: 926-9.
273. Gough JE, Scotchford CA, Downes S. Cytotoxicity of glutaraldehyde crosslinked collagen/poly(vinyl alcohol) films is by the mechanism of apoptosis. J Biomed Mater Res 2002; 61: 121-30.
274. Wagner MS, Castner DG. Characterization of adsorbed protein films by time-of-flight secondary ion mass spectrometry with principal component analysis. Langmuir 2001; 17: 4649-60.
275. Kim YP, Hong MY, Kim J, et al. Quantitative analysis of surface-immobilized protein by TOF-SIMS: effects of protein orientation and trehalose additive. Anal Chem 2007; 79: 1377-85.
276. Ngo P, Ramalingam P, Phillips JA, Furuta GT. Collagen Gel Contraction Assay. 2006. p. 103-9.
277. Dykstra MJ, and Reuss, L.E. Biological electron microscopy: Theory, techniques, and troubleshooting 2ed. New York: Kluwer Academic/Plenum Publishers 2003. p.373-376.
278. Stevenson MD, Sieminski AL, McLeod CM, Byfield FJ, Barocas VH, Gooch Keith J. Pericellular conditions regulate extent of cell-mediated compaction of collagen gels. Biophys J 2010; 99: 19-28.
279. Wang H, Castner DG, Ratner BD, Jiang S. Probing the orientation of surface-immobilized immunoglobulin G by time-of-flight secondary ion mass spectrometry. Langmuir 2004; 20: 1877-87.
280. Damljanovic V, Lagerholm BC, Jacobson K. Bulk and micropatterned conjugation of extracellular matrix proteins to characterized polyacrylamide substrates for cell mechanotransduction assays. Biotechniques 2005; 39: 847-51.
281. Achilli M, Mantovani D. Tailoring mechanical properties of collagen-based scaffolds for vascular tissue engineering: The effects of pH, temperature and ionic strength on gelation. Polymers 2010; 2: 664-80.
282. Lake SP, Barocas VH. Mechanical and structural contribution of non-fibrillar matrix in uniaxial tension: a collagen-agarose co-gel model. Ann Biomed Eng 2011; (in press).
283. Bloom RJ, George JP, Celedon A, Sun SX, Wirtz D. Mapping local matrix remodeling induced by a migrating tumor cell using three-dimensional multiple-particle tracking. Biophys J 2008; 95: 4077-88.

284. Provenzano PP, Eliceiri KW, Campbell JM, Inman DR, White JG, Keely PJ. Collagen reorganization at the tumor-stromal interface facilitates local invasion. Bmc Medicine 2006; 4.

285. Georges PC, Hui JJ, Gombos Z, et al. Increased stiffness of the rat liver precedes matrix deposition: implications for fibrosis. Am J Physiol Gastrointest Liver Physiol 2007; 293: G1147-54.

286. Pathak A, Kumar S. Biophysical regulation of tumor cell invasion: Moving beyond matrix stiffness. Integr Biol 2011; 3: 267-78.

287. Sen S, Dong M, Kumar S. Isoform-specific contributions of alpha-actinin to glioma cell mechanobiology. PLoS ONE 2009; 4: e8427.

288. Otey CA, Carpen O. Alpha-actinin revisited: a fresh look at an old player. Cell Motil Cytoskeleton 2004; 58: 104-11.

289. Quick Q, Skalli O. Alpha-actinin 1 and alpha-actinin 4: contrasting roles in the survival, motility, and RhoA signaling of astrocytoma cells. Exp Cell Res; 316: 1137-47.

290. Ulrich TA, Lee TG, Shon HK, Moon DW, Kumar S. Microscale mechanisms of agarose-induced disruption of collagen remodeling. Biomaterials 2011; (in press).

291. Yang YL, Motte S, Kaufman LJ. Pore size variable type I collagen gels and their interaction with glioma cells. Biomaterials 2010; 31: 5678-88.

292. Beningo KA, Dembo M, Wang YL. Responses of fibroblasts to anchorage of dorsal extracellular matrix receptors. Proc Natl Acad Sci U S A 2004; 101: 18024-9.

293. Klein EA, Yin L, Kothapalli D, et al. Cell-Cycle Control by Physiological Matrix Elasticity and In Vivo Tissue Stiffening. Curr Biol 2009; 19: 1511-8.

294. Galli R, Binda E, Orfanelli U, et al. Isolation and characterization of tumorigenic, stem-like neural precursors from human glioblastoma. Cancer Res 2004; 64: 7011-21.

295. Lee J, Kotliarova S, Kotliarov Y, et al. Tumor stem cells derived from glioblastomas cultured in bFGF and EGF more closely mirror the phenotype and genotype of primary tumors than do serum-cultured cell lines. Cancer Cell 2006; 9: 391-403.

296. McLendon RE, Rich JN. Glioblastoma Stem Cells: A Neuropathologist's View. J Oncol 2011; 2011: 397195.

297. Pollard SM, Yoshikawa K, Clarke ID, et al. Glioma stem cell lines expanded in adherent culture have tumor-specific phenotypes and are suitable for chemical and genetic screens. Cell Stem Cell 2009; 4: 568-80.

298. Huang Z, Cheng L, Guryanova OA, Wu Q, Bao S. Cancer stem cells in glioblastoma-molecular signaling and therapeutic targeting. Protein Cell 2011; 1: 638-55.

299. Tilghman RW, Cowan CR, Mih JD, et al. Matrix rigidity regulates cancer cell growth and cellular phenotype. PLoS ONE 2010; 5: e12905.